Functional Characterisation of Plant-Specific Mitochondrial Outer Membrane Proteins in *Arabidopsis thaliana*

Szymon Kubiszewski-Jakubiak, M.Sc.

A thesis submitted for the degree of Doctor of Philosophy

The University of Western Australia
School of Chemistry and Biochemistry
ARC Centre of Excellence in Plant Energy Biology

April 2015

Declaration

The work contained in this thesis is my own except, where stated. These experiments and associated work were carried out in The Australian Research Council Centre of Excellence in Plant Energy Biology at the School of Chemistry and Biochemistry. The material presented in this thesis has not been presented for any other degree.

Szymon Kubiszewski-Jakubiak

22nd of September 2014

Acknowledgements

First of all I would like to thank my primary supervisor, Jim, for quick response to an email, in which I asked him if he had a PhD position open. Thank you for kick-starting my PhD studies at the "Centre" and for numerous valuable lessons about work in the field of research and in the laboratory.

My greatest thanks go to Monika for taking over as my supervisor and for taking such good care of me after I arrived in Perth for the first time and in the lab and for all the help during the last couple of years, especially during the process of writing. Thank you for many stimulating discussions over coffee. Scientific or otherwise. I guess Polish genes are thicker than water. I'd also like to thank Owen for introducing me to the lab and the outer membrane project. Cheers, mate! Thanks to all Whelanites and Murchlings. This endeavour wouldn't be possible without you all. Thanks to amazing Jenny, Jude and Deb for their tremendous hard work and help. I'd be lost without it.

Since my arrival in Perth I have met some amazing people who made this PhD time an unforgettable experience. I'm so lucky I have met you all. Ray, thank you for teaching me about scientific scepticism and logical fallacies. Faz, thank you for all the crazy parties and being there, when I needed you. Terima Kasih! Cristián, thank you for the amazing time we had in Perth and later in Santiago. Gracias! Ell, thank you for listening, when I had to talk to someone. I really appreciate it. Bradshaw, thank you for all the lels during the last months of my PhD. You really get me. And Max, “You Stupid Idiot”, thanks for always laughing at my Happy Endings references. I’ll always remember it. Merci!

To my Polish mates back home. Thank you for making me feel like I have never left. Jaś, thank you for our daily chats and so many laughs. They were absolutely essential #ft4l. Madzia, thank you for being the voice of reason and the voice of tomfoolery.

Na koniec chciałbym podziękować moim Rodzicom za to, że zawsze są i zawsze mogę na nich liczyć. Ta praca nie byłaby możliwa gdyby nie Wasza pomoc. Dziękuję.

Abstract

Plant mitochondria represent a fascinating model of mitochondrial evolution and biogenesis. Unlike their counterparts in fungi and animals, plant mitochondria coexist with another endosymbiotic organelle, the chloroplast. Therefore, significant differences in mitochondrial biology have been observed to arise during plant mitochondrial evolution. One of them is a low level of conservation of the outer membrane proteome between plants and other groups of organisms. Whilst the mitochondrial outer membrane proteome has been studied in model organisms such as *Saccharomyces cerevisiae* or *Neurospora crassa,* the components present in *Arabidopsis thaliana* (Arabidopsis) have been mostly deduced from orthology and are still poorly characterised. A recent study, using quantitative shotgun mass spectrometry of highly enriched Arabidopsis mitochondria, identified 42 mitochondrial outer membrane proteins, 27 of which haven't previously been observed to localise to this organelle and several of which appeared to be plant-specific. Therefore it was this project's aim to characterise two of these novel mitochondrial outer membrane and plant-specific proteins encoded by At5g24650 and At3g27930.

The protein encoded by At5g24650 was found to be on the mitochondrial outer membrane proteome and belongs to a preprotein and amino acid transporter family of proteins (PRAT). This protein has previously been shown to be dual targeted to the mitochondria and chloroplast and is unique in that it is the only dually located protein transporter. Furthermore this protein is predicted to contain a conserved PRAT domain and sterile alpha motif (SAM) domain. The latter of which is known to be involved in protein-protein interaction and RNA binding. Utilising T-DNA insertional knockout lines, the function of At5g24650 was investigated and found to have a potential role in the import of tRNAs into mitochondria. This finding is an exciting contribution to the field of mitochondrial tRNA import and could be the first case of a plant-specific mitochondrial tRNA import receptor protein. Moreover, it could be used as an important tool for regulation or modification of the expression of mitochondria-encoded proteins.

An additional protein encoded by At3g27930 was identified as plant specific and located on the mitochondrial outer membrane. Bioinformatic analysis identified it to belong to the Porin3 superfamily that includes the voltage dependant anion channel (VDAC) and translocase of the outer membrane 40 (TOM40). Functional characterisation of this protein termed OM47 found that whilst not essential for plant viability it might have a more specialised plant specific role involved in plant senescence. The porin nature of this protein and its putative function in senescence might link it to the programmed cell death, process, which is still not very well described in plants. This discovery could be applied in order to engineer plants, which senesce later and therefore are more efficient.

Abbreviations

AAC	ADP/ATP carriers
ADP	adenosine diphosphate
AOX	alternative oxidase
ATP	adenosine triphosphate
BSA	bovine serum albumin
cDNA	complementary DNA
CL	cardiolipin
COX	cytochrome *c* oxidase
DNA	deoxyribonucleic acid
EF	elongation factor
Eno2p	enolase 2 protein
ER	endoplasmic reticulum
ERMES	ER-mitochondria encounter structure
ERMIONE	ER-mitochondria organizing network
ETC	electron transport chain
Fe-S	iron sulphur cluster
FL	full-length construct
gDNA	genomic DNA
GFP	green fluorescent protein
Hsp	heat shock protein
IF	initiation factor
IMAC	immobilized metal ion affinity chromatography
IMS	intermembrane space
LPS	lipopolysaccharide
MAM	mitochondria associated membranes
Mdm	mitochondrial distribution and morphology
MIA	mitochondrial intermembrane space import and assembly
MINOS	mitochondrial inner membrane organizing system
Mmm	maintenance of mitochondrial morphology
MS	Murashige and Skoog
NADH	nicotinamide adenine dinucleotide

NADPH	nicotinamide adenine dinucleotide phosphate
NBT	nitroblue tetrazolium
ND2	type II NAD(P)H dehydrogenase
OM	outer membrane
PAM	presequence translocase-associated import motor
PC	phosphatidylcholine
PCD	programmed cell death
PCR	polymerase chain reaction
PE	phosphatidylethanolamine
PG	phosphatidylglycerol
PI	phosphatidylinositol
PiC	phosphate carrier
pK	proteinase K
PRAT	preprotein and aminoacid transporter
PS	phospatidylserine
RNA	ribonucleic acid
RNS	reactive nitrogen species
ROS	reactive oxygen species
rRNA	ribosomal RNA
RS	tRNA synthetase
SAM	sorting and assembly machinery
SD	synthetic defined
SDS	sodium dodecyl sulphate
SDS-PAGE	sodium dodecyl sulphate-polyacrylamide gel electrophoresis
SMP	synaptotagmin-like mitochondrial and lipid-binding protein
SOD1	superoxide dismutase
SSU	small subunit of ribulose-1,5-phosphate
T-DNA	transfer DNA
TCA	tricarboxylic acid cycle
TIM	translocase of the inner membrane
TOM	translocase of the outer membrane
TPR	tetratricopeptide repeat
TR	truncated construct

TRic	tRNA import component
tRNA	transfer RNA
VDAC	voltage dependant anion channel
$\Delta\psi$	membrane potential

Table of Contents

Introduction

Chapter 1 - Introduction

1.1 Mitochondria – Overview

1.1.1 The endosymbiotic theory and the origin of semi-autonomous organelles

The origin of the endosymbiotic theory

In 1967, Lynn Margulis (as Sagan) [1] published “On the Origin of Mitosing Cells”, in which she presented a theory of the origins of eukaryotic cells and organelles contained within them. Margulis proposed that mitochondria originated from the bacterial ancestors, which were incorporated into a primordial eukaryotic single cell organism, about 2 billion years ago. According to that theory a second endosymbiotic fusion took place when a free-living cyanobacterium capable of photosynthesis was incorporated and gave rise to today’s plastids (chloroplasts) [2, 3]. However, the concept that prokaryotes could be the ancestors of some organelles is much older than the work of Lynn Margulis. In the late 19th century, Andreas Schimper made a fundamental observation, that there are similarities between the division of chloroplasts and cyanobacteria. Konstantin Mereschkowsky brought this to attention in “On the nature and origin of chromatophores (plastids) in the plant kingdom” [4].

Bacterial origin of mitochondria

Over the course of evolution, endosymbionts have transformed into highly specialised compartments of eukaryotic cells. Mitochondria are often referred to as semi-autonomous organelles due to the fact that even though they contain their own genomes and protein biosynthesis machinery, the majority of proteins building the organelles are encoded by the nuclear genome. In fact, the discovery of organellar DNA within the mitochondria in the 1960s and the translation systems, much different from the cytosolic one, became major arguments for the endosymbiont hypothesis of organelle origin [5]. The development of technology in DNA cloning, sequencing and various omics approaches led to detailed characterization of organellar genomes and genes. Molecular data from the genome organization, small subunit (SSU) of rRNA sequence and proteome studies suggested that origin of these genomes is in fact bacterial and allowed to

identify the living phyla of prokaryotic organisms, which these organelles are closely related to and it is now widely accepted that mitochondrial origin is in the phylum of α-Proteobacteria (Alphaproteobacteria) of the Rickettsial subdivision [5-7]. Over the past 50 years, various groups reported in detail the molecular and biochemical evidence for the endosymbiotic origin of organelles [8-10].

Models of the endosymbiotic theory

There are two prevalent and competing models of the endosymbiotic theory. They are usually referred to as the “archezoan scenario” and the “symbiogenesis scenario” [3, 11]. The first one assumes that the host - archezoan, which engulfed the mitochondrial ancestral cell, was a hypothetical primordial eukaryote, which had a basic plan of a typical eukaryotic cell but was lacking the mitochondria. This model most closely resembles the classical endosymbiotic theory descreibed by Lynn Margulis. However the latest phylogenetic studies and the identification of the mitochondrion-related organelles led to the abandonment of this hypothesis [5]. The "symbiogenesis scenario" on the other hand, describes the situation where, the host was a prokaryotic cell, which evolved into eukaryotic cell after the endosymbiotic event. This means that the evolution of mitochondria, nuclei and other compartments would occur simultaneously. Often cited example of symbiogenesis scenario is the hydrogen hypothesis, which states that the relationship between the anaerobic host (an autotrophic archeabacterium) and the aerobic symbiont (a heterotrophic eubacterium) was based on the fact that the symbiont was able to respire but produced molecular hydrogen as a waste product. This created a metabolic advantage for both host and the symbiont, which became a driving force for the establishment of the symbiosis and what we know today as the eukaryotic cell [12].

Mitochondria-derived organelles

A group of ultrastructurally simple, eukaryotic organisms, such as diplomonads, parasabalids and microsporidia, formerly known as Archezoa, were thought to lack mitochondria. They were thought to split from the main trunk of the eukaryotic tree before the mitochondrial acquisition event occurred. This assumption was in agreement with the initial analyses of SSU rRNA and the

translation elongation factors (EFs) [13, 14]. However, what was also observed in their nuclear genomes was the presence of certain genes such as Hsp60 and Hsp70, which are typical mitochondrial-derived proteins, encoded by the nuclear genome and subsequently imported to mitochondria. Moreover, they turned out to contain double membrane organelles, which correspond to mitochondria, namely hydrogenosomes and mitosomes [13, 14] thus proving the archezoan scenario less likely. Hydrogenosomes and mitosomes are considered mitochondria derived organelles since they are double membrane bound organelles and share the conserved mechanism of mitochondrial protein import. Unlike mitochondria they don't typically contain their own genomes [14]. Hydrogenosomes are known to be the site of iron-sulfur (Fe-S) cluster biogenesis and they generate ATP in the anaerobic process of fermentation of pyruvate to acetate, carbon dioxide and molecular hydrogen by substrate level phosphorylation [15]. Mitosomes on the other hand don't possess the ability to generate the energy in form of ATP. It seems that the only function of these organelles is the synthesis of Fe-S clusters [16].

1.1.2 Mitochondrial morphology

Mitochondria are usually portrayed in textbooks as tiny bean-shaped organelles spread evenly around the cell. In reality, they can exhibit a variety of shapes ranging from singular spheres to complicated networks and their form depends on the organism, the type of the cell as well as cell's metabolic state [17]. They consist of four distinct subcompartments: the outer mitochondrial membrane, the intermembrane space, the inner mitochondrial membrane and the mitochondrial matrix.

The outer membrane of mitochondria acts as an interface between the organelle and the cytosolic environment. It mediates a variety of processes such as the protein import, macromolecule diffusion and cellular signalling [18]. The outer membrane is a smooth, phospholipid bilayer, rich in porins (channel proteins of β-barrel confirmation such as voltage dependant anion channel, VDAC), which is permeable to small molecules (between 2-6 kDa), which allows the free flow of

metabolites between the cytoplasm and the intermembrane space (IMS) [19]. The mitochondrial outer membrane will be described further in the section 1.3.

The intermembrane space (IMS) is a crucial subcompartment of mitochondria, which harbours various proteins involved in a variety of processes such as energy production (via oxidative phosphorylation) as well as transport of certain proteins, metal ions and metabolites. It partakes in the detoxification of harmful molecules and finally is the site of some of the processes of the apoptosis. The most common feature of proteins present in the IMS is the presence of the disulfide bonds [20]. Proteins present in the IMS can be divided into 3 classes: proteins with Cx_3C motif (such as small TIM proteins responsible for the transport of hydrophobic membrane proteins) [21], proteins with Cx_9C motif such as cytochrome *c* oxidase (COX) proteins involved in cytochrome *c* oxidase assembly as well as an mitochondrial intermembrane space import and assembly 40 receptor Mia40) [20, 22] and finally proteins lacking the aforementioned motifs e.g. complex III subunits and superoxide dismutase (SOD1) [23].

The inner membrane of mitochondria is another crucial subcompartment of mitochondria especially because of its function in the energy transduction. It contains the electron transport chain machinery proteins. The IMS and the inner membrane proteins are responsible for generation of the proton gradient necessary for the chemiosmotic production of ATP. Probably most notable features of the inner membrane are the structures, formed by it, referred to as the mitochondrial cristae. The function of cristae is to increase the surface of the inner membrane, which allows for more efficient energy production [24].

The matrix is the aqueous compartment, enclosed by the two membranes. It contains the mitochondrial genome together with its protein synthesis machinery and TCA cycle enzymes.

1.1.3 Functions of Mitochondria

Mitochondrial genome

Even though mitochondria have kept their bacterial double membrane structure and the machinery to synthesize energy, in the course of evolution they have gained a multitude of new functions within the host cell. The gain of new

mitochondrial functions was dependent on the loss of most of the genetic information from the bacterial progenitor genome, which was transferred to the nucleus. What were left are small, usually circular DNA molecules, which encode for a small number of, crucial to the mitochondrial function, proteins. The sizes of mitochondrial genomes vary between different species. The human mitochondrial genome encodes for 13 proteins of the electron transport chain, 22 transfer RNAs and 2 ribosome coding RNAs [25, 26]. Plant mitochondrial genomes are usually much larger. *Arabidopsis thaliana* (Arabidopsis) mitochondrial genome for example, encodes for around 30 proteins in 366 kb of DNA [27]. Different sizes of the mitochondrial genomes among different species translates to a varying coding capacity, however most mitochondrial genomes encode for similar components such as respiratory complexes proteins (I-IV), the ATP synthase subunits, cytochrome *c* biogenesis proteins, ribosomal proteins, ribosomal RNAs and finally the transfer RNAs [27].

Mitochondrial dynamics

As early as 1914, Lewis and Lewis observed that mitochondria in chick embryo tissue culture are dynamic and constantly change their morphology [28]. They observed that mitochondria go through a series of morphological changes: first the single mitochondria fuse with each other creating elongated rods, then more complicated threads and finally form composite networks which subsequently divide back to singular organelles [28]. Hence the number, morphology and distribution of mitochondria are the result of two ongoing, opposing processes: fusion and division (fission) [29, 30]. Initial studies of the nature of these processes were conducted in the early 1990s using genetic screens of *Saccharomyces cerevisiae* (budding yeast). This led to the discovery of the first proteins essential for distribution and morphology of yeast mitochondria. It seems that the best described pathways: fusion and fission, often rely on proteins with GTPase activity conserved in animals such as fruit flies, worms, mice and humans as well as plants such as Arabidopsis, which indicates that the fundamental mechanisms controlling mitochondrial behaviour have been maintained during evolution [31]. However, budding yeast remains the best-described model organism in the mechanics of mitochondrial dynamics.

Three proteins: Fzo1, Mgm1 and Ugo1 are thought to be involved in the fusion process in yeast mitochondria. Hales and Fuller (1997) reported that Fzo1 is essential during fusion of mitochondria in fruit fly spermatogenesis [32]. It belongs to a family of large, transmembrane GTPases (known as mitofusins in mammals), which build high molecular weight complexes in the outer membrane. Mammalian mitochondrial outer membranes contain two mitofusin isoforms: Mfn1 and Mfn2 [29, 33]. Mitochondrial genome maintenance (Mgm1) protein is a dynamin- related GTPase required to promote fusion of mitochondria in yeast, specifically the inner membrane [34]. A mammalian orthologue to Mgm1 named Opa1 (optic atrophy) has also been identified [29, 31]. The third component of the yeast mitochondrial fusion machinery is Ugo1 (ugo: Japanese for fusion), which is thought to co-ordinate the fusion of both the outer and inner membranes by physically connecting with Mgm1 and Fzo1. No homologues of Ugo1 have been found in animals [29].

So far there has been no report of any plant mitochondrial protein required for mitochondrial fusion. No homologues of yeast Fzo1 and Ugo1 proteins have been identified. A plant protein that exhibits highest homology to Mgm1 is termed DRP3A, however, it is believed that DRP3A is responsible for the fission process in Arabidopsis, not fusion [35]. Although specific proteins essential for mitochondrial fusion in plants have not yet been identified, it has been demonstrated that plant mitochondria also undergo fusion events. In 2004, Arimura *et al.* observed mitochondrial fusion using the photoconvertible fluorecent protein Kaede, in onion epidermal cells, which when exposed to light (350-400 nm) can be irreversibly changed from green to red. The presence of yellow mitochondria indicates mixing of red and green protein localised in matrix, thus proving that fusion indeed occurs [36].

Similar to fusion, the mitochondrial fission pathway is best described in yeast [29]. Dynamin-related protein (DRP) called Dnm1 is essential for fission in yeast . DRPs are the main factors responsible for mitochondrial fission in most eukaryotic organisms, including higher plants [35, 37]. Dnm1 is a cytosolic protein containing a GTPase domain on the N-terminus and a GED domain (GTPase effector) on the C terminus, which allows self-assembly. Mutants without Dnm1 function present nets of connected mitochondria, caused by fusion events without

fission activity [38]. Ingerman *et al.* described a mechanism where Dnm1 self-assembles into spiral-like structures, which are targeted to the outer membrane and take part in GTP hydrolysis-driven constriction and scission of mitochondria [39]. According to Mozdy *et al.,* (2000), the process of mitochondrial fission in yeast requires a cytosolic protein Fis1 (fission), which is anchored to the outer membrane of mitochondria and acts as a receptor for Dnm1 and two cytosolic proteins: Mdv1 and Caf4 [40]. Homologues of dynamin-related proteins have been identified in animals and plants indicating a high level of conservation throughout evolution [33].

Similarly to yeast, dynamin-related proteins take part in mitochondrial fission in Arabidopsis and rice. Several dynamin-like genes have been identified in Arabidopsis two of which, *DRP3A* and *DRP3B,* are suggested to be involved in plant mitochondrial fission [35, 37]. Green fluorescent protein (GFP) labelled DRP3A and DRP3B (formerly known as ADL2a and ADL2b), were found attached to constriction sites and tips of mitochondria [41]. In addition, mutant plants with knockouts in *DRP3A* and *DRP3B* as well as plants overexpressing constructs with disrupted GTPase domain are characterized by a reduction in the number of mitochondria per cell, larger mitochondria and mitochondrial tubulation [41]. Two orthologues of Fis1 have been identified in Arabidopsis: BIGYIN1 and BIGYIN2 (also known as FISION1A and FISION1B). Both BIGYIN1 and BIGYIN2 are outer membrane proteins and knockouts in their genes lead to an increase in mitochondrial size and a decrease in the number of mitochondria in the cell, thus suggesting their role in mitochondrial fission [37]. According to Arimura *et al.* (2008), ELM1 (also known as NETWORK1) is a plant specific protein, which localizes to the outer membrane of mitochondrion and possibly takes part in recruiting DRP3A and DRP3B during fission in Arabidopsis [42]. It has been also shown recently, that plants deficient in cardiolipin (CL), the key membrane component; exhibit dysfunctional fission of mitochondria in Arabidopsis. This might be due to the stabilizing function of CL towards the DRP3 protein [43].

Unlike the majority of yeast and mammalian cells, in which mitochondria are mostly tubular and/or form extensive networks [44], typical plant cells are characterised by highly fragmented mitochondria, which could indicate that in plant species the process of fission dominates over fusion of these organelles [43].

Respiratory pathways

Mitochondria play a critical role in the generation of energy in eukaryotic cells and they are responsible for the production of majority of energy derived from the breakdown of carbohydrates, which is converted into ATP by oxidative phosphorylation process. The classic pathways of the respiration are glycolysis, the mitochondrial tricarboxylic acid (TCA) cycle and the mitochondrial electron transport chain. Plant respiratory metabolism possesses several unique features such as multiple entry points of starch and sucrose or the presence of the non-phosphorylating electron transport systems [45]. The tricarboxylic acid cycle (TCA cycle), also known as the Krebs cycle, is the core of the metabolic reactions of the process of respiration. It takes place in the mitochondrial matrix and consists of eight enzymes, which link products of oxidation of pyruvate and malate (generated in the cytosol in the process of glycolysis) to CO_2 while generating the reducing power in the form of NADH.

Probably the most known function of mitochondria is the synthesis of most of the cell's energy in the form of adenosine triphosphate (ATP). Mitochondria perform the last step of aerobic respiration, in which the bulk of ATP is synthesized in the process of oxidative phosphorylation. This process occurs between the mitochondrial inner membrane and the IMS and is mediated by complexes of proteins known collectively as the electron transport chain (ETC), located in the inner membrane: complex I (NADH dehydrogenase), complex II (succinate dehydrogenase), complex III (cytochrome c reductase), complex IV (cytochrome c oxidase) and the terminal complex V (ATP synthase). The ETC generates an electrochemical gradient via co-transfer of protons across the inner membrane and electrons to oxygen. The proton gradient formed by this chain of oxidation and reduction events powers the ATP synthase, which catalyses the synthesis of ATP from ADP and inorganic phosphate [46], [47]. Mitochondrial ATP synthase (also referred to as the F-ATPase) is an evolutionary conserved protein, which homologs are present in mitochondria, chloroplasts and bacteria [48]. It consists of membrane extrinsic sector F_1 (catalytic) and membrane intrinsic sector F_0 (proton translocating) [48].

Plant mitochondria (as well as some protists and fungi) possess an alternative respiratory pathway. In addition to complex I, or the NADH

dehydrogenase, plant mitochondria contain type II NAD(P)H dehydrogenases or ND2s that also have the ability to use the NADH or NADPH to reduce ubiquinone. Unlike the complex I, these proteins face the IMS or matrix of the inner mitochondrial membrane [49] and do not contribute to the translocation of protons but rather indirectly power the ATP synthesis while competing with the ETC for the electrons [49]. Multiple isoforms of these proteins exist for example Arabidopsis mitochondria contain two NDA isoforms (internal side of the inner membrane), four NDB isoforms (external side of the inner membrane) and one NDC isoform, which is an internal NAD(P)H dehydrogenase [50].

Probably the most studied plant mitochondrial protein (and a component of the alternative respiratory pathway) is the alternative oxidase (AOX). Since its discovery in 1971 [51] its exact role in the respiration hasn't been elucidated. It was initially hypothesized to act as the overflow pathway for electrons, when COX reaches its capacity [52]. This was shown to be inaccurate, when Ribas-Carbo *et al*. performed the oxygen isotope discrimination study, demonstrating that AOX and COX compete for electrons [53]. Whilst several hypotheses of AOX function exist, all point to similar conclusion that AOX acts as a buffer for fluctuations of respiration, which could potentially lead to the oxidative stress [54]. A number of studies have shown that AOX is induced at a gene and protein level by a variety of stresses [55], which can signal the nucleus to launch expression of various stress responsive genes in the process of the mitochondrial retrograde signalling [56-58].

Other functions

The essential role of mitochondria in all eukaryotic organisms is the biogenesis and assembly of iron-sulphur (Fe-S) clusters. These molecules are essential cofactors of various cytosolic and mitochondrial proteins such as complex I and III and are involved in multiple processes such as photosynthesis, assimilation of sulphur and nitrogen, metabolism of amino acids, synthesis of plant hormones as well as repair of DNA and the protein biosynthesis [59].

Apart from pyruvate and malate, which are the most prevalent substrates of the mitochondrial matrix in darkness or in non-photosynthetic tissues, various metabolites such as e.g. amino acids can also be metabolized. This occurs via transamination or direct oxidation of amino acids, especially of protein storing

plants such as legumes [60]. The resulting TCA intermediate can re-enter the cycle. However mitochondria can also contribute to biosynthesis of amino acids. This process is powered by the production and export of 2-oxoglutarate, which is used in the reaction of transamination and assimilation of ammonia. Ammonia and 2-oxoglutarate are used as substrates in the GS/GOGAT cycle, which results in synthesis of glutamate and downstream of other amino acids [61].

Mitochondria mediate the synthesis of various other crucial molecules such as biotin - a cofactor of many carboxylases [62]. They contain enzymes responsible for the synthesis of some phospholipids, which link mitochondria to endoplasmic reticulum (a liaison, which in plants is yet to be elucidated). This process takes place at the mitochondria-associated membrane (MAM) of ER, fraction, which is enriched in phospholipid synthesis enzymes [63]. Mitochondria are also involved in cell death. By releasing the cytochrome *c*, which acts in part as an activator of the cascade of caspases, mitochondria initiate the disassembly of all of the cell constituents in the process of programmed cell death (PCD).

1.2 Mitochondrial Biogenesis - Macromolecule Import

1.2.1 Mitochondrial Protein Import

Overview

Mitochondria have multiple functions in all eukaryotic cells including processes such as energy metabolism, synthesis and degradation of various molecules as well as the programmed cell death [64]. Whilst they possess their own genomes over the evolutionary time, the vast majority of genes were lost or their function was transferred to the nucleus and subsequently encode for only about 50 proteins and a number of ribosomal and transfer RNAs. Hence about 1000 proteins, which build these organelles in plants [65], yeast [66] and up to 1500 in mammals [67], are encoded by the cell's nucleus, translated in the cytosol and subsequently imported into mitochondria. The current knowledge regarding the mechanisms of protein translocation comes from comprehensive genetic and biochemical studies of yeast. Whilst studies within other species are relatively limited, it appears that these mechanisms are highly conserved amongst the higher eukaryotes. The presence of gene orthologs and protein complexes of the

yeast protein import machinery is well documented across plants, animals, and fungi and to lesser extent in some protists [18, 68-71]. The examples of protein import pathways and components described below refer to yeast studies unless stated otherwise.

The Translocase of the Outer Membrane (TOM) complex is responsible for the recognition of the mitochondrial protein precursors and for translocating them onto another multi-subunit complex, the Translocase of the Inner Membrane (TIM). In fact, there are two TIM complexes in the mitochondrial inner membrane: TIM23 and TIM22. The former mediates the translocation of proteins with the N-terminal presequence, or the targeting signal via so called "general import pathway". Proteins carrying the presequence are either completely imported to the matrix, which requires energy in the form of ATP and the Presequence translocase Associated import Motor (PAM) or in case of the lateral sorting into the inner membrane, the import is solely dependant on the membrane potential ($\Delta\psi$). TIM22 complex is responsible for the translocation of the proteins, which contain the internal targeting signal or the carrier proteins via the "carrier import pathway". Upon translocation via TOM, proteins destined for the IMS are imported via Mitochondrial Intermembrane space import and Assembly (MIA) machinery. The Sorting and Assembly Machinery (SAM) is responsible for integration of the β-barrel proteins into the outer membrane. Small Tim proteins, soluble chaperones found in IMS, mediate in the carrier and the β-barrel protein translocation [72].

The TOM complex

The TOM complex mediates the transport of numerous kinds of precursor proteins, containing diverse import signals, across the outer membrane. The central component of the complex, Tom40, is a transmembrane pore in the β-barrel conformation, which acts as the gate for all mitochondrial precursor proteins [73]. It is essential for viability in yeast, being the first membrane protein demonstrated to be so [72]. It has been demonstrated, that the prevalent isoform of Tom40 in Arabidopsis, AtTom40-1 is similarly an essential protein when knocked out by a T-DNA insertion [72]. Additionally to the central Tom40 pore, TOM complex consists of Tom20, Tom70/72, Tom22 and the small Tom5, Tom6

and Tom7 subunits. These additional subunits play role in supporting the structure of the complex and/or function as receptors [74]

Tom20 and Tom70/72, the cytosolic facing receptors of the complex, distinguish between different kinds of precursor proteins. Tom20 recognizes the N-terminal presequences, which are present in about 70% of mitochondrial proteins and are usually 6-90 amino acids long [75] while Tom70/72 bind the precursor proteins with the integral targeting sequence [76]. Interestingly, neither Tom20 nor Tom70/72 receptors have been identified in plants by homology based searched. However, plant Tom20 receptor is likely to have arisen independently through convergent evolutionary mechanism. Plant Tom20 receptor was identified by biochemical means and unlike its yeast or mammalian analogues is anchored to the outer membrane by its C-terminus and has also been described as having a unique recognition site for precursor proteins namely two atypical tetratricopeptide repeat (TPR) folds, each 43-44 amino acid in length (unlike the yeast and mammalian Tom20 containing only one TPR, 34-residue in length) [77, 78].

The Tom22 receptor is a transmembrane receptor of the TOM complex, spanning through the outer membrane with its N-terminus on the cytosol side and the C-terminus on the IMS side [79]. Tom22 forms a so-called *cis* recognition site (together with Tom20) on the cytosol side of the outer membrane as well as the *trans* recognition site on the IMS site (together with the IMS-facing region of Tom40 and Tom7). It is responsible for the stabilization of the Tom40 channel of the complex [79]. Tom9, the plant ortholog of Tom22, is highly conserved in different plant species and is characterized by the lack of the cytosolic domain of Tom22. It is being hypothesized that Tom9 has lost its cytosolic domain to avoid the misstargeting of chloroplast preproteins to mitochondria [80].

Tom5 is hypothesized to be involved in the biogenesis of Tom40 as well as assisting Tom22 in the transfer of protein precursors into the Tom40 channel [81]. Additional small subunits, Tom6 and Tom7 are similarly involved in the assembly of Tom40, where the former acts as the promoter via interaction with the intermediates of early assembly and the latter destabilizes the process of assembly of the complex [82, 83]. The Arabidopsis genome contains orthologs to all of the small Toms though only Tom7 has been identified biochemically as a part of the TOM complex in potato [84, 85]

To date only one plant specific outer membrane receptor has been identified termed outer membrane protein 64 (OM64). It is been shown to be a paralog to the chloroplast Toc64 protein import receptor to which it exhibits 67% sequence identity. Lister et al. (2007) showed that depletion of OM64 resulted in a small decrease in the import rate of some mitochondrial protein precursors (such as plant specific ATP synthase subunit F_Ad) with only a minor phenotypic change as shown in T-DNA knock out lines [86]. Though interestingly an embryo lethal phenotype could only be observed when OM64 was deleted in combination with all three isoforms of Tom20 [18].

The mechanism of the translocation of protein precursors containing the N-terminal presequences is the best-understood pathway of mitochondrial protein import. After being recognized by the Tom20 receptor, protein precursors interact with the *cis* recognition site (cytosolic domains of Tom22 and Tom5) and subsequently perform the so-called polar slide formed with the Tom40, after which they interact with the *trans* recognition site (IMS domains of Tom40, Tom7 and Tom22). This movement inward the complex happens probably due to the increasing affinity of the interactions between the protein precursors and the components of the complex [87].

The SAM complex

A key characteristic of the outer membrane of Gram-negative bacteria is the presence of proteins in a β-barrel confirmation. As such eukaryotically derived β-barrel proteins are also present in the outer membranes of mitochondria and chloroplasts whose import is distinct to that of the general import pathway. β-barrel proteins are initially recognized by the TOM complex, translocated through Tom40 and transferred onto IMS protein complexes formed by the small Tims [88]. These hexameric chaperone complexes are responsible for guiding specific precursor proteins onto their respective sorting machineries. The Tim9-10 complex recognizes the β-barrel proteins and carrier proteins, whilst the Tim8-13 complex recognizes Tim23 protein [89, 90]. Subsequently, the β-barrel proteins are integrated into outer membrane, by the SAM complex, upon the recognition of the so-called β-signal. The β-signal has been identified as a conserved sequence, present in the last predicted, transmembrane β-strand, which is characterized by

large polar residues, mostly lysine and glutamate [91]. The SAM complex consists of the core protein, Sam50, which is integrated in the outer membrane and forms a pore across it [91] and two additional subunits, namely Sam35 and Sam37 (also termed metaxin in mammalian models [92]). The bordering Sam35 and Sam37 face to the cytosol side of the complex. Sam35 has shown to be the receptor of β-signal, which binds the proteins and overhangs the pore of Sam50. Sam50 has been suggested to be responsible for folding of the β-barrel precursors, which are subsequently released to the membrane by Sam37 [93]. Orthologs of Sam50 and Sam37 exist in plants and both have been shown to be outer membrane proteins involved in import of β-barrel precursor proteins. Depletion of Sam37 in Arabidopsis has been described to cause decrease in import and altered phenotype suggesting its crucial role in mitochondrial protein import [86]. Several additional protein components have been shown to interact with SAM complex in yeast such as Mdm10 (also known as Tom13), Mdm12, Mmm1, Mmm2 and Fcj1, which are also involved in the Tom40 assembly [94]. There are two hypotheses of the function of the Mdm10-containing SAM complex. One of them assumes it releases the β-barrel precursors from the SAM complex while the other states that it is involved in assembly of α-helical subunits of TOM complex like Tom22 and it has been also postulated that the Tom7 subunit regulates the assembly of the TOM complex by dissociation of Mdm10 from SAM complex [95, 96]. Mdm10, Mdm12, Mmm1, Mmm2 and Fcj1 have all been previously identified from mutants known to be defective in maintaining mitochondrial morphology and distribution. Moreover, mutations in Mdm10, Mdm12, Mmm1 and Mmm2 have been shown to cause aberrations in β-barrel assembly pathway. [97, 98]. All these proteins contribute to the endoplasmic reticulum-mitochondria encounter structure (ERMES) described below.

The ERMES complex

In 2009 Kormann et al. identified a protein complex, which tethers the endoplasmic reticulum (ER) and mitochondria in yeast by physically binding two organelles with each other. This was achieved by screening for yeast mutants, which had a phenotype that could be rescued by expression of a synthetic protein designed to tether the mitochondria to ER. By using this approach subunits of the

ER-mitochondria encounter structure (ERMES) complex where first identified [99]. Interestingly mutations in components of ERMES complex also results in various morphological aberrations of mitochondria as well as physiological dysfunctions such as inability to grow on non-fermentable media [99].

There are at least four subunits forming ERMES: Mdm10 and Mdm34, which are localized on the mitochondrial outer membrane, Mmm1, which is integrated in the ER membrane and Mdm12, which resides in the cytosol. These subunits come together to form the complex, which physically bind these two organelles however it has been suggested that ERMES plays roles in other cellular processes such as mitochondrial morphology, replication of mitochondrial DNA, protein import and the homeostasis of phospholipids [97, 99-101].

ERMES orthologs have yet to be identified in plants. Homology based searches against the genome of Arabidopsis resulted in some potential candidate proteins. Whilst sequence identity of these was quite low (29-42%) [72] they were shown to contain the synaptotagmin-like mitochondrial and lipid-binding protein (SMP) domains, which belong to the tubular lipid-binding protein (TULIP) domain superfamily present in several ERMES components [102].

The MINOS complex

Both TOM and SAM outer membrane complexes have been shown to interact with the mitochondrial inner membrane organizing system (MINOS) complex [103]. The complex consist of six subunits: Fcj1/mitofilin, Mio10, Aim5, Aim13, Aim 37 and Mio27. It has been suggested that MINOS is mainly involved in maintenance of the cristae architecture of the mitochondrial inner membrane [104]. However its involvement in the import of β-barrel precursor proteins [103] and IMS proteins [105] has also been proposed.

There are no confirmed orthologs of MINOS complex in plants, however candidate orthologs have been identified with 27-32% sequence identity in Arabidopsis genome [72].

A model of a functional and physical link between TOM, SAM, ERMES and MINOS complexes has been proposed and termed ER-mitochondria organizing network (ERMIONE) and described as a large network involved in communication, morphology and biogenesis of mitochondria and ER [103].

The MIA pathway

Proteins of the mitochondrial intermembrane space are characterized by multiple cysteine moieties (responsible for formation of disulfide bridges), which take form of characteristic motifs such as Cx_3C (small Tims) and Cx_9C (COX proteins). Mitochondrial IMS sorting signal (MISS) around these cysteine motifs has been identified and is responsible for targeting these proteins to the IMS through the MIA pathway [106] a specialised pathway involving two proteins Mia40 (which acts as the receptor) and Erv1 (a sulfhydryl oxidase), involved in the import and folding of IMS proteins functioning as a disulfide relay system in the IMS.

After translocation through the TOM complex, the IMS-destined precursor protein is transiently bound to Mia40. This occurs through the cysteine-proline-cystein (CPC) domain of Mia40, which is responsible for the formation of a disulfide bond [107]. It has been shown in yeast that Mia40 is located in close proximity to TOM complex by interacting with the inner membrane protein mitofilin/Fcj1 (mentioned above as the component of MINOS complex). Mitofilin/Fcj1 functions at contact sites of inner and outer membrane therefore it can facilitate Mia40 in the interception of newly translocated IMS precursor proteins [105]. Subsequently, Mia40 catalyses the formation of disulfide bonds within the precursor molecule, which causes the release of the precursor and reduction of Mia40. Erv1 performs the oxidation of Mia40 and the import cycle can be repeated [108].

Unlike in yeast, plant Mia40 is not an essential protein and its depletion has no obvious deleterious effect on Arabidopsis growth. Additionally it has been shown that AtMia40 localizes to both the mitochondria and peroxisomes [68] with its function in peroxisomes unknown. The same study also showed that the Arabidopsis ortholog to Erv1, like its yeast ortholog, is essential Dual targeting of Mia40 and its substrates suggest that in higher plants Mia40 might have more diverse functionality [109].

The TIM22 complex

Precursor proteins containing internal targeting sequences are imported through and into the inner membrane by the TIM22 complex. The majority of

these proteins belong to mitochondrial metabolite carriers such as ADP/ATP carriers (AAC) and the dicarboxylate carrier and the phosphate carrier (PiC) and thus this pathway has been termed the carrier import pathway. Moreover TIM22 complex also mediates import of other inner membrane import components such as Tim17, Tim22 itself and Tim23 [110]. Because of their high hydrophobicity, following translation precursors must be secured by the chaperones of Hsp70 and Hsp90 families, which stop the aggregation and support targeting to the outer membrane [111]. Delivery of the precursor-chaperone complex involves recognition by Tom70 receptor, which has been shown to bind not only the internal targeting signal but the chaperones as well. Interestingly maximum of three Tom70 dimers are assembled per precursor during this process [112]. The release of the precursor from its chaperone complex requires energy in the form of ATP however, which protein is involved in the release of precursor onto Tom40 pore is yet to be elucidated [113].

While still being traversed across the Tom40 pore, precursors are recognized by the small Tim complex in the IMS - Tim9-10. The Tim9-10 complex (about 70 kDa in size) consists of three Tim9 and three Tim10 subunits in a form of a hexamer. Its role is to bind precursor's hydrophobic regions while they appear on the IMS side of the outer membrane [89]. Subsequently, it shuttles the precursor onto the TIM22 complex of the inner membrane, which is responsible for the membrane potential-dependent insertion of multispanning inner membrane proteins into the inner membrane [110]. The TIM22 complex consists of peripheral protein Tim12, which interacts with Tim9-10 complex, and is integrated with the membrane Tim18, Tim22 and Tim54 subunits. Tim22 has been shown to conduct two functions: it is responsible for the recognition of internal targeting signals and acts a pore, which responds to membrane potential [113].

Association of Tim9-10 complex with Tim12 initiates the targeting of carrier precursor proteins. Subsequently, the IMS-facing domain of Tim54 recognizes substrate-loaded Tim9-10-12 complex and passes it onto the Tim22, which is followed by the release of the precursor into the membrane and assembly of functional dimers in case of a majority of metabolite carriers [113].

All subunits of this complex have been shown to be essential in yeast with Tim18 shown to be also part of the Sdh3 (complex II subunit) suggesting

involvement in both mitochondrial biogenesis and electron transfer [114]. Plant orthologs can only be identified for Tim22, with two identical genes encoding Tim22 in Arabidopsis. Characterisation of T-DNA insertional knock-out lines suggests that while one is essential for viability the other most likely a result of a recent gene duplication is a pseudogene that is not expressed as it cant rescue the embryo lethality of the other [72].

The TIM23 complex

The vast majority of proteins imported to mitochondria possess a cleavable presequence on the N-termini [75]. These preproteins after translocation through Tom40 pore associate with the IMS-facing domain of the Tom22 receptor [115]. The preprotein whilst still being transported through the Tom40 pore, is recognized by the TIM23 complex of the inner membrane [116]. The TIM23 complex consists of the twin pore proteins Tim23 and Tim17 and the accessory protein Tim50. The IMS-facing region of Tim23 and a large IMS domain of Tim50 form the preprotein receptor. Tim50 is also suggested to have the maintenance function of the Tim23 channel, when preprotein is absent, by preventing the dissipation of membrane potential caused by ion leakage [117, 118]. Tim17 regulates the twin pore assembly of the TIM23 complex as well as mediates protein sorting and voltage sensing however the molecular mechanism is yet to be described [119, 120]. An additional membrane component - Tim21, has been shown to dynamically interact with TIM23 complex and is involved in facilitation of the transfer of the preprotein from the TOM complex onto TIM23 complex [121-123].

Preproteins are either translocated into the matrix or upon recognition of a hydrophobic "" signal laterally released into the membrane. The membrane potential is responsible for the delivery, translocation and opening of the channel of TIM23 complex by the electrophoretic "dragging" of the positive charge of the presequence across the membrane. In fact, it has been demonstrated, that the minimal system required for import and integration of a preprotein, with the "stop transfer" signal, into the inner membrane consists of the presequence translocase (TIM23 complex), the membrane and the membrane potential by reconstituting the purified presequence translocase into the cardiolipin-rich liposome [124]. The

core components of TIM23 complex together with Tim21 are therefore referred to as TIM23^{SORT}. It has been also demonstrated that the TIM23^{SORT} interacts with respiratory chain complex III subunit, bc_1 and the cytochrome *c* oxidase (complex IV). This interaction supports the membrane potential-dependent preprotein insertion [124, 125].

The Arabidopsis genome encodes for three isoforms of Tim17 protein. AtTim17-1 and AtTim17-2 are characterized by a C-terminal extension, which is only present in plants. This extension has been shown to bind specific substrates as well as physically link the inner and the outer membranes [126]. Interestingly, all three isoforms of Tim17 in Arabidopsis are characterized by different expression patterns. While AtTim17-1 has low expression in various tissues and throughout the development, it has been shown to be upregulated during germination and can be induced with UV [127, 128]. The most abundant is the AtTim17-2 isoform and it is expressed throughout the development and peaks during germination unlike AtTim17-3, which is moderately expressed and without specificity to tissue or stage of development. Mutant studies demonstrated that AtTim17-2 is an essential isoform in Arabidopsis while no phenotype was observed when AtTim17-3 was depleted. This could be explained by the fact that while AtTim17-2 is not the most orthologous to ScTim17 protein, its plant-specific extension may confer the essential function.

There are also three isoforms of Tim23 present in Arabidopsis mitochondria. It has been shown that all three isoforms have the highest level of expression during germination however the most abundant is the AtTim23-2 isoform [129]. Mutant studies showed that depletion of the single isoform didn't cause changes in the phenotype however double crosses had an embryo-lethal phenotype with seeds aborted later in the development suggesting that at least two isoforms are needed for seed viability [72].

The Arabidopsis ortholog to Tim21, similarly to its yeast counterpart, interacts with the TIM23 complex and the respiratory complex III [130]. Depletion of AtTim21 has been shown to cause seedling lethality [131] unlike ScTim21, which is a non-essential protein [132]. Overexpression of AtTim21 resulted in increased size (plants/mitochondria) and higher intracellular ATP levels and increased expression of several subunits encoding respiratory components [131].

Interestingly there are two additional Tim21-like genes in Arabidopsis [133]. Both proteins, referred to as AtTim21-like 1 and -2 contain the conserved Tim21 protein domain however they are phylogenetically distinct from Tim21. They have been shown to be plant specific and originate in green algae. Both AtTim21-like proteins have been shown to located in the mitochondria and contain N-terminal targeting presequence. Furthermore it has been suggested that as observed with AtTim21, both AtTim21-like proteins have the ability to interact with the TIM23 complex and the respiratory complexes I and III [133].

The Arabidopsis genome encodes for one Tim50 protein, while Tim50 is essential in yeast there seems to be some discrepancy when it comes to studies on its viability in plants. Kumar *et al.* described the AtTim50 knock out line as viable with only minor phenotypic changes. However further analysis revealed the line to be a functional knock-down and not a knock-out line. An additional line resulting in a truncated Tim50 protein instead exhibited an retarded growth phenotype supporting the theory that Tim50 in Arabidopsis is also an essential protein [72].

Complete translocation of proteins into the matrix requires energy from ATP hydrolysis and is mediated by the presequence translocase-associated import motor (PAM) and the mitochondrial heat shock protein 70 (Hsp70). The peptide-binding domain and the ATPase domain of Hsp70 are main factors contributing to the complete translocation of the preproteins into the matrix [134]. Several components of PAM are responsible for recruitment of Hsp70 to the TIM23 complex and its regulation: Pam16, Pam17, Pam18, Tim44 and Mge1. It is being suggested that Pam17 initiates this process by displacing Tim21 and together with Tim44 bind the Pam16-18 complex. Subsequently the Hsp70 is recruited to, what now is referred to as $TIM23^{PAM}$ and together with Mge1 it drives the ATP-dependent import into matrix [135-137].

The final step of the import of matrix proteins is the processing of the presequence, which is mediated by the mitochondrial processing peptidase (MPP). MPP cleaves the presequence off the preprotein entering the matrix, which is subsequently degraded by the presequence peptidase (PreP). Interestingly the plant MPP has been shown to have additional function in electron transport. It has

been shown to be an integral component of the cytochrome bc_1 complex unlike its mammalian and yeast counterparts.

Since the endosymbiotic event, variations of mitochondrial protein import have evolved across different species. With the increasing number of sequenced genomes it is feasible to gain new information about pathways of mitochondrial protein import. A Mitochondrial Protein Import Components (MPIC) Database (http://www.plantenergy.uwa.edu.au/applications/mpic) has been generated, which provides searchable information on the protein import apparatus from plant and non-plant species [138].

1.2.2 Mitochondrial tRNA Import

Overview

Contrary to many textbooks, mitochondrial biogenesis in the majority of eukaryotes does not solely rely on the import of proteins but also requires the import of cytosolic transfer RNAs (tRNAs). Since the first report by Suyama (1967), who reported that tRNAs isolated from the mitochondria of the protozoan *Tetrahymena* hybridize to the nucleus rather than mitochondria [139], the hypothesis of tRNA import into mitochondria was largely ignored. It was not until 1992 when Small *et al*. showed the first direct evidence for the mitochondrial tRNA import, using transgenic plants in which a tagged tRNA gene transcript could be found in both cytosolic and mitochondrial fractions [140]. Only after these experiments, the phenomenon of tRNA import was widely accepted by the scientific community though despite its broad occurrence in many organisms it is still an area of research in its infancy.

Mitochondrial tRNA import is a widespread process and the number of mitochondrial genes encoding for tRNAs varies between species. Some mitochondrial genomes encode for a complete set of tRNAs (e.g. human and yeast), other lack a significant number (e.g. Arabidopsis) and some are completely devoid of tRNA genes (e.g. trypanosomes) summarized in [141]. Organisms which possess mitochondrial genomes encoding for a complete number of necessary tRNAs are only present among the supergroup of Opisthokonta (i.e. Fungi and

Metazoans) however this is not true for all opisthokonts. This led to belief that the tRNA import machinery evolved several times independently. However if tRNA import were polyphyletic in origin, different mechanisms would have to evolve in a relatively short time. This could explain why closely related species can import different number of tRNAs. Moreover some species like humans and yeast have been predicted to contain a complete set of mitochondrial tRNA genes yet the tRNA import in these groups can still be observed. The occurrence of this putatively redundant import and the fact that tRNA import is widely represented could indicate that mitochondrial tRNA import is derived from the ancestor of all eukaryotic organisms and diverse pathways and numbers of imported tRNAs are due to the evolution of one, conserved pathway [141].

Prior to import into mitochondria, tRNAs must undergo a number of processing and targeting steps. After transcription in the nucleus tRNAs undergo various modifications such as 5' and 3' processing, addition of CCA terminus and aminoacylation. Subsequently they are exported from the nucleus into the cytosol, where they interact with multiple proteins, and are diverted from the cytosolic protein biosynthesis machinery and targeted to mitochondria [142, 143].

Mechanisms of tRNA import in yeast

Despite the fact that the yeast mitochondrial genome is predicted to encode a full set of tRNA genes, it has been demonstrated that a fraction of the $tRNA^{Lys}$ is imported from the cytosol. While $tRNA^{Lys}$(CUU) is imported into yeast mitochondria, the isoacceptor $tRNA^{Lys}$(UUU) remains in the cytosol [144]. The mechanism of $tRNA^{Lys}$(CUU) import in yeast has been well described. The targeting of $tRNA^{Lys}$(CUU) is dependent on enolase 2 (Eno2p), which binds it specifically and guides to mitochondria. Subsequently this tRNA-Eno2p complex binds to the precursor of mitochondrial lysyl-tRNA synthetase (pre-LysRS) and is co-imported via the general protein import pathway [145, 146]. Interestingly, it has been shown *in vitro,* that $tRNA^{Lys}$(CUU) rearranges its conformation while being associated with the targeting complex. Instead of a classic L-form of tRNA, the 3' end is in close proximity to the TΨC loop [147]. Mitochondrial genome of yeast encodes for $tRNA^{Lys}$(UUU), which is capable of decoding both of the lysine codons, hence import of the cytosolic $tRNA^{Lys}$(CUU) seems redundant. However,

it has been demonstrated that in stress conditions such as temperature of 37°C it becomes essential for growth [148]. Recent genetic and biochemical studies have identified three novel components of the $tRNA^{Lys}$(CUU) import pathway: Rpn13, Rpn8 and Doa1, which have been shown to interact with tRNA and the pre-LysRS and regulate this import pathway [149]. On the other hand a recent study showed that $tRNA^{Lys}$(CUU) import in yeast can occur independent of LysRS *in vivo*, which suggests an alternative mechanism for the import of this tRNA species in yeast [150].

Import of $tRNA^{Gln}$(CUG) and $tRNA^{Gln}$(UUG) into yeast mitochondria has been recently observed however it seems to engage a different import mechanism [151]. The import of $tRNA^{Gln}$(CUG) and $tRNA^{Gln}$(UUG) into isolated mitochondria has been demonstrated to occur independent from membrane potential and any cytosolic factors. Immunofluorescence experiments confirmed the presence of both cytosolic $tRNA^{Gln}$ and the cytosolic glutaminyl synthetase (GlnRS) [151]. This would suggest that yeast evolved more than one independent pathway of tRNA import and unlike other eukaryotes, their mitochondria do not synthesize $tRNA^{Gln}$ via the transamidation pathway [152].

Mechanisms of tRNA import in mammals

It has been demonstrated that mammalian mitochondria are also able to import tRNAs despite encoding a complete set of mitochondrial tRNA genes. *In vivo* localization of imported tRNA species was shown, when nuclear-encoded $tRNA^{Gln}$(CUG) and $tRNA^{Gln}$(UUG) have been found in RNA fractions extracted from rat and human mitochondria. *In vitro* import experiments suggest that import is specific to tRNAs, requires ATP, but is independent from a membrane potential. Thus, $tRNA^{Gln}$ import into mitochondria in mammals engages a pathway, which is independent from the protein import pathway [153].

Mechanisms of tRNA import in protozoa

Mitochondrial genomes of protozoans such as *Trypanosoma bruce*i and *Leishmania spp*. have been predicted to be devoid of tRNA genes hence all of the tRNAs present in their mitochondria must be imported from the cytosol [154]. It has been proposed that tRNA itself can determine whether it will engage the cytosolic translation or be imported into mitochondria. Two closely related tRNA

molecules: $tRNA^{Met}$ initiator and $tRNA^{Met}$ elongator were shown to have a different localization in the cell due to their specific subregions of the T stem [155]. Studies have shown that T stem localization signal is most likely present in all tRNAs in trypanosomes. It has been shown that $tRNA^{Met}$ initiator binds the eukaryotic translation initiation factor 2 (eIF2) in the cytosol, which prevents it from being targeted to mitochondria whereas $tRNA^{Met}$ elongator binds to the eukaryotic translation elongation factor 1a (eEF1a), which is a prerequisite to target this tRNA to mitochondria in *T. brucei* [156]. It is currently unknown how tRNAs are traversed across the two mitochondrial membranes in trypanosomatids, however a study has shown that VDAC knockout cells of *T. brucei* import tRNAs as efficiently as their wild type counterparts suggesting that porin is not responsible for this process [157]. It has been also demonstrated that ATP is a requirement for tRNA import in trypanosomatids [158, 159], however membrane potential is not [160]. Recent *in vivo* study provided evidence that two components of the protein import machinery, Tim17 and Hsp70, may be involved in the translocation of tRNA across the inner membrane in *T. brucei* [161].

An RNA import complex (RIC) has been described in *Leishmania tropica.* It has been reported that RIC consists of 11 subunits and can drive the ATP-dependant import of tRNAs into phospholipid vesicles [162, 163]. To explore the possibility of this mechanism being conserved among other trypanosomatids, the Rieske subunit of complex III (RIC6) from *T. brucei* was studied [164]. The RNAi knockdowns of RIC6, both *in vivo* and *in vitro*, showed no effect on the tRNA import rate. Moreover, RIC6 has been shown to be crucial in respiration and membrane potential maintenance [164]. Interestingly, the bloodstream stage of *T. brucei*, which relies on glycolysis, has been shown to be capable of tRNA import [165, 166]. These findings corroborate previous observations, that respiratory subunits and membrane potential are not involved in tRNA import in trypanosomatids [158, 160, 165]. The nature of the RIC complex in *L. tropica* remains questionable and is currently under scrutiny [167].

Mechanisms of tRNA import in plants

All species of plant mitochondria import tRNA however the number of different imported tRNA species varies greatly among species [168-170]. A study

showed that a single nucleotide change in $tRNA^{Ala}$, which was previously shown to inhibit the aminoacylation of $tRNA^{Ala}$ by the alanyl-tRNA synthetase (AlaRS), could inhibit the import of tRNAs into plant mitochondria indicating that AlaRS could be involved in the import mechanism [171]. The number of tRNAs imported into mitochondria of *Chlamydomonas reinhardtii*, at least for a subset of tRNA molecules, corresponds to the codon usage in mitochondrial translation [172]. It has been reported that *in vitro* import of tRNA is an ATP- and membrane potential-dependent process in *Solanum tuberosum*, however it doesn't require cytosolic factors. [173]. The voltage-dependent anion channel (VDAC) has been suggested as the major component of the translocation process of tRNAs in plant mitochondria. It has been demonstrated that VDAC antibodies as well as the VDAC inhibitor, ruthenium red, can inhibit the tRNA import *in vitro*. Further experiments using specific antibodies showed that TOM20 and TOM40 proteins could be involved in recognizing the tRNA and act as receptors of this process [174]. Addition of a synthetic presequence negatively influenced the import of proteins but not the import of tRNAs into isolated mitochondria [174]. It is clear that there is a connection between the protein import and the tRNA import machinery in plant mitochondria, however the fact that cytosolic factors are not essential and that tRNA doesn't compete with the protein import pathway suggests that tRNAs might be imported through a different mechanism.

1.3 Mitochondrial Outer Membrane

The mitochondrial outer membrane acts as the interface between the mitochondrion and the cytosol and is a mediator of intracellular signalling, transport of small molecules and the import of macromolecules such as proteins and RNAs, membrane biogenesis, mitochondrial morphology and cell death. It is a smooth, highly porous membrane, which allows the passive transport of molecules not larger than 5 kDa [19]. Larger molecules are transported actively through specific protein pores whereas macromolecules such as proteins and RNAs are imported through specialized translocons as described above.

The lipid composition of the mitochondrial outer membrane is similar to other membranes. The major phospholipids are phosphatidylcholine (PC) - 40 %,

phosphatidylethanolamine (PE) - 30 %, phosphatidylinositol (PI) and phospatidylserine (PS) - 5 %. Unlike other membranes, mitochondrial membranes also consist of phosphatidylglycerol (PG) and cardiolipin (CL) [175, 176]. While enzymes present in mitochondria synthesize CL, PE and PG; PI, PC and PS are synthesized in the ER and therefore must be imported between the membranes. This process takes place in mitochondria-associated membranes of ER (MAM) [177].

The protein composition of the mitochondrial outer membrane has been studied in yeast, *Neurospora crassa* and recently in *Trypanosoma brucei* [178-180]. These studies identified 82, 30 and 82 outer membrane proteins respectively. In plants 42 mitochondrial outer membrane proteins have been identified by quantitative shotgun mass spectrometry of highly enriched mitochondria from Arabidopsis [181], 27 of which haven't been observed to localise in mitochondria. Identified proteins range from proteins specific to plants with undescribed functions to putative morphology and signalling components. The study showed complexity of biogenesis and function of plant mitochondria but also the extent, to which the composition of plant mitochondrial outer membrane changed between the bacterial ancestor and the present organelle. The comparison of the *Escherichia coli* outer envelope proteins to that of Arabidopsis mitochondrial outer membrane showed, that a significant number of proteins was lost during evolution. Proteins such as specific nutrient uptake β-barrel proteins, lipoproteins and lipopolysaccharide (LPS) trafficking proteins are no longer present in plant mitochondria, which reflects the changes in environment of the endosymbiont. Four VDAC isoforms, TOM40 and SAM50 proteins are the sole mitochondria outer membrane proteins retained from the bacterial ancestor (reviewed in [182]). Majority of the 42 Arabidopsis mitochondrial outer membrane proteins seem to be of the host origin and their function has not been elucidated making it an excellent platform for future research.

1.4 Project Proposal and Aims

Plant mitochondria represent a fascinating model of mitochondrial biogenesis and evolution. Whilst many of the components of the protein import

apparatus and other processes such as morphology and distribution have been identified by their direct orthology to the well-characterised yeast and mammalian models, it is increasingly apparent that several plant specific differences exist.

Previous studies within the laboratory had identified several novel plant specific outer mitochondrial membrane proteins. Therefore, it was this project's aim to functionally characterise several of these candidates as detailed below:

a) To functionally characterise two mitochondrial outer membrane proteins encoded by At3g49560 and At5g24650 genes. These proteins belong to the preprotein and amino acid transporter (PRAT) family and previous studies have suggested that they are dual-targeted to both mitochondria and chloroplasts [183] in addition to being located on the mitochondrial outer membrane. Unlike other PRATs, these two proteins also contain the sterile alpha motif (SAM) domain, which previously shown to be implicated in protein-protein interaction and RNA binding. The combination of these two domains is specific to plants therefore they were chosen for functional characterisation.

b) To functionally characterise the novel, plant specific β-barrel protein encoded by At3g27930. This protein has been previously identified as a novel outer mitochondrial membrane protein by proteomic analysis predicted to belong to the Porin3 superfamily. This superfamily also contains proteins of vital importance in mitochondrial outer membrane such as VDAC and Tom40, which are highly conserved throughout all species and thus the plant specific protein encoded by At3g27930 is of significant interest to determine what plant specific role could have diverged or have been acquired throughout evolution.

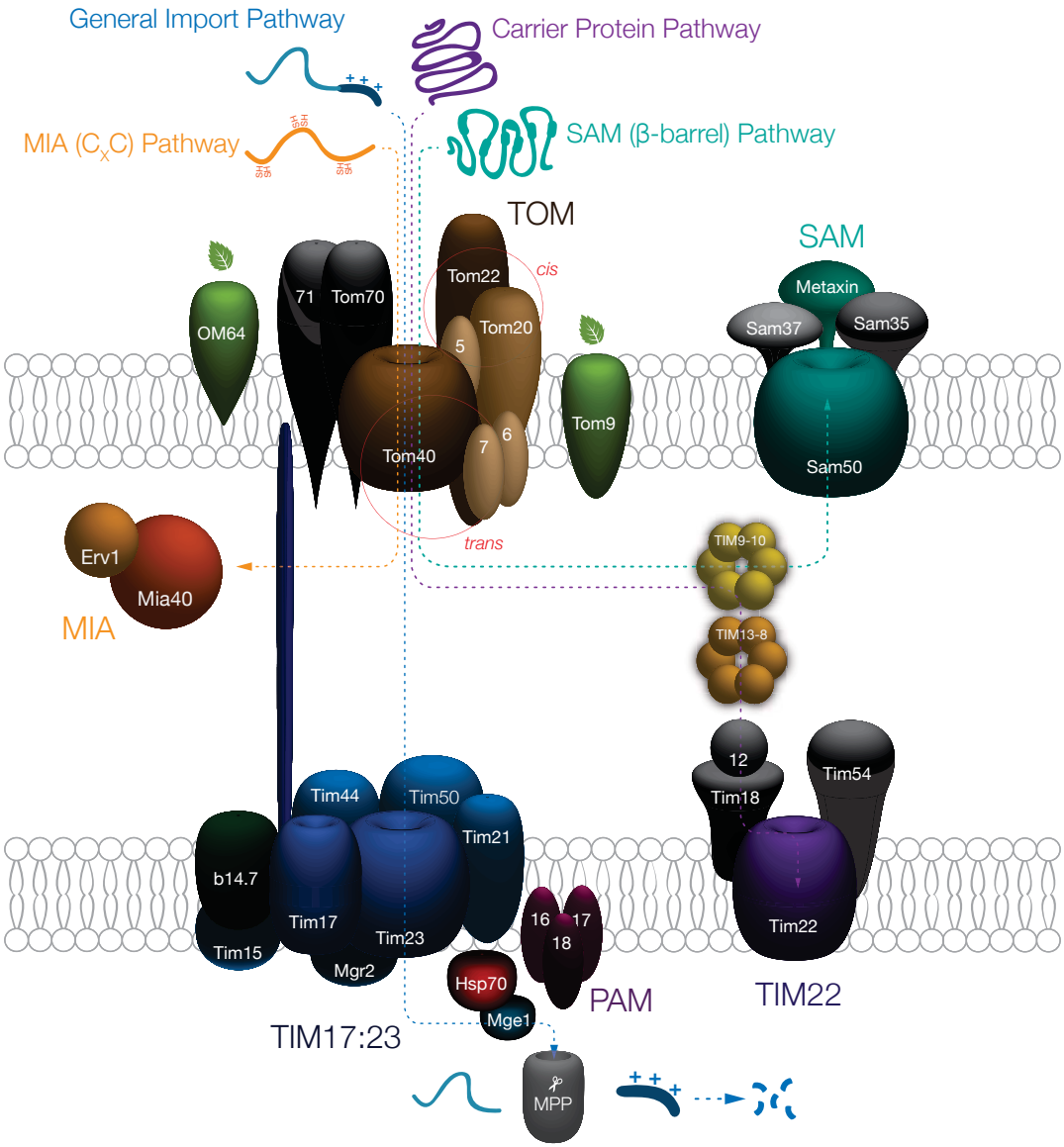

Figure 1.1 Mitochondrial protein import machinery

A schematic representation of the mitochondrial protein import machinery. Plant specific protein import components are indicated by 🍃. The major import pathways are indicated. Protein precursors initially pass through the Translocase of the Outer Membrane (TOM) complex. Insertion of β-barrel proteins into the outer membrane occurs via the Sorting and Assembly Machinery (SAM). Carrier Protein pathway proteins translocate into the inner membrane via the small TIMs (TIM9-10 and TIM13-8) through to the TIM22 complex. Cysteine rich proteins of the IMS are imported via the MIA pathway (Mitochondrial Intermembrane space and Assembly). Proteins located in the matrix and containing an N-terminal cleavable presequence are translocated via the TIM17:23 channel. The presequence is removed via Mitochondrial Processing Peptidase (MPP) and the subsequent transit peptide is degraded by matrix-located peptidases.

Material and methods

Chapter 2 - Material and methods

2.1 Materials

2.1.1 Plant growth and media

Arabidopsis thaliana (Arabidopsis), ecotype Columbia (Col-0) plants were used in this study. Seeds were planted on Murashige and Skoog (MS) medium plates (30 g/l (w/v) sucrose, 4.3 g/l (w/v) MS powder, 0.5 g/l 4-morpholineethanesulfonic acid (MES) and 1 ml/l of Gamborg B5 vitamins). Seeds were stratified for 48h at 4°C and grown for 14 days at 22°C under lamps of 100 umol m^{-2} s^{-1} light intensity in a long day (16 hour day/8 hour night) photoperiod. Tissue was harvested and used for isolation of mitochondria, chloroplasts and for plate-based phenotyping.

Alternatively seeds were planted on soil mix consisting of grade 2 vermiculite, perlite and soil in 1:1:3 ratio. Seeds were stratified at 4°C for 48 h and grown at 22°C under lamps of 100 umol m^{-2} s^{-1} light intensity in a long day (16 hour day/ 8 hour night) photoperiod. Plants were used for bulking of seed, *Agrobacterium*-mediated transformation and dark induced senescence assays as well as reactive oxygen species (ROS) determination, starch determination assays and soil-based phenotyping.

2.1.2 Bacterial growth and media

Lysogeny broth (LB) media for bacterial growth (10g/l tryptone peptone, 10 g/l NaCl, 5 g/l yeast extract) were sterilized by autoclaving. Agar plates were prepared by adding 15g/l of agar before the sterilization. Bacterial cultures were grown in 37°C unless stated otherwise.

2.1.3 Bacterial strains

DH5α: F– Φ80*lac*ZΔM15 Δ(*lac*ZYA-*arg*F) U169 *rec*A1 *end*A1 *hsd*R17 (rK–, mK+) *pho*A *sup*E44 λ– *thi*-1 *gyr*A96 *rel*A1

Bl21 (DE3) pLysS: F^-, *ompT*, $hsdS_B$ (r_B^-, m_B^-), dcm, gal, λ(DE3), pLysS, (Cam^R)

Rosetta2 (DE3) pLysS: F^-, *ompT*, $hsdS_B$ (r_B^-, m_B^-), *gal dcm* (DE3) pLysSpRARE2[3] (Cam^R)

2.1.4 Yeast growth and media

Yeast peptone dextrose (YPD) media for yeast growth (20 g/l Difco peptone, 10 g/l yeast extract) were sterilized by autoclaving followed by addition of filter-sterilized 40 % (w/v) glucose solution to the final concentration of 2 % (v/v) glucose. Agar plates were prepared by addition of 20g/l of agar before sterilization. Yeast cultures were grown at 30°C.

Synthetic defined (SD) media for yeast selection (6.7g/l yeast nitrogen base without amino acids, 0.6 g/l amino acid dropout powder (Clontech, Mountain View) were sterilized by autoclaving followed by addition of filter-sterilized 40 % (w/v) glucose solution or sterile 40 (v/v) glycerol to the final concentration of 2 % (v/v) or 2.5 % (v/v) respectively. Yeast cultures were grown in 30°C for 3-5 days depending on the experiment.

2.1.5 Yeast strains

Wilde type strain, BY4742:
MATα, *his3Δ1*; *leu2Δ0*; *lys2Δ0*; *ura3Δ0*

ScVDAC1(-) mutant strain, YNL055c (*por*):
MATα, *his3Δ1*; *leu2Δ0*; *lys2Δ0*; *ura3Δ0*; UNL055c::kanMX4

2.1.6 Sterile distilled water

Sterile water (MQ) was prepared by double deionization and filtering through the Millipore Milli-Q plus® ultra pure water system (Millipore, Sydney). Alternatively the molecular grade DNase and RNase free water (MP Biomedicals, Solon, Ohio) was used.

2.1.7 Seed sterilization protocols

Arabidopsis seeds were sterilized using the gas sterilization method. Aliquots of 50-100 µl of seeds were placed in a desiccator together with a beaker filled with 50 ml of bleach. In order to start the sterilization, 3 ml of concentrated HCl was added to bleach, which caused the production of chlorine gas. Desiccator was closed immediately and seeds were sterilized for 3 h. Alternatively the ethanol method was used. Aliquots of 50 µl of seeds were treated with 1 ml of sterilization solution (0.05 % (v/v) Triton X-100 in 70 % (v/v) ethanol) for 5 min on a rotary spinner. Tubes were moved to the laminar flow and seeds were washed once with 1 ml of 70 % (v/v) ethanol and once with 1 ml of 100 % (v/v) ethanol, which was removed prior to drying. Seeds were left in the tube to dry or resuspended in 100 % (v/v) ethanol and transferred on a sterile Whatman paper filters to dry.

2.2 Bioinformatic analysis

2.2.1 Protein sequence analyses

Amino acid sequences of studied proteins were retrieved from The Arabidopsis Information Resource (TAIR, http://www.arabidopsis.org/) TAIR 10 genome release. Alignments of sequences were generated using ClustalW2 - Multiple Sequence Alignment tool (http://www.ebi.ac.uk/Tools/msa/clustalw2/) set to default settings. Shading of the alignment was carried out using BOXSHADE 3.21 (http://www.ch.embnet.org/software/BOX_form.html). Protein domains were predicted using The Conserved Domain Database (CDD) (http://www.ncbi.nlm.nih.gov/Structure/cdd/wrpsb.cgi) [184]. Transmembrane alpha-helices were predicted using Dense Alignment Surface (DAS) prediction tool (http://www.sbc.su.se/~miklos/DAS/) [185]. The β-strands were predicted using the transmembrane strands and topology of beta-barrel outer membrane protein prediction web server - PRED TMBB (http://bioinformatics.biol.uoa.gr/PRED-TMBB/) based on a Hidden Markov Model [186]. Protein sequence identity and similarity scores were estimated using the Matrix Global Alignment Tool (MatGAT) v2.01 [187].

2.2.2 Phylogenetic analysis

Orthology study was performed by protein sequence homology search using basic local alignment search tool (BLASTP) [188] against following species in their respective databeses: *Homo sapiens* (human, http://www.hprd.org), *Caenorhabditis elegans* (roundworm http://www.wormbase.org), *Neurospora crassa* (mould, http://www.ncbi.nlm.nih.gov), *Dictyostelium discoideum* (slime mould, http://dictybase.org/) and *Saccharomyces cerevisiae* (budding yeast http://www.yeastgenome.org), Phytozome v9.1 (http://www.phytozome.net/) for *Brassica rapa* (Br), *Capsella rubella* (Cr), *Chlamydomonas reinhardtii* (Cr), *Cucumis sativus* (Cs), *Eucalyptus grandis* (Eg), *Glycine max* (Gm), *Medicago truncatula* (Mt), *Oryza sativa* (Os), *Physcomitrella patens* (Ps), *Populus trichocarpa* (Pt), *Ricinus communis* (Rc), *Selaginella moellendorfii* (Sm), *Solanum tuberosum* (St), *Vitis vinifera* (Vv), *Volvox carteri* (Vc), and *Zea mays* (Zm) for higher plants and green algae; Cyanidioschyzon merolea Genome Project (http://merolae.biol.s.u-tokyo.ac.jp/) for *Cyanidioschyzon merolea* (red algae) and Online resource for community annotation of eukaryotes OrcAE (http://bioinformatics.psb.ugent.be/orcae/overview/Ectsi) for *Ectocarpus siliculosus* (brown algae). Direct orthologs of studied proteins were identified using the threshold of e-value lower than $1e^{-10}$. For proteins exhibiting high conservation to other known protein families the threshold was raised to $1e^{-50\text{-}100}$. Phylogenetic analysis was generated using MEGA 5.2.2 [189]. The alignment of full-length protein sequences was generated using Clustal option. Generation of the phylogenetic tree was carried out using the maximum likelihood tree setting according to the Jones-Thornton-Taylor model after 1000 replications.

2.3 Cloning protocols

2.3.1 RNA isolation protocol

Total RNA from Arabidopsis tissue was isolated using the RNeasy Plant mini kit (Qiagen, Sydney) according to the manufacture's instructions. In a standard RNA isolation about 100 mg of tissue was ground to a fine powder in the presence of liquid nitrogen using a sterile mortar and pestle. The RNA was eluted in molecular grade DNase and RNase free water and analysed on the agarose gel

prior to reverse transcription and PCR. Quantification was performed by measuring the absorbance at 260 nm of 1 µl of RNA on a Nanodrop spectrophotometer (Thermo Scientific, Melbourne).

2.3.2 cDNA synthesis protocol

The first strand cDNA was synthesized by reverse transcription of the total RNA using the SuperScript™ III Reverse Transcriptase (Invitrogen, Melbourne) according to manufacturer's instructions. Generally 1-5 µg of total RNA was used with oligo $(dT)_{12-18}$ primers.

2.3.3 Yeast genomic DNA isolation protocol

The yeast genomic DNA (gDNA) was isolated according to the method described in [190]. A 100-200 µl liquid yeast culture (OD_{600} = 0.4) was centrifuged and the supernatant was discarded. Cells were resuspended in 100 µl of 200 mM lithium ethanoate (LiOAc), 1 % (w/v) sodium dodecyl sulphate (SDS) solution and incubated in 70°C for 5 min followed by addition of 300 µl of 96-100 % (v/v) ethanol. The reaction was centrifuged for 3 min at 15 000 x g and the pellet was washed in 70 % (v/v) ethanol. The washed pellet was dissolved in 100 µl of molecular grade water, centrifuged for 15 sec at 15 000 x g to pellet the debris and resulted supernatant containing yeast gDNA was transferred to a fresh tube and used for amplification of yeast coding sequences.

2.3.4 Restriction enzyme digestion

Restriction enzyme digestion was performed by adding 10 units of enzyme per 1000 ng of DNA in a total reaction volume of 20 µl. Reaction was assembled on ice and incubated for 2 h under enzyme specific temperature and buffer conditions. The resulting digestion was visualized by the electrophoresis on an agarose gel.

2.3.5 Bacterial transformation

Plasmids were transformed to chemically competent cells, DH5α (Roche, Sydney), Bl21 (DE3) pLysS or Rosetta2 (DE3) pLysS (Promega, Sydney) using a heat shock protocol. A 50-100 µl of thawed competent cells were incubated with 5-10 µl of DNA (100 ng) for 30 min on ice followed by heat shock at 42°C for 45 s. The cells were returned on ice for 2 min and 200-500 µl of LB or super optimal broth with catabolite respression (SOC) medium was added. The cells were incubated at 37°C for 1 h at 200 revolutions per minute (rpm) and 50-100 µl of transformation reaction was plated on LB agar plates containing the appropriate antibiotics.

2.3.6 Yeast transformation

Several 2-3 mm colonies of BY4742 or YNL055c yeast strains were inoculated into 1 ml of yeast peptone dextrose (YPD), vortexed, transferred to flasks containing 50 ml of YPD and incubated for 16-18 h in 30°C with shaking at 250 rpm to stationary phase of OD_{600} > 1.5. The overnight culture was transferred into flasks containing 300 ml of YPD to produce the final OD_{600} of 0.2-0.3 and further incubated for 3 h in 30°C with shaking at 230-270 rpm until OD_{600} of 0.5 was reached. Cells were placed in 50 ml falcon tubes and centrifuged at 1000 x g for 5 min at room temperature in a swing out rotor. The supernatant was discarded and cells were resuspended in 20 ml of sterile MQ water. Cells were pulled and centrifuged again at 1000 x g for 5 min, the supernatant was discarded and pellets were resuspended in 1.5 ml of freshly prepared sterile 1 x Tris EDTA/lithium acetate (TE/LiAc). Resuspended cells were used in transformation reactions.

A 100 µl aliquot of competent yeast cells was mixed with 10 µl of herring testes carrier DNA (10 mg/ml), which was denatured in 95°C for 10 min prior to the transformation and 100 ng of plasmid DNA of choice. The reaction was mixed with 600 µl of polyethylene glycol/lithium acetate (PEG/LiAc) solution, vortexed at high speed and incubated in 30°C for 20 min with shaking at 350 rpm. The reaction was mixed with 70 µl DMSO followed by heat shock at 42°C for 15 min with occasional agitation of the tube. The reactions were placed on ice for 1-2

min, centrifuged at 1000 x g for 30 sec and resuspended in 0.5 ml of 1 x Tris EDTA (TE).

Finally, the cells (50-200 µl) were plated on selection media and incubated in 30°C for 3-5 days.

2.3.7 Plasmid protocols

Plasmids mini preparations were used to screen colonies after cloning. A 2 ml LB aliquot containing the appropriate antibiotic was inoculated with a single colony and incubated over night at 37°C and shaking at 200 rpm. Cultures were pelleted by centrifugation for 1 min at 14 000 rpm. Plasmid DNA was isolated using the QuickLyse® Miniprep Kit (Qiagen, Sydney) according to manufacturer's instructions. Plasmid concentration was estimated by spectrophotometric measurement using a NanoDrop spectrophotometer.

Plasmid midi preparations were carried out for plasmid constructs used in *in vitro* translations, *in vitro* transcriptions, bacterial protein expression and glycerol stocks. A single colony was inoculated into 40 ml of LB media containing the appropriate antibiotics and incubated over night at 37°C and shaking at 200 rpm. The cultures were pelleted in falcon tubes by centrifugation at 4°C for 15 min at 5 000 rpm. Plasmid DNA was isolated using the QIAGEN Plasmid Midi Kit (Qiagen, Sydney) according to manufacturer's instructions. Plasmid concentration was estimated by spectrophotometric measurement using a NanoDrop spectrophotometer.

2.3.8 Polymerase Chain Reaction (PCR)

PCR was performed using either genomic DNA, cDNA, which was reverse transcribed from mRNA or plasmid DNA. A typical PCR consisted of 1 µl of cDNA or genomic DNA and 20 pmol of forward and reverse primers. Each reaction was assembled on ice using the Platinum High Fidelity PCR system according to manufacturer's instructions (Invitrogen). Typically an amplification reaction consisted of 94°C for 2 min, followed by 35-40 cycles of denaturation at 94°C for 4 min, annealing at 55°C for 30 s and extension at 72°C for 2 min, followed by

cooling to 4 C. The products of amplification were visualized by agarose gel electrophoresis. PCR products for cloning were gel extracted using a QIAquick Gel Extraction Kit (Qiagen, Sydney) according to manufacture's instructions.

Coding sequences of genes of interest were amplified from cDNA libraries using gene specific primers containing Gateway® recombination sites (Apendix I).

2.4 Organelle manipulation protocols

2.4.1 Protein synthesis protocols

2.4.1.1 [^{35}S]-methionine labelled precursor proteins

Radiolabelled precursor proteins were *in vitro* transcribed and translated using the TNT® Coupled Transcription Translation Rabbit Reticulocyte system (Promega, Melbourne). The reaction (reticulocyte lysate, RNA polymerase, amino acids, buffer, RNase inhibitor and [^{35}S]-labelled methionine) was assembled on ice in an eppendorf tube. Plasmid DNA (0.2-0.4 µg) was added and reaction incubated at 30°C for 2 h, after which 2 µl of the reaction was removed for a subsequent sodium dodecyl sulphate-polyacrylamide gel electrophoresis (SDS-PAGE) analysis (see Section 2.4.1). Remaining sample was stored at -80 C.

2.4.1.2 Protein expression and purification

Small Scale (Test) Expression: Bacterial strain Bl21 (DE3) pLyS was transformed with appropriate plasmid encoding wanted recombinated (purification tag containing, typically a 6xHis tag) protein. A single colony was inoculated into 2 ml of LB media containing appropriate antibiotics and incubated over night at 37 °C and 1400 rpm. The next day 100 µl of the preculture was moved to a fresh 2 ml of LB containing selection antibiotic. The culture was incubated at 37°C at 1400 rpm for 1 h followed by removing 100 µl of the culture (sample before the induction) and adding 2 µl of 1 M IPTG to induce the expression. After the induction 100 µl samples were taken from the culture every hour for 4 h. All samples were pelleted and pellets were resuspended in loading buffer and analysed by SDS-PAGE.

Large Scale Expression: Single colony was inoculated into 50 ml of LB containing appropriate antibiotics and incubated over night at 37°C and 220 rpm. The next day, the preculture was used to inoculate 500 ml of fresh LB containing appropriate antibiotic and incubated at 37°C and 220 rpm. After 1 h the culture was induced by adding 500 µl of 1 M IPTG. After 4 h incubation the culture was pelleted at 8 000 g for 10 min at 4 C. Pellet was used for protein purification by means of denaturing or native immobilized metal ion affinity chromatography (IMAC) using Profinia™ Protein Purification system (Biorad, Sydney).

Denaturing lysate preparation: The weight of the bacterial pellet was determined and pellet was resuspended in 10 volumes of the denaturing IMAC wash buffer 1 (6 M Urea, 300 mM KCl, 50 mM KH_2PO_4, 5 mM imidazole, pH 8.0). To lyse the bacterial cell, the resuspended pellet was sonicated on ice (25 % output, 4 times at 1 min interval) followed by centrifugation at 16 000 g for 20 min at 4°C to clarify the lysate. Pellet was discarded while the supernatant was filtered through a 0.8 um Milipore filter. The clarified lysate was inserted into Profinia.

The purification was carried out according to manufacturer's instructions. Purified protein was used to generate an antibody (denaturing IMAC) or to generate the shuttle protein for import assays (native IMAC).

2.4.2 RNA synthesis protocols

2.4.2.1 [^{32}P]-labelled tRNA^{Ala} synthesis

Radiolabelled tRNA^{Ala} probes were *in vitro* transcribed using the Riboprobe® System-T7 kit (Promega, Melbourne). The synthesis reaction (buffer, T7 polymerase, ribonucleotides, RNase inhibitor, BstNI-digested plasmid DNA encoding tRNA for Alanine and an [α-^{32}P] uridine 5'-triphosphate) was assembled on ice in an eppendorf tube and incubated for 2.5 h at 37 C. After the incubation 1 µl of DNase RQ1 was added and incubated for 15 min followed by addition of 40 µl of MQ water. Free radioactivity was eliminated by spinning down the reaction through a G-25 Sephadex column according to manufacturer's instructions (Roche, Sydney).

To test the radiolabelled probe, 2 µl of the reaction was resolved on a denaturing (7 M Urea) 15 % polyacrylamide gel (Section 2.5.1). The gel was fixed

in 20 % (v/v) ethanol and 10 % (v/v) acetic acid solution and dried for 2 h. After drying, the gel was exposed in the phosporimaging cassette for an hour to test the probe before import.

2.4.3 Mitochondrial isolation protocols

The protocol used for isolation of mitochondria from Arabidopsis seedlings was based on methods by [191]. All mitochondrial isolation steps were performed at 4°C and centrifugations were carried out using Beckman AvantiJ26XP or AvantiJ301 (Beckman Coulter) with a JA-25.50 rotor unless otherwise stated.

Two-week old seedlings growing on MS plates (approximately 200 µg of seeds), were collected on the day of the prep and ground using a mortar and a pestle at 4°C, in grinding medium (0.3 M sucrose; 25 mM tetrasodiumpyrophosphate; 2 mM EDTA (disodium salt); 10 mM KH_2PO_4; 1 % (w/v) BSA; pH 7.5) followed by filtering using 4 layers of disposable and one layer of tough miracloth into a conical flask. Any solid material was reground. The filtered homogenate was transferred to 6-8 prechilled 50 ml centrifuge tubes and centrifuged for 5 min at 2 500 g, 4°C. Supernatant was transferred to fresh tubes and centrifuged for 20 min at 17 500 g, 4°C. The supernatant was discarded while the pellet was dispersed in residual buffer followed by addition of 1 ml of 1 X wash medium (0.3 M sucrose; 10 mM TES; 1 % (w/v) BSA; pH 7.5). Pellets from 4 tubes were combined into one, filled with 1 X wash buffer and two-centrifugation step was repeated.

The PVP Percoll gradient was assembled using a gradient former (Bio-Rad, model 485) and a peristaltic pump (Gilson, Miniplus 2) by mixing 4.4 % (w/v) PVP heavy gradient solution (17.5 ml 2 X wash buffer, 9.8 ml Percoll, 7.7 ml 20 % (w/v) PVP-40) and a light gradient solution (17.5 ml 2 X wash buffer, 9.8 ml Percoll, 7.7 ml MQ water). Crude mitochondrial fraction was layered over a 0-4.4 % (w/v) PVP Percoll gradient using a Pasteur pipette and centrifuged at 40 000 g for 40 min at 4°C without breaks off, resulting in the separation of mitochondria from chloroplasts and thylakoids. Typically mitochondria formed a yellow band in the lower section of the gradient or located in the heavy solution on the bottom of the gradient in a form of a cloud. The upper sections of the gradient were removed by

aspiration and the mitochondrial fraction was removed using a Pasteur pipette. The mitochondrial fraction was washed twice using 1 X wash buffer by centrifugation at 31 000 g for 15 min with slow deceleration. The mitochondrial pellet was collected and kept on ice and used immediately in the import assays.

2.4.4 *In vitro* import assays

2.4.4.1 Import of precursor proteins into plant mitochondria

Import of radiolabelled precursor proteins was performed according to methods described by [192]. Freshly isolated mitochondria (100 µg) were incubated in an import reaction mix (0.3 M sucrose; 50 mM KCl; 10 mM Mops; 5 mM KH_2PO_4; 0.1 % (w/v) BSA, 1 mM $MgCl_2$; 1 mM methionine; 0.2 mM ADP; 0.75 mM ATP; 5 mM succinate; 5 mM DTT; 5 mM NADH; 5 mM GTP) in an eppendorf tube for 3 min on ice, followed by addition of 10 µl of thawed radiolabelled precursor protein. The reaction was incubated at 25 °C for 20 min at 350 rpm.

Placing the reaction on ice terminated the protein import. Typically reaction was split to 2 aliquots, of which 1 was treated with 50 µg of proteinase K (pK) in order to digest any precursor protein, which hasn't been imported to mitochondria or was bound to the outer mitochondrial membrane. In order to inhibit pK digestion, 1 µl of 100 mM PMSF was added to the pK-treated reaction. The mitochondria were pelleted by centrifugation at 20 000 g for 3 min at 4°C. Pellets were resuspended in sample buffer (SB) - 2 X Laemmli buffer (125 mM Tris-HCl, pH 6.8; 4 % (w/v) SDS, 3 % (v/v) glycerol, 20 % (v/v) B-mercaptoethanol, 0.05 % (w/v) bromophenol blue) and boiled fro 3 min. The denatured mitochondrial proteins were resolved on a 12 % or 16 % polyacrylamide gel (SDS PAGE); gels were dried and exposed to a phosphorimaging plate for 24 h (Section 2.5.1).

2.4.4.2 Import of tRNA into plant mitochondria.

Import of radiolabelled Arabidopsis [^{32}P]-$tRNA^{Ala}$ was carried out according to methods described by [193]. Freshly isolated mitochondria were incubated in the import reaction mix described in section 2.3.4.1 for 3 min on ice. The reaction

was then incubated with 4 µg of purified pDHFR shuttle protein for 5 min on ice. Finally 4 µl of the radiolabelled [^{32}P]-tRNA^{Ala} was added to reaction (approximately 4 000 cpm) and incubated for 20 min at 25 C, 350 rpm. After the incubation, reaction was put back on ice and treated with 100 µl of RNase mix (50 µg/ml RNase A; 375 U/ml RNase T1 in 1 X wash buffer) in order to eliminate any tRNA molecules, which bound to the mitochondrial outer membrane or haven't been imported. Reactions were treated with 800 µl of STOP solution (300 mM sucrose; 5 mM EDTA, 5 mM EGTA, 1 % (w/v) BSA). Reactions were centrifuged at 9 000 rpm for 4 min in the aeresol-tight benchtop centrifuge. Supernatant was discarded and the wash procedure was repeated 2 times by addition of 1 ml of the STOP solution. Pellet was washed 3 times in order to eliminate the residual RNases. Washed pellet was treated with 100 µl of tRNA extraction buffer (10 mM $MgCl_2$; 10 mM Tris-HCl, pH 7.5; 2.5 % SDS; 10 mM EDTA; 10 mM EGTA) and 100 µl of phenol, added immediately after and mixed by fast pipetting followed by shaking on a vortex for 10 min. Extraction reactions were centrifuged at 13 000 rpm for 10 min at 4 °C and aqueous phase (top layer) containing extracted tRNA was recovered and transferred to eppendorf tubes containing 250 µl of 100 % ethanol and 4 µl of 5 M NaCl. The tubes were stored in -20 °C over night in order to precipitate the tRNA. Followed the precipitation, tubes were centrifuged at 13 000 rpm for 25 min at 4°C. Ethanol was removed and tubes were left in room temperature (RT) for 10 min to ensure all remaining ethanol evaporated. Samples were resuspended in 20 µl of tRNA loading buffer (95 % (v/v) formamide; 20 mM EDTA; 0.05 % bromophenol blue; 0.05 % xylen cynol) and incubated at 60 °C for 2 min. Samples were resolved on a denaturing (7 M Urea) 15 % polyacrylamide gel with a diluted radiolabelled transcript (1 µl of 1 000 cpm) as a size control. Gel was fixed in the solution of 20 % (v/v) ethanol and 10 % (v/v) acetic acid, dried and exposed in the phosphorimaging cassette for 48 h (Section 2.5.1).

2.4.5 Mitoplast preparation

Rapture of the mitochondrial outer membrane was carried out by creating an osmotic shock. This allowed pK treatment to access the inner membrane and the inter membrane space. Following or before the import assay, mitochondria were centrifuged at 10 000 rpm at 4 °C for 5 min. Pellets were resuspended in 10

µl of SEH buffer (0.25 mM sucrose; 1 mM EDTA; 10 mM Hepes-KOH, pH 7.4) and 155 µl of 20 mM Hepes-KOH, pH 7.4 was added. Reactions were mixed and incubated for 15 min on ice followed by addition of 25 µl of sterilized 2 M sucrose and 10 µl 3 M KCl. Reactions were mixed and incubation on ice was continued for 30 min. Reactions were centrifuged at 10 000 rpm at 4 °C for 5 min and resulting pellets were used for gel analysis or for *in vitro* import assays depending on the experiment.

2.4.6 Mitochondrial pK titration

Freshly isolated mitochondria were treated with proteinase K (pK) prior to *in vitro* import assays. The mitochondrial pellets were resuspended in 1 ml of 1 X wash buffer. Resuspended mitochondrial pellets were treated with 0, 0.4, 2, 4 and 8 µg of pK for 30 min on ice. The pK reactions were stopped by the addition of 1 µl of 100 mM PMSF. The reactions were washed with 1 X wash buffer by centrifugation twice at 1 000 rpm for 5 min and once at 10 000 rpm for 10 min. The final pellet was resuspended in SB and used for Western blot (WB) or 1 X wash buffer and used for *in vitro* import assay.

2.4.7 Chloroplast isolation protocol

The Arabidopsis chloroplast isolation was performed according to the method described in [194]. Two week-old seedlings were collected from MS plates, which were placed in darkness the night before the isolation. Seedlings were collected using a sharp razor blade and homogenized with a Polytron mixer (13 mm rotor) at low speed (setting 2/3) for 1-2 sec in 25 ml of ice-cold isolation buffer (0.3 M sorbitol; 5 mM $MgCl_2$ x 6 H_2O; 5 mM EDTA; 20 mM HEPES-KOH; 10 mM $NaHCO_3$; 50 mM ascorbic acid; pH 8.0). The homogenate was filtered through a single layer of gaze and the recovered material was homogenized three more times resulting in four 25 ml homogenate aliquots. The tissue was discarded and the homogenate was centrifuged in 4 °C for 4 min at 3000 rpm. The supernatant was discarded and the pellet was carefully resuspended in approximately 1 ml of residual isolation buffer and overlayed on the Percoll

gradient followed by centrifugation in 4 °C for 6 min at 3500 rpm in a swing-out rotor with slow breaks.

The Percoll gradient was prepared in 15 ml centrifuge tubes and consisted of 3 ml of lower layer solution and 7 ml of upper layer solution. The Percoll solution (95 % (v/v) Percoll; 3 % (w/v) PEG 6000; 1 % (w/v) Ficoll; 1 % (w/v) BSA) and the gradient mix (25 mM HEPES-KOH; pH 8.0; 10 mM EDTA; 5 % (w/v) sorbitol) were prepared on the day of the isolation and stored on ice or stored frozen in -20°C. The lower layer solution (2.55 ml Percoll solution, 0.45 ml gradient mix) was placed in the tube followed by overlaying with the upper layer solution (2.1 ml Percoll solution, 4.06 gradient mix; 0.84 ml water).

The lower band containing intact chloroplasts was recovered, by removing the upper layer, and washed in a fresh 15 ml centrifuge tube by filling the tube with wash buffer (50 mM HEPES-KOH; 0.3 M sorbitol; 3 mM $MgSO_4$; pH 8.0) and centrifuging in 4 °C for 4 min at 3000 rpm. The pellet was resuspended in a small volume of wash buffer and the protein concentration was measured according to the method described in section 2.5.4.

2.5 Gel electrophoresis

2.5.1 Polyacrylamide gel electrophoresis

Polyacrylamide gels were assembled using the Bio-Rad PROTEAN II™ system (Bio-Rad, Sydney). In order to assemble the gel for protein analyses a separating component was prepared (375 mM Tris-HCl, pH 8.8, 12 % (w/v) acrylamide, 0.1 % (w/v) SDS, 0.05 % ammonium persulphate (AMPS), 0.05 % (v/v) TEMED) degased for 5 min, poured first and allowed to set. After setting of the separating component, the stacking component was prepared (125 mM Tris-HCl, pH 6.8, 4 % (w/v) acrylamide, 0.1 % (w/v) SDS, 0.05 % (w/v) AMPS, 0.05 % (v/v) TEMED) and poured on the separating component. Before loading, samples were resuspended in 2 X Laemmli buffer and boiled for 3 min. The gels were resolved in a Tris-glycine buffer system (25 mM Tris-HCl pH 8.3, 200 mM glycine, 1 % (w/v) SDS) for 10 h at 10 mA per gel (limited voltage to 250 V) or for 4.5 h at 20 mA per gel (limited voltage to 250 V). The gels, which were not used for Western blotting, were stained in a Coomasie solution (0.1 % (w/v) Coomasie blue

R-250, 40 % (v/v) ethanol, 10 % (v/v) glacial acetic acid) for 2-3 h followed by destaining in 37.5 % (v/v) ethanol, 15 % (v/v) glacial acetic acid, 2.5 % (v/v) glycerol solution for 2 h.

For separation and analyses of tRNAs a denaturing gel (7 M Urea, 15 % (w/v) acrylamide, 1 X Tris/Borate/EDTA (TBE) buffer, 0.4 % (w/v) AMPS, 0.04 (v/v) % TEMED) was used and resolved in 1 X TBE buffer system for 2.5 h at constant voltage of 220 V and 15 mA per gel.

The gels of *in vitro* import assays were dried under the vacuum drier for 2-3 h at 80 °C (Bio-Rad Gel Dryer, model 583, Bio-Rad). Dried gels were wrapped in cling wrap and exposed to phosphorimaging plate (Fuji, BAS-TR2040) in a phosphorimaging cassette (Fuji, 2040) for 24 h (protein gels) or 48 h hours (tRNA gels). The exposed plates were scanned with the phosphorimaging scanner (Bio-Rad, PMI, Personal Molecular Imager).

2.5.2 Blue Native-Polyacrylamide gel electrophoresis (BN-PAGE)

Mitochondrial complexes were solubilized in 5 % (v/v) digitonin in digitonin extraction buffer (30 mM HEPES-KOH, 150 mM potassium acetate, 10 % (v/v) glycerol, pH 7.4) and separated by BN-PAGE according to [195] as described previously [196]. Following the separation gel was transferred onto a polyvinyl difluoride (PVDF) membrane and subjected to immunodetecion. In case of large scale *in vitro* protein import assays, gels were stained with colloidal Coomasie Brilliant Blue, dried and radiolabelled proteins were detected as outlined above.

2.5.3 Agarose gel electrophoresis

For visualization, separation and purification of DNA, the agarose gel electrophoresis was performed. An agarose gel (1 % (w/v) agarose, 1 X Tris/acetic acid/EDTA (TAE) buffer (40 mM Tris-HCl, 1.14 ml/L glacial acetic acid, 1 mM EDTA, pH 8.0) was prepared. In order to visualize DNA, 1 mg/L of ethidium bromide was added to the gel mix before setting. The gels were inserted into a Bio-Rad gel tank containing 1 X TAE buffer. Samples were prepared in 6 X loading buffer (60 mM Tris-HCl, pH 7.5, 6 mM EDTA, 0.06 % (w/v) bromophenol blue, 30

% (v/v) glycerol) and resolved at 80 V for 50 min or before the dye front reached the ¾ of the length of the gel. Resolved samples were visualized using a UV transilluminator (Bio-Rad, .

2.5.4 Coomasie protein assay

Mitochondrial or chloroplast protein was measured by diluting 1 µl of the mitochondrial fraction in 1 ml of 50 % (v/v) of Coomasie® Plus Protein Assay Reagent (Thermo Scientific, Melbourne). The samples were mixed and the absorbance of the reaction was measured at 595 nm. The amount of protein was determined using a bovine serum albumin (BSA) standard curve.

2.5.5 Quantification of import

Quantification of imported radiolabelled proteins was carried out using the Quantity One® 1-D Analysis Software (Bio-Rad, Sydney). The intensity of the radiolabelled protein was determined by measuring the pixel density per mm^2 of the protein band. The highest pixel density was expressed as 1 and the remaining bands expressed relatively.

2.6 Western blotting

2.6.1 Blotting

Proteins resolved on an SDS-PAGE were transferred to a Hybond-C extra nitrocellulose membrane (Thermo Scientific, Melbourne). The gel was incubated in transfer buffer (39 mM glycine; 48 mM Tris-HCl, pH 8.3; 0.037 % (w/v) SDS, 20 % (v/v) methanol) for 1 h on a rocker. Prior to transfer, 10 pieces of Whatman® filter paper and 1 piece of membrane (same measurements as the gel), were incubated in transfer buffer for 10 min. The paper (3 sheets), membrane, gel and the remaining sheets of paper were assembled and the transferred was carried out for 1 h at 0.8 mA per cm^2 using a semi-dry transfer unit (Hoefer, TE77X). After the transfer the membrane was briefly stained in Ponceau stain (0.1 % (w/v) Ponceau powder, 5 % (v/v) acetic acid) to visualize the transferred proteins to confirm the

consistency of the transfer and to mark the weight markers using a pencil. The membrane was washed with TBS-Tween 20 (150 mM NaCl; 10 mM Tris-HCl pH 7.4; 0.1 % (v/v) Tween-20) and used for immunodetecion.

2.6.2 Immunodetecion

Immunodetection was performed using a variety of antibodies, typically polyclonal antibodies raised in rabbits. Prior to immunodetecion the membrane was incubated in the blocking solution (blocking reagent diluted 1:10 in 1 X TBS-Tween 20) (Roche, Sydney) for 1 h in RT on a rocker or over night at 4°C. The membrane was washed in 1 X TBS-Tween 20 and incubated in the primary antibody for 1 h in RT on a rocker or over night at 4°C. Following the incubation the membrane was rinsed twice in 1 X TBS-Tween 20 followed by one 15 min and two 5 min washes. After the washing the membrane was incubated in the secondary antibody solution (1:10 000 dilution of the monoclonal antibody raised in mouse) for 1 h in RT on a rocker. The secondary antibody was washed by rinsing twice, in 1 X TBS-Tween 20 followed by one 15 min and two 5 min washes. In order to detect the signal the membrane was placed in a plastic envelope and treated with 3 ml of detecting solution (3 ml of Solution A, 30 µl of Solution B) (BM, Chemiluminescence Blotting Substrate POD, Roche, Sydney) and incubated for 1 min. The excess of the detecting solution was discarded. The membrane was wrapped with cling wrap and detected immediately using the Fuji LAS 1000 Transiluminator (Fuji, Tokyo).

2.7 Green Fluorescent Protein Localisation

2.7.1 Biolistic transformation

Arabidopsis suspension cell cultures and spring onion epithelial cells were transiently transformed using a Bio-Rad PDS-1000/He biolistic instrument (Bio-Rad, Sydney). The DNA construct containing the full coding sequence was fused to green fluorescent protein at C- or N-terminus under control of the 35S tobacco mosaic virus promote. The plasmid DNA (5 µg) was precipitated onto gold micro carriers prior to bombardment by adding 3 mg of sterilised 1.6 um gold particles

in 50 % (v/v) glycerol solution to the DNA followed by adding 50 µl of 2.5 M $CaCl_2$ and 20 µl of 100 mM spermidine and simultaneous vortexing at 600 rpm for 90 seconds. Gold particles were allowed to settle and supernatant was subsequently removed. The pellet was washed with 140 µl of 70 % (v/v) ethanol by agitating the tube and allowing it to set. Subsequently the supernatant was removed. The pellet was then washed for the second time with 140 µl of 100 % (v/v) ethanol followed be the removal of the supernatant. Finally, 56 µl of 100 % ethanol was added to the tube and the resuspended pellet was transferred onto a single macro carrier (Bio-Rad, Sydney).

The 5-day-old Arabidopsis suspension cell culture of 2.5 ml was coated onto a 55 mm filter paper disk (Whatman, Maidstone, UK) by blunt ended pipette. The liquid was removed by application of vacuum through a 47 mm glass filter holder assembly (Millipore, Sydney) and transferred onto osmoticum plates. Additionaly the epidermis of the spring onion was carefully pealed and placed alongside the cell culture disc. The plates were incubated for 2 h at 22°C prior to transformation.

The bombardment was carried out according to the following parameters: He preassure - 1300 psi, rupture disc pressure - 1100 psi, chamber vacuum 27 inch / Hg, platform spacing 9 cm and a hepta adaptor with the single macro carrier containing the DNA precipitated gold particles placed in the centre with six 'blank' macro carriers surrounding it. Following the bombardment the plates were transferred to 22°C cabinets where they were incubated in the dark for 24-48 h before the fluorescent microscopy analysis.

2.7.2 Fluorescent microscopy

GFP localisation was performed by co-transformation of the experimental coding sequence fused to GFP with the control plasmid containing a known targeting sequence fused to the red fluorescent protein (RFP). The GFP and RFP localisation was visualised with an Olympus BX61 fluorescence microscope 460-480 nm excitation 495-540 nm emission (GFP) and 535-555 nm excitation 495-540 nm emission (RFP). Images were captured and analysed using Olympus CellR software (http://www.olympusaustralia.com.au/Product/Detail/316/Cell-R-M).

2.8 *Agrobacterium*-mediated stable transformation of plants

2.8.1 Transformation of *Agrobacterium tumefaciens* competent cells

Plasmids were transformed to competent *Agrobacterium* cells, GV 1330-C58 without the pSoup plasmid using a freeze-thaw protocol. A 100 µl of thawed competent cells were added to 1 µg of plasmid DNA and frozen in liquid nitrogen followed by thawing the reaction in 37 °C water batch for 5 min. Reaction were gently mixed with 500 µl of LB by pipetting and incubated at 28°C for 2-4 h with gentle shaking. Reactions were centrifuged at 4 000 x g for 2 min and the pellets were resuspended in 100 µl of LB. Subsequently reactions were plated on LB plates containing appropriate antibiotics and incubated at 28 °C for 2-3 days.

2.8.2 *Agrobacterium* floral dip of Arabidopsis

A 1 ml LB aliquot was inoculated with 2-3 mm colonies of transformed *Agrobacterium* in a 50 ml tube and incubated for 8-9 h in 28°C at 220 rpm in the dark without the addition of antibiotics. Followed by addition of 10 ml LB without antibiotics, the preculture was incubated overnight in 28°C at 220 rpm in the dark until OD_{600} was approximately 1.7-2.0. Silwet solution (40 ml of MQ water containing 5 g sucrose and 25 µl of Silwet) was added to the preculture prior to dipping. Young flowers of at least four plants for each construct were dipped in the *Agrobacterium* culture by inverting and gentle agitating for 5-10 sec. The dipping was repeated after 7 days to allow plants to recover. Plants were grown in conditions described above until the life cycle was completed and seeds were collected.

2.8.3 Selection of Arabidopsis primary transformants

The screen for T_1 transformants was performed by collecting the seeds from dipped plants and selecting them on the MS plates with 5 mg/ml glufosinate ammonium (Basta). Plants resistant to Basta were green while the non-transformed plants remained pale.

2.9 Dark induced senescence assay

Leaves from 4-week-old plants were excised and the chlorophyll was measured using the SPAD 500 chlorophyll meter (Minolta, Japan). Leaves were incubated on a paper square (Whatman, Maidstone) damped with MQ water in an obscured petri dish for 3 days. After incubation in the dark, the leaves were uncovered and the senescence-related chlorophyll breakdown was measured. Five leaves per plant and three plants per genotype were sampled.

2.10 Determination of ROS and starch accumulation

The reactive oxygen species (ROS) in the form of O_2^- were visualized according to method described in [197]. Individual leaves were excised from plants exposed to normal growth conditions as well as from plants subjected to the dark induced senescence assay and placed in 600 μM solution of nitroblue tetrazolium (NBT) for 3 h. After incubation in NBT leaves were placed in 80 % (v/v) ethanol for 48 h to remove the chlorophyll. Five leaves per plant and three plants per genotype were sampled.

The leaf accumulation of starch was measured by incubating leaves in 80 % (v/v) ethanol for 24 h, twice, in order to remove the chlorophyll followed by 3 washes in MQ water and 5 min incubation in 50 % (v/v) solution of Lugol (Sigma). Leaves were destained in water for 60 min before being imaged. Leaves were collected in the morning and at the end of the day. Five leaves per plant and three plants per genotype have been sampled.

TRic1 and TRic2

Chapter 3 - TRic1 and TRic2

3.1 Introduction

Mitochondria import most of their proteins from the cytosol, a process mediated by independent protein translocation systems located in the outer membrane (TOM and SAM complexes) and inner membrane (TIM complexes). The TIM17:23 complex, responsible for the translocation of presequence-containing proteins, consists of integral membrane proteins Tim17 and Tim23. Preproteins, containing internal targeting signals, are imported by the TIM22 complex. Proteins Tim17, Tim22 and Tim23 belong to the preprotein and amino acid transporter (PRAT) family [183, 198], which evolved from a single eubacterial LivH amino acid permease, characterized by four transmembrane domains and a conserved motif: $[G/A]X_2[F/Y]X_{10}RX_3DX_6[G/A/S]GX_3G$ [198].

Arabidopsis genome encodes for 17 PRATs, of which 10 are localized in mitochondria, with three genes encoding Tim17, three genes encoding Tim23, two genes encoding Tim22 and two genes, which are yet to be characterised while the other ones are present in plastids and are putative metabolite transporters such as outer envelope protein 16 (OEP16). Yeast and brown algae, *Ectocarpus,* contain only three members of the PRAT family: Tim17, Tim23 and Tim22, which clearly shows that this gene family has expanded over evolutionary time in the plant kingdom. A recent study on two mitochondrial PRAT proteins: NADH dehydrogenase B14.7 like (B14.7) protein, which was previously identified to be a Complex I subunit in Arabidopsis [199-201] and Tim23-2, showed that both are present in Complex I and TIM17:23 complexes [130]. It is being hypothesised that the dual location of these PRATs gives them two functions and might be an evolutionary mechanism for regulation of mitochondrial biogenesis caused by oxidative damage or increased respiratory demand of Complex I.

A previous study characterizing the locations of the PRAT gene family in Arabidopsis, found that the PRAT proteins encoded by At3g49560 and At5g24650 were dual-targeted to both mitochondria and chloroplasts. *In vitro* protein import assays and green fluorescent protein (GFP) localization analysis identified the protein encoded by At5g24650 to be located on the mitochondrial

outer membrane protein [183], which was confirmed by a large Arabidopsis mitochondrial outer membrane proteome study [181]. Interestingly, these two proteins, apart from containing the PRAT consensus sequence also contain a sterile alpha motif (SAM) consensus sequence at their C-termini a domain that has been shown to have multiple functions such as protein-protein and RNA binding [202]. The SAM domain is present in many other organisms, a recent study in *Drosophila melanogaster* (fruit fly) revealed that Smaug protein's SAM domain is capable of RNA-binding with a cluster of positively charged residues [203]. Similar results were obtained when examining a Smaug homolog in yeast called Vts1 (VTI1-2 suppressor protein1), which also consists of the SAM domain with the RNA-binding capability [204]. The protein encoded by At5g24650 may have a unique plant specific function as phylogenetic analysis reveals that proteins containing both a PRAT and SAM domains can only be identified in plants [183]. Moreover, these two proteins were identified in the green algae such as *C. reinhardtii* and *V. carteri* but not in red or brown algae suggesting that they evolved early in response to specific needs of plants and have been conserved throughout the evolution of land plants.

3.2 Aims

The aim of this set of experiments was to investigate the function of proteins encoded by At3g49560 and At5g24560. The focus of this set of experiments was to investigate the interesting characteristics of these two proteins such as combination of the PRAT and SAM domain motifs and their phylogenies. We were interested in determining their putative functions in mitochondrial biogenesis processes such as protein import as well as the tRNA import. The presence of the SAM domain in these proteins and results obtained from *in vitro* tRNA import assays led to the hypothesis of these two proteins being putatively involved in the process of tRNA import into plant mitochondria. Therefore, they were referred to as tRNA import component 1 (TRic1) (encoded by At3g49560) and tRNA import component 2 (TRic2) (encoded by At5g24560). In addition, we were interested in determining the possible involvement of TRic proteins in mitochondrial-encoded protein synthesis as well as their association in putative protein complexes. Finally the functional complementation of the knock out line was performed. The experiments were carried out as follows:

1. Bioinformatic analysis of TRic1 and TRic2
2. Characterization of the T-DNA insertion single and the double knock out lines.
3. *In vitro* import of various protein precursors.
4. *In vitro* import of $tRNA^{Ala}$ into isolated mitochondria.
5. Analysis of mitochondrial *in organello* synthesis of proteins.
6. Analysis of protein complexes.
7. *In vivo* complementation of *tric1:2* line.

3.3 Results

3.3.1 Bioinformatic analysis of TRic1 and TRic2 proteins

Amino acid sequences of TRic1 and TRic2 proteins were retrieved from The Arabidopsis Information Resource (TAIR, http://www.arabidopsis.org/) TAIR10 genome release. Alignments of sequences were generated using ClustalW2 - Multiple Sequence Alignment tool (http://www.ebi.ac.uk/Tools/msa/clustalw2/) with default settings. Shading of the alignment was performed using BOXSHADE 3.21 (http://www.ch.embnet.org/software/BOX_form.html). Four predicted transmembrane domains (amino acids: 61-77, 119-124, 141-148 and 169-178 for TRic1 and 52-72, 114-119, 137-149 and 164-173 for TRic2) were highlighted in the form of green boxes over the sequences as predicted by Transmembrane Prediction server, DAS (http://www.sbc.su.se/~miklos/DAS/). The PRAT and SAM domains were predicted using The Conserved Domain Database (CDD) (http://www.ncbi.nlm.nih.gov/Structure/cdd/wrpsb.cgi) [184] and sequence consensuses were highlighted in blue for PRAT: $[G/A]X_2[F/Y]X_{10}RX_3DX_6[G/A/S]GX_3G$ (amino acids 65-186 for TRic1 and 57-181 for TRic2) [198] and red for SAM: $WLX_2LRLHKYX_{19}LX_4VX_3GAX_2K$ (amino acids 203-252 for TRic1 and 200-247 for TRic2) [204] (Figure 3.1.1 A).

The amino acid residues (Tyrosine, Y; Leucine, L and Lysine, K), of the SAM domain previously shown to be involved in RNA binding [204], are highlighted and are conserved in both TRic1 and TRic2. Variants of Smaug proteins, TRic1 and TRic2 as well as Vts1 protein sequences were aligned and the conserved residues were highlighted (Figure 3.1.1 B) indicating high conservation of RNA-binding residues of the SAM domain across different organisms.

The sequence identity and similarity scores between TRic1 and TRic2 protein sequences were estimated using Matrix Global Alignment Tool (MatGAT) version 2.01 [187]. The similarity score was estimated at 91 % and identity at 83 % indicating that both isoforms are highly similar proteins and most likely result form a recent gene duplication event (Figure 3.1.1 C).

In order to identify TRic orthologs present in other species, sequences of Arabidopsis TRic proteins retrieved from TAIR (http://www.arabidopsis.org) were

used to find direct orthologs by sequence homology using BLASTP [188] against *Homo sapiens* (human, http://www.hprd.org), *Caenorhabditis elegans* (roundworm http://www.wormbase.org), *Neurospora crassa* (mould, http://www.ncbi.nlm.nih.gov), *Dictyostelium discoideum* (slime mould, http://dictybase.org/) and *Saccharomyces cerevisiae* (budding yeast http://www.yeastgenome.org) in their respective databases. After manually checking the results from the BLAST searches, proteins were considered orthologous if the e-value representing the significance was lower than $1e^{-10}$. For proteins, which exhibited high conservation to known PRAT proteins the threshold was raised to $1e^{-50\text{-}100}$. This search revealed no significant orthologs among these groups hence it was concluded that TRic proteins are most likely specific to the plant kingdom. To study this further, protein sequences of TRic orthologs were retrieved from the genomic databases: Phytozome v9.1 (http://www.phytozome.net/) for *Brassica rapa* (Br), *Capsella rubella* (Cr), *Chlamydomonas reinhardtii* (Cr), *Cucumis sativus* (Cs), *Eucalyptus grandis* (Eg), *Glycine max* (Gm), *Medicago truncatula* (Mt), *Oryza sativa* (Os), *Physcomitrella patens* (Ps), *Populus trichocarpa* (Pt), *Ricinus communis* (Rc), *Selaginella moellendorfii* (Sm), *Solanum tuberosum* (St), *Vitis vinifera* (Vv), *Volvox carteri* (Vc), and *Zea mays* (Zm) for higher plants and green algae; Cyanidioschyzon merolea Genome Project (http://merolae.biol.s.u-tokyo.ac.jp/) for *Cyanidioschyzon merolea* (red algae) and Online resource for community annotation of eukaryotes OrcAE (http://bioinformatics.psb.ugent.be/orcae/overview/Ectsi) for *Ectocarpus siliculosus* (brown algae). The elimination process was repeated using e-value thresholds as described above. It was ensured that none of the orthologs found by the BLAST search was a direct homolog to other PRAT proteins such as Tim17, Tim23, Tim22 and OEP16. By process of elimination direct orthologs of TRic proteins were identified in 16 plant species (including green algae) and are not present in *Homo sapiens*, *Caenorhabditis elegans*, *Neurospora crassa*, or *Dictyostelium discoideum*. TRic orthologs were also not found in red and brown algae, however they are present in early plant taxa such as green algae, which suggests they might have evolved in response to plant needs in the early evolution of land plants, which corroborated previous findings. The phylogenetic analysis was carried out using MEGA 5.2.2 [189]. The full-length protein alignments were

first generated using the Clustal option followed by the generation of the phylogenetic tree using the maximum likelihood tree setting according to the Jones-Thornton-Taylor model after 1000 replications (Figure 3.1.2).

3.3.2 Characterization of the mutant lines

The initial screening and genotyping of the single knock out lines in At3g49560 and At5g24650 was undertaken by Dr Monika Murcha, who obtained the single mutant lines from The Arabidopsis Biological Resource Centre (http://abrc.osu.edu/) and the European Arabidopsis Stock Centre (http://arabidopsis.info/). The following lines: SALK_112126 and SALK_032707 insertion lines in At3g49560 and SALK_149871 and SALK_053383 insertion lines in At5g24560 were screened for homozygosity by PCR-based genotyping using specific primers designed with T-DNA Primer Design (http://signal.salk.edu/tdnaprimers.2.html) (Figure 3.2.1 A). These mutant lines were grown in long day conditions (16 hour day/8 hour night at 22°C under 100 µmol m^{-2} s^{-1} light intensity). No obvious phenotypic changes were identified in any of the single mutant lines (data not shown), therefore lines SALK_112126 (TRic1) and SALK_149871 (TRic2) have been cross-fertilised in order to generate a double knockout line *tric1::2.*

To confirm the functional knockouts of proteins encoded by At5g24650 and At3g49560, immunodetection against total mitochondrial protein isolated from *tric1*, *tric2* and *tric1::2* lines was carried out (Figure 3.2.1 B). Specific antibodies, raised to the recombinant protein of amino acids 1-180 of TRic1 and amino acids 1-180 of TRic2 were used. Immunodetection using TRic1 antibody (Ab) resulted in the detection of a band of 28 kDa in Col-0 (Figure 3.2.1 B, lane 1). This band was not evident in mitochondria isolated from *tric1::2* (Figure 3.2.1 B, lane 2) confirming that the *tric1::2* is a functional knockout line of TRic1. Similarly, detection with antibodies raised against TRic2 against mitochondria isolated from each of the single KO lines and from the *tric1::2* line was carried out and a band of 28 kDa in Col-0 was detected (Figure 3.2.1 B, lane 5) however band wasn't evident in the *tric1::2* (Figure 3.2.1 B, lane 6). In the case *tric1* and *tric2* lines the insertions caused the absence of the specific isoforms in their respective lines

while the other isoform could be still detected at low levels due to the very high sequence similarity of TRic isoforms, which caused the antibodies to cross-react (Figure 3.2.1 B, lanes 3, 4, 7 and 8). The cross reactivity of the Tric1 Ab was previously tested against recombinant, full-length Tric1 and Tric2 proteins with polyhistidine (6xHis) tags [205].

Immunodetection against total chloroplast protein isolated from Col-0, single lines KO lines and the *tric1::2* was similarly carried out. A protein band of 28 kDa can be detected in chloroplasts isolated from Col-0 (Figure 3.2.1 B, panel chloroplasts, lanes 1 and 2) but not in the *tric1::2* chloroplasts (Figure 3.2.1 B, lanes 7 and 8). These results show that in the *tric1::2* line, the insertions cause the absence of the TRic proteins just like in the case of mitochondria.

The presence of TRic1 protein was confirmed in mitochondrial and chloroplastic compartments while no protein was detected in the cytosol (Figure 3.2.1 C).

The *tric1::2* plants revealed a severely pale leaf phenotype and moderately retarded growth phenotype. A detailed phenotypic analysis was carried out as outlined in [206] according to the described parameters. The *tric1::2* plants exhibited delayed development, when grown on MS media with 0 % (w/v) sucrose, reaching the radicle emergence stage (0.5) on average 6 days later than wild type (Col-0) plants (Figure 3.2.2 A, i). The *tric1::2* plants did not develop past the principal growth stage 1 (leaf development), when grown on 0 % (w/v) sucrose media for 14 days. When grown on MS media with 3 % (w/v) sucrose, the *tric1::2* plants exhibited only mild growth retardation and were able to reach all developmental stages (hypocotyl and cotyledon emergence, 0.7; fully opened cotyledons, 1.0 and 2 rosette leaves >1 mm, 1.02) on average 1-2 days later than Col-0 plants and complete the principal growth stage 1 until stage 1.04 (4 rosette leaves > 1 mm), after which they were transplanted to soil (Figure 3.2.2 A, ii).

The soil-based phenotyping was initiated after approximately 14 days from sowing and showed that *tric1::2* plants reached the 10 rosette leaves stage (1.10) on average 5 days later than Col-0 plants. However, first visible flower buds stage (5.10) was observed at day 18, which was on average 7 days before Col-0 plants and first open flower stage (6.0) was reached at day 30, 4 days before Col-0. The flowering time, however, was longer than in Col-0 plants and wasn't complete

until day 65, which was on average 11 days after Col-0 plants (Figure 3.2.2 A, iii). The severe pale phenotype of *tric1::2* plants (Figure 3.2.2 B, i) and generally slower development affecting the roots (Figure 3.2.2 B, ii) and adult plants (Figure 3.2.2 B, iii) was consistently observed throughout the development.

3.3.3 *In vitro* protein import into Col-0, *tric1::2* and *tom20-2.3.4* mitochondria

Protein precursors selected for the *in vitro* protein import experiments included an N-terminal presequence-containing protein (AOX), a carrier protein (ANT), a β-barrel protein (Tom40) and a dual-targeted to mitochondria and chloroplasts monodehydroascorbate reductase (MDHAR). *In vitro* translation of these proteins using the rabbit reticulocyte lysates in presence of [^{35}S]-methionine resulted in products of 36 kDa, 38 kDa, 47kDa and 36 kDa respectively (Figure 3.3, lane 1). Proteins containing a cleavable extension, which is removed from the protein by the mitochondrial processing peptidase (MPP) after translocation through the inner membrane, produced shorter, mature products. Incubating precursor proteins with mitochondria isolated from Col-0 and *tric1::2* plants resulted in the accumulation of the processed, mature form of the protein over time (Figure 3.3 A), which was measured as the rate of the protein import. To avoid the false positive results, which could occur due to the release of the MPP from raptured mitochondria during the isolation process, the reactions were treated with proteinase K (pK) to digest protein external to mitochondria. The protein imported into mitochondria was protected from degradation by the presence of the mitochondrial membranes.

In vitro protein uptake reactions were assembled and sampled over a time course of 5, 10 and 20 min in order to determine the rate of protein uptake into mitochondria from Col-0 and *tric1::2* plants (Figure 3.3 A, lanes 2-4 vs 5-7). Products of the reactions were separated by SDS-PAGE and imaged by storage phosphor autoradiography. Intensity of the mature products, protected by pK, was quantified in three replicates (Figure 3.3 A). The maximal intensity of the replicates was normalised to one, and other values expressed relatively. The normalised results were graphed (n = 3, P value < 0.05, student's t test, +/- SE).

Protein precursors used in the experiment represented a wide spectrum of mitochondrial proteins encoded in the nucleus, which follow different import pathways, however no significant changes in the rate of protein import were observed. This indicated that neither of the TRic isoforms is essential for the process of mitochondrial protein import of the tested precursors.

The triple knockout of three Tom20 isoforms (*tom20-2.3.4*) mitochondria were used as an additional control of the protein import, which was carried out as described above. As reported previously [86], plants lacking Tom20 are viable, however exhibit retarded growth and leaf morph ology phenotype as well as significant reduction in the protein import rate. The rate of AOX import into these mitochondria was observed to be 20 % lower comparing to Col-0 mitochondria. Similar results were observed for Tom40 (30 %) and ANT (25 %) (n = 3, P value < 0.05, student's t test, +/- SE). The import of dual-targeted MDHAR seems to be unaffected in the absence of TOM20 isoforms (Figure 3.3 B), which corresponds to the import of another dual-targeted protein gluthatione reductase (GR), thus the results obtained in this experiment corroborate previous findings [86].

3.3.4 *In vitro* import of $tRNA^{Ala}$ into Col-0, *tric1::2* and *tom20-2.3.4* mitochondria

In vitro transcription of the Arabidopsis $tRNA^{Ala}$ using the *in vitro* transcription T7 polymerase kit in the presence of [^{32}P]-UTP resulted in the radiolabelled product used in all tRNA import experiments. The $tRNA^{Ala}$ was chosen as it is one of the known cytosolic tRNAs, which are imported into Arabidopsis mitochondria *in vivo* [171]. Incubation of radiolabelled $tRNA^{Ala}$ with mitochondria isolated from Col-0, *tric1::2* and *tom20-2.3.4* plants, resulted in import and internalisation of tRNA import was measured by the presence of the band corresponding to the size of the radiolabelled probe (Figure 3.4, lane T). To ensure the band corresponds to imported probe and not binding of the radiolabelled tRNA to the outside of mitochondria, reactions were treated with RNase to digest any external un-imported tRNA probe (Figure 3.4 A, lanes 3-4 and 7-8). Therefore the presence of a band within these lanes represents imported tRNA protected from RNase degradation within the mitochondrial membranes. The assay was repeated in technical duplicate (Figure 3.4 A, lanes 1-

2, 3-4, 5-6, 7-8) to ensure band intensity was consistent between samples and not compromised during the extraction process.

The amount of import was measured as band intensity (pixel density/mm^2). The intensity of the imported, RNase-protected substrate was quantified in three experimental replicates. The maximal intensity from the three replicates was set to one and the other values expressed relative to this value. Mitochondria isolated from *tric1::2* seedlings imported tRNA at approximately 80 % lower then Col-0 (Figure 3.4 B) (n = 3, P value < 0.05, student's t test, +/- SE).

The tRNA import ability was also tested in *tom20-2.3.4* mitochondria that previously were seen to exhibit a significant decrease in the protein import ability using precursors of the general import pathway [86]. Salinas *et al*. suggested that Tom20, among other proteins such as VDAC and Tom40, could be involved in the tRNA import recognition and translocation in *S. tuberosum* mitochondria [174]. In order to determine whether Tom20 plays a role in the tRNA import the *tom20-2.3.4* mitochondria were subjected to the *in vitro* tRNA import assay as described in Chapter 2 (Figure 3.4 C). A decrease in signal intensity of approximately 20 % was observed in mitochondria isolated from *tom20-2.3.4* mutant plants (Figure 3.4 D) (n = 3, P value < 0.05, student's t test, +/- SE).

3.3.5 *In vitro* tRNA^{Ala} import into Col-0 mitochondria is sensitive to pK treatment

In order to confirm that mitochondrial outer membrane protein composition plays a role in mediating the tRNA import, mitochondria from Col-0 plants were isolated as described above with the additional step of pretreatment in the presence of pK. Mitochondria were incubated in growing concentrations of pK (0, 0.4, 2, 4 and 8 µg) followed by addition of 100 mM PMSF to inhibit the digestion. pK-treated mitochondria were used in *in vitro* tRNA import assays as described above. By incubating radiolabelled tRNA^{Ala} with mitochondria isolated from Col-0 plants, the sensitivity of the internalisation of tRNA import to pK was measured by the presence of the band corresponding to the size of the radiolabelled probe (Figure 3.5, lane 1). Products of the import reaction were resolved on 7 M urea polyacrylamide gel in the presence of 1 X TBE and imaged by storage phosphor autoradiography.

The *in vitro* import of tRNA into pK-treated mitochondria isolated from Col-0 plants was shown to be sensitive to the protease digestion, which was indicated by the disappearing band corresponding to the imported $tRNA^{Ala}$ molecules (Figure 3.5, lanes 2-5). Additionally pK-treated mitochondria were used for immunodetecion of various mitochondrial proteins using polyclonal antibodies against the truncated variant of TRic1 (without the SAM domain, aa: 1-100) as well as markers for peripheral outer membrane components: Tom20-2, 20-3, 20-4, metaxin and mtOM64), integral outer membrane components (Tom40), inner membrane components (RISP) and matrix located mtHSP70. The TRic1 Ab was shown to detect both of the isoforms of TRic when incubated against recombinant, 6xHis-tagged TRic1 and TRic2 proteins (Figure 3.5 B). When incubated with pK-treated mitochondria, shift in the apparent size of the band corresponding to TRic1 was observed suggesting that TRic1 is an integral outer membrane component (Figure 3.5 B, lanes 3-6). The red arrow indicates the shift.

3.3.6 *In organell*o protein synthesis in mitochondria is affected in *tric1::2* plants

Mitochondrial genome-encoded proteins require cytosolic tRNAs and the functional tRNA import apparatus to be synthesized. In order to see, whether *in organello* protein synthesis was affected, mitochondria from Col-0, *tric1*, *tric2* and *tric1::2* plants were isolated as described above and incubated in the presence of [^{35}S]-methionine (Figure 3.6 A). *In organello* protein synthesis reactions were assembled and sampled every 10 (lanes 1, 4, 7 and 10), 30 (lanes 2, 5, 8, 11) and 60 min (lanes 3, 6, 9, 12) in order to determine the rate of incorporation of [^{35}S]-methionine into mitochondria-encoded proteins. Products of the reaction were separated by SDS-PAGE and imaged by storage phosphor autoradiography. Resulted products were quantified as previously described and represented as graphs for each of the proteins (Figure 3.6 B).

In organello synthesis of mitochondria-encoded proteins such as atp1, cob, cox2, nad9, nad6 and atp9 was observed by incorporation of [^{35}S]-Methionine over time and their apparent molecular weight was determined according to previous studies. It has been observed that rate in which mitochondria of *tric1::2* plants synthesize proteins was down to 70 % (atp1), 30 % (cob), 45 % (cox2) 55 % (nad9) 40 % (nad6) comparing to Col-0. No significant

changes were observed in *in organello* synthesis of apt9. *In organello* synthesis of *tric1* mitochondria was 76 % (atp1), 44 % (cob), 47 % (cox2), 63 % (nad9) and 65 % (nad6) while *tric2* was 76 % (atp1), 39 % (cob), 49 % (cox2) 55 % (nad9) and 55 % (nad6) down comparing to Col-0. These results indicated that mitochondria devoid of TRic proteins have decreased ability to synthesize some mitochondrial-encoded proteins.

3.3.7 TRic proteins associate with protein import machinery

It has been previously observed that outer and inner membrane complexes are dynamic and multiple interactions were reported between protein import components, respiratory chain components and proteins maintaining the mitochondria morphology [207, 208]. Recent studies in plant mitochondria showed evidence for physical link between the outer and inner membranes through the Tim17-2 [126] as well as interaction between Tim23, Tim21, and two Tim21-like proteins with respiratory complexes [133]. As mentioned before, a PRAT protein B14.7, a complex I subunit, has been also shown to interact with TIM17:23 complex [130]. Previous studies identified TRics as outer membrane proteins in mitochondria and inner envelope membrane in chloroplasts [181, 183], however other members of the PRAT family of proteins are known to localize to the mitochondrial inner membrane.

In order to determine the integration of TRic1 and TRic2 proteins within mitochondrial protein complexes, a large-scale *in vitro* protein import assay into isolated Col-0 mitochondria, using radiolabelled TRic1 and TRic2 proteins was carried out followed by Blue Native PAGE (BN-PAGE) analysis. To confirm that incorporation of TRics into protein complexes was a result of specific import and accumulation, a time-course experiment was performed where samples were collected at 5, 10 and 20 minutes for radiolabelled TRic1 (Figure 3.7, lanes 2-4) and TRic2 (Figure 3.7, lanes 5-7). Radiolabelled Tim23 (lane 1) and Tom40 proteins (lane 8) were used as controls. The resulting products were resolved on BN-PAGE and imaged as described previously.

Import and assembly of TRics was evident within TOM complex as shown by comigration with radiolabelled Tom40 (Figure 3.7, indicated by *). Moreover,

these results show that radiolabelled TRic is assembled into three complexes, two large complexes migrating at approximately 500 kDa (indicated by **) and 300 kDa (indicated by *) and a smaller 100 kDa complex (***). Interestingly the position at approximately 100 kDa corresponds to TIM17:23 complex. These findings suggest that TRics could be interacting with both TOM and TIM machinery and are consistent with the preliminary yeast 2 hybrid (Y2H) assay results, which revealed that TRics have ability to interact with Tom40, Tom20 as well as Tim17-2, Tim23 and Tim50 (personal correspondence, Monika Murcha).

3.3.8 *In vivo* complementation of *tric1::2* line

As shown previously, *tric1::2* line exhibits pale leaf morphology and delayed growth phenotype, which could indicate changed mitochondrial and chloroplast functions. In order to functionally complement the tric1::2 line *in vivo*, two constructs were generated: the full length TRic2 (FL) (aminoacids 1-259) and truncated form of TRic2 lacking the SAM domain (TR) (aminoacids 1-180). The tric1::2 plants were transformed using *Agrobacterium*-mediated floral dip transformation, where both constructs were expressed under a strong, constitutive cauliflower mosaic virus (CaMV) 35s promoter (Figure 3.8.1 A).

In order to determine the effect of the complementation on the ability to import tRNA *in vitro*, mitochondria from complemented lines were isolated as described previously and used for the *in vitro* import. *In vitro* tRNA import reactions were assembled and sampled after 20 min to measure the uptake of radiolabelled tRNA into mitochondria from Col-0, tric1::2, FLA and FLD mitochondria (Figure 3.8.1 B, lanes 1 vs 2 vs 3 vs 4). Products of the reactions were separated by gel electrophoresis and imaged as described before. The intensity of the imported, RNase-protected substrate was quantified in three experimental replicates and the normalised results were graphed (Figure 3.8.1 B). These results suggest that complementation of *tric1::2* plants with the full-length construct resulted in significant restoration of the import ability of tRNA *in vitro*.

Lines complemented with the full-length construct (FLA) or with truncated construct (TRA) were grown in the long day conditions as described above. Complementation of the *tric1::2* line with FL construct showed a significant

restoration of the phenotype while complementation with the TR construct resulted in no phenotypic restoration (Figure 3.8.2 A). Quantitative phenotypic analysis of Col-0, *tric1::2*, FL and TR lines was performed as described above. These results suggested that the SAM domain of TRics is crucial for their function and lack thereof leads to severe morphological and physiological changes.

3.4 Discussion

Mechanisms of tRNA import into mitochondria are highly variable between different groups of organisms and it has been suggested that evolution of these mechanisms was very rapid. Despite the fact, that first direct evidence of mitochondrial tRNA import was shown in plants [140], the mechanism is still very poorly described and very little experimental data from plant studies is available. Up until recently the only evidence for plant mitochondrial protein engagement in tRNA import came from the study on potato mitochondria, which showed a link to protein import components Tom20 and Tom40 as well as VDAC [174]. The evidence for the dynamic nature of mitochondrial outer and inner membranes and interactions between them invited a closer examination of interesting mitochondrial proteins, specifically the preprotein and amino acid transporter (PRAT) proteins: TRic1 and TRic2, which have been shown to be only present in photosynthesizing eukaryotes. These two proteins have been previously identified as residing in the mitochondrial outer membrane, unlike the rest of the PRAT family of proteins as well as having a C-terminal sterile alpha motif (SAM) domain implicated in RNA binding in yeast and fruit fly. The role of TRics in Arabidopsis mitochondria was investigated by looking at various aspects of mitochondrial biogenesis in Col-0 as well as knockout and complemented lines.

The SAM domain has been described as implicated in a range of functions such as mediating interaction between proteins as well as in RNA binding. The sequence analysis revealed that the SAM domain of TRics forms similar structures to known RNA binding proteins such as Vts1 protein in yeast and Smaug protein in fruit fly. Amino acid residues (Y, L and K), implicated in RNA binding in these proteins are conserved in TRic1 and TRic2. This data led to hypothesis of TRics functioning as putative outer membrane tRNA import components. The

characterization of TRic proteins was complicated by them being encoded by two genes At3g49560 and At5g24560. Therefore a double knockout, *tric1::2* line, had to be generated, which exhibited severe phenotypic changes i.e. chlorotic leaves and retarded development. This suggested that TRics must confer a vital function in mitochondria while not being essential in Arabidopsis.

As other members of the PRAT family of proteins (such as Tim17, Tim22 and Tim23) are directly involved in the protein import mechanism, the import rate of various radiolabelled protein precursors was studied in *tric1::2* plants. These results show that import process of none of the tested precursors is dependent on the presence of TRic proteins. Tested precursors included a variety of proteins encoded by the nucleus and subsequently imported to mitochondria, which represent four distinct import pathways such as: presequence-containing matrix protein (AOX), an outer membrane β-barrel protein (Tom40), a dually-located protein targeted to mitochondria and chloroplasts (MDHAR) and a plant carrier protein (ANT). Interestingly, a recent study reported that in chloroplasts, TRics (named HP30-1 and HP30-2) are inner plastid envelope membrane proteins cooperating as components of the transit sequence-less protein import [209] and that they are specific to chloroplasts. Moreover, they are compared to the TIM22 complex, which mediates the import of carrier proteins and other inner membrane proteins, which contain internal targeting sequences in mitochondria. Contrary to these findings, data obtained in our laboratory suggests that TRics are dually targeted to chloroplasts and to mitochondria [183]. Nevertheless, these reports raise an interesting question of how PRAT proteins could have evolved several distinct functions in different membranes of different organelles. In fact, another study has shown that TRic proteins localized in chloroplasts might be involved in cysteine and methionine transport across the inner envelope membrane (personal correspondence, Kathrin Philippar).

The next step was to investigate, whether *tric1::2* mitochondria have impaired ability to import tRNAs *in vitro*. A protein shuttle system to efficiently target tRNA into Arabidopsis mitochondria was used, which consisted of a nucleic acid binding protein, dehydrofolate reductase (DHFR) fused to a mitochondrial targeting sequence to target the tRNA into the mitochondrial matrix [193]. Results from this *in vitro* import assay showed that the capability to import $tRNA^{Ala}$ in

tric1::2 plants was significantly decreased as compared to controls, making it the first evidence of any plant mitochondrial protein involved in the process of tRNA import using reverse genetic approach.

Although the pDHFR shuttle system is artificial, it raises exciting questions about the nature of the plant RNA import in general. It has been previously demonstrated that tRNAs can be imported in plant mitochondria *in vitro* at low levels in the absence of any protein factors [173]. However, in multiple species tRNA import is very often dependent on various cytosolic factors, which are required for targeting and trafficking of tRNA molecules into mitochondria. Targeting of $tRNA^{Lys}$ into yeast mitochondria is dependant on coordinated interaction with enolase 2 (Eno2p) and the precursor of mitochondrial lysyl-tRNA synthetase (preLysRS) [144, 145]. Studies in trypanosomes have shown that $tRNA^{Met}$ initiator binds to the cytosolic eukaryotic translation initiation factor 2 (eIF2) which diverts it from being targeted to mitochondria while $tRNA^{Met}$ elongator binds to the eukaryotic translation elongation factor 1a (eEF1a), which targets this tRNA to the mitochondrion [155, 156]. It seems that tRNA targeting to mitochondria almost always involves at least one protein and in that sense the pDHFR system resembles the *in vivo* mechanism of mitochondrial tRNA import studied in some organisms. It is therefore of importance for the field of tRNA import to establish wether plants also require carrier proteins or if there might be two parallel mechanisms existing (with and without any protein cofactors involved) as it is suggested for yeast $tRNA^{Lys}$ and $tRNA^{Gln}$.

It has been reported that a mutation of U_{70} to C_{70} in Arabidopsis $tRNA^{Ala}$ can block its aminoacylation, which prevents the import of $tRNA^{Ala}$ *in vivo*, hence it has been suggested that alanyl-tRNA synthetase (AlaRS) is necessary for $tRNA^{Ala}$ import in plants [171]. To test this hypothesis the Arabidopsis $tRNA^{Ala}$ and the precursor of AlaRS were co-expressed in yeast [210]. Despite the efficient import rate of the AtAlaRS into yeast mitochondria, neither the import of the Arabidopsis $tRNA^{Ala}$ nor the yeast cytosolic $tRNA^{Ala}$ isoacceptors was observed. This suggests that there has to be another component involved in the mitochondrial import of the plant tRNAs, which isn't present in yeast mitochondria. Moreover, recombinant TRic1 and TRic2 proteins have been shown to directly bind to the T-arm of the Arabidopis $tRNA^{Ala}$ in an experiment carried out recently (personal

correspondence, Pedro Teixeira) suggesting their ability to bind tRNA directly. This was confirmed by the lack of binding of tRNA to recombinant TRic proteins with mutationally altered amino acid residues previously shown to be responsible for RNA bidning (i.e. Y, L, K) (personal correspondence, Pedro Teixeira).

Efficient mitochondrial biogenesis relies on the functional protein import and translation of a small number of crucial mitochondrial proteins encoded by the mitochondrial genome. In Arabidopsis, mitochondrial genome encodes for nine subunits of Complex I (*nad1-7*, *nad4L* and *nad9*), one subunit of Complex II (*sdh4*), one subunit of Complex III (*cob*) three subunits of Complex IV (*cox1-3*), four subunits of Complex V (*atp1*, *atp6* and *atp8-9*) as well as several cytochrome *c* biogenesis proteins, ribosomal proteins, ribosomal RNAs as well as 22 tRNA genes, of which four are duplicated [27]. The 18 genes encoding for different tRNA species are not enough to translate mitochondria-encoded genes, hence tRNAs isoacceptors for five amino acids (Alanine, Arginine, Leucine, Threonine and Valine) are necessary and have to be imported from the cytosol [170]. Results obtained from an *in organello* protein synthesis assay suggest that, translation of mitochondria-encoded proteins is affected by the depletion of TRics in single KO lines and to more extent in the *tric1::2* line. Decreased tRNA import might lead to impaired translation of these crucial subunits of respiratory complexes and proteins involved in other metabolic pathways and might be the reason for the severe phenotype of *tric1::2*.

As mentioned previously, the dynamic and intertwining character of outer and inner membrane protein complexes in mitochondria is becoming increasingly evident with growing number of studies on components of protein complexes such as TOM and TIM as well as recently identified ERMES and MINOS complexomes in yeast. Moreover, the dynamic nature of mitochondrial membrane complexes is also occurring in plants with Tim17-1 and Tim17-2 physically linking the outer and inner membranes, Tim23 and B.14.7 having a dual function in translocation of preproteins to mitochondrial matrix via TIM complex and regulation of Complex I and finally with Tim21 and two Tim21-like proteins interacting with respiratory chain machinery. Previous localisation studies identified TRic2 as outer membrane proteins via GFP-tagging, which was confirmed by a comprehensive mass spectrometry analysis of highly purified mitochondrial outer

membrane fractions from Arabidopsis. It was surprising to see a PRAT protein present in the outer membrane as other members of this family have been shown to consistently span the inner membrane with their four transmembrane regions. However several lines of evidence including previous findings and the subsequent protease titrations and immunodetection confirm TRic integral outer membrane localisation (Figure 3.5 B). The preliminary Y2H interaction studies (data not shown) have shown that TRic2 has the ability to interact with both outer membrane (Tom40 and Tom20) and inner membrane (Tim17-2, Tim23, Tim50) components. These results are in line with previous findings linking Tom40 and Tom20 with the *in vitro* tRNA import in potato mitochondria and it is therefore possible that TRics might contribute to a larger complex involving components of protein import from both membranes or have the dynamic ability to interact with protein complexes on both membranes as previously demonstrated for Tim17-2. As obtained data suggest that SAM domain of TRics is putatively responsible for import of tRNAs into mitochondria, it is crucial to establish the topology of the these proteins. The shift of the protein size caused by the protease K titration (Figure 3.5 B) indicates that TRics are integral to the outer membrane, however it is unclear whether the C-terminal SAM domain is facing the cytosol, which would contribute to its possible receptor function.

In conclusion, this study investigated two PRAT proteins (TRic1 and TRic2) in order to gain insight into their function in plant mitochondrial biogenesis. Several approaches were undertaken and it was concluded that TRics are plant specific, mitochondrial outer membrane proteins, which are crucial but not essential in Arabidopsis. Data obtained from *in vitro* protein import assays suggests that TRics are not involved in the process of translocation of any of the tested preproteins into mitochondria. However, it is clear that TRics are possibly involved in the process of tRNA import in plants. As this data is an exciting contribution to the field of tRNA import in plants it is an incremental step in understanding of the process.

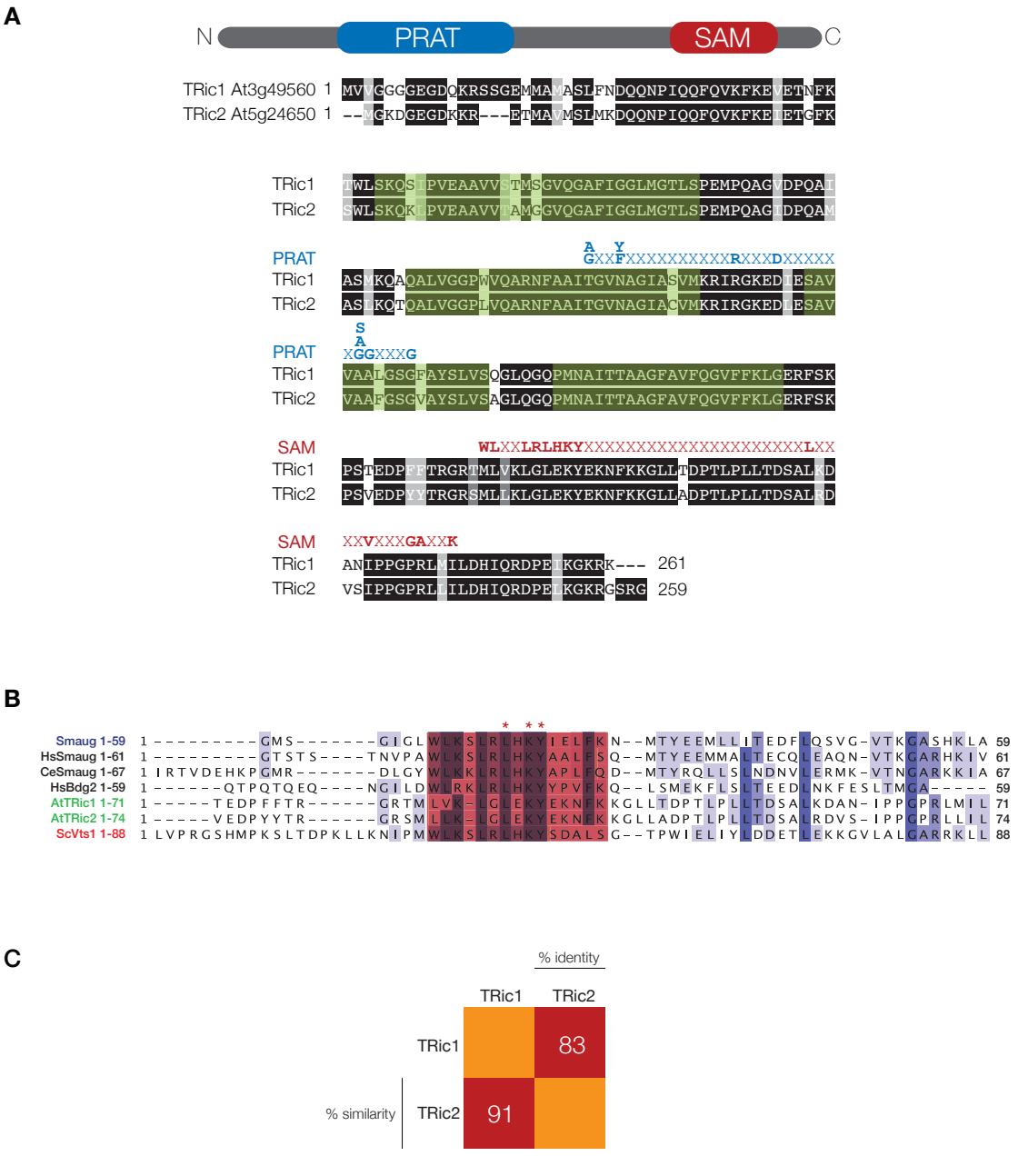

Figure 3.1.1 Bioinformatic analysis of Tric1 and Tric2.

A Diagram showing the predicted PRAT and SAM domains and a comparison of the protein sequences of TRic1 and TRic2. The predicted transmembrane domains are represented as green boxes, PRAT domain was highlighted in blue and SAM domain in red. The protein sequence alignment was generated using ClustalW2 - Multiple Sequence Alignment (http://www.ebi.ac.uk/Tools/msa/clustalw2/), default settings. Shading of the alignemnt was performed using BOXSHADE 3.21 (http://www.ch.embnet.org/software/BOX_form.html), default settings.

B Sterile Alpha Motif (SAM) sequence predictions. SAM domain of Vts1 from *Saccharomyces cerevisiae* recognizes and binds RNA. Aminoacid residues (Y, L and K) involved in RNA binding are conserved in both TRic1 and TRic2 proteins. Variants with reduced RNA binding (*Drosophilia* Smaug) are indicated according to Aviv *et al*., 2003. The RNA binding domain is represented as a red box.

C Matrix showing the percentage similarity and identity scores of amino acid sequences of TRic1 and TRic2 generated using MatGAT (Campanella *et al*., 2003)

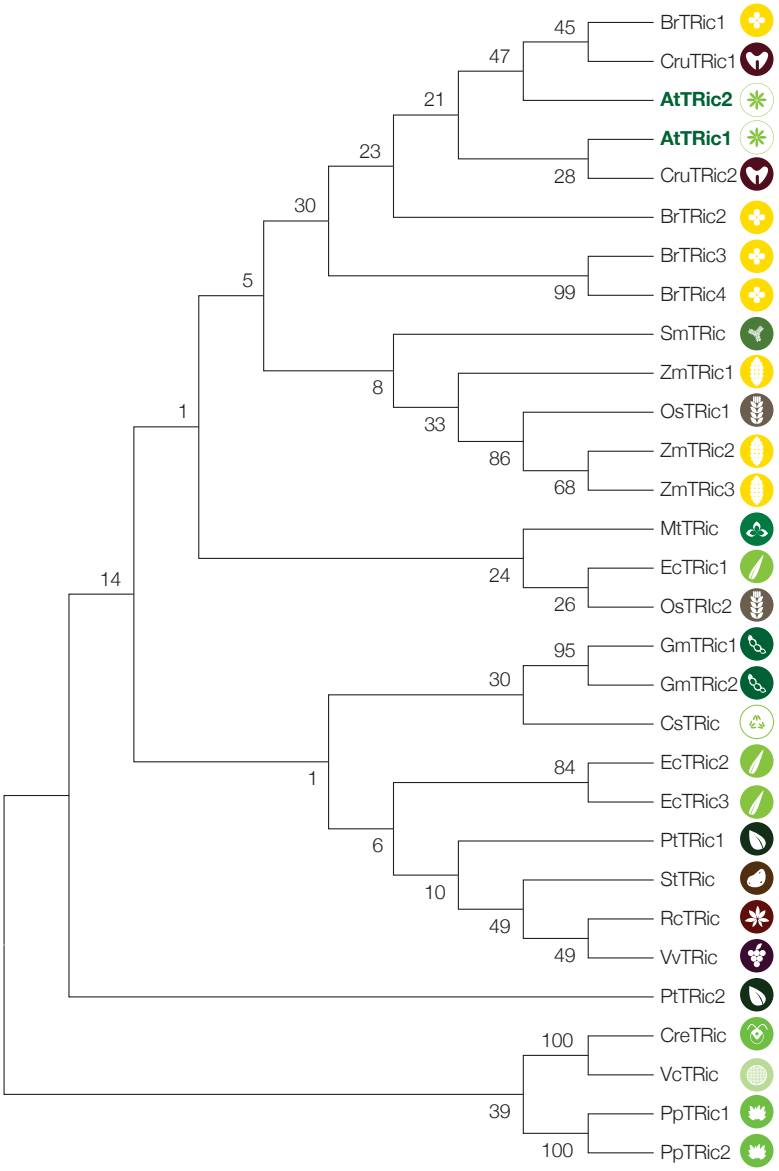

Figure 3.1.2 Phylogenetic analysis of TRic proteins

Sequences of TRic proteins were retrieved from various databases: Phytozome v9.1 (http://www.phytozome.net/), dictyBase (http://dictybase.org/), Cyanidioschyzon merolea Genome Project (http://merolae.biol.s.u-tokyo.ac.jp/) and Online resource for community annotation of eukaryotes OrcAE (http://bioinformatics.psb.ugent.be/orcae/overview/Ectsi). The phylogenetic analysis was carried out using MEGA 5.2.2 (Temura et al., 2011). Full-length protein alignments were generated using the Clustal option. The phylogenetic tree was generated using the maximum likelihood tree setting according to the Jones-Thornton-Taylor model after 1000 replications.

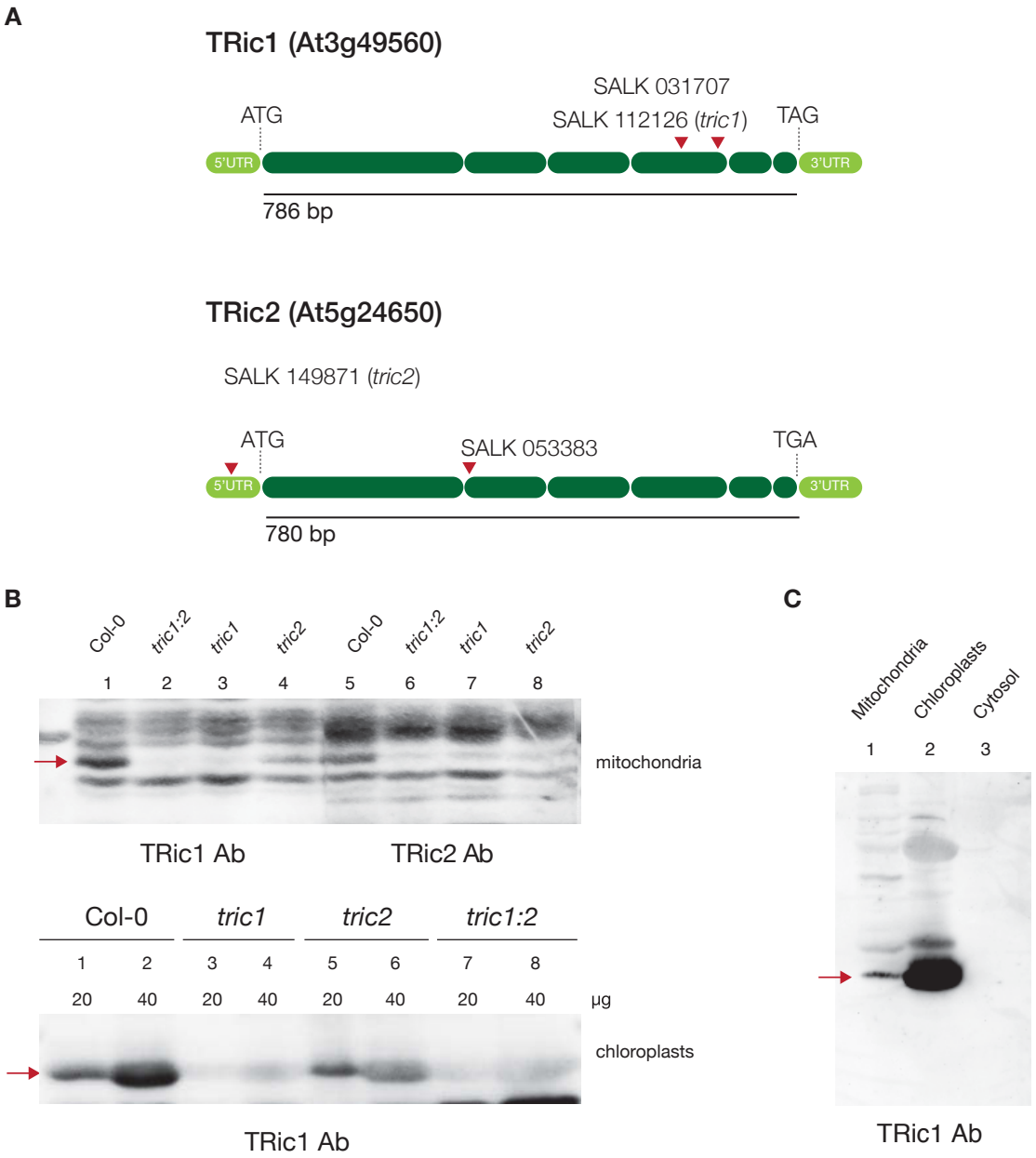

Figure 3.2.1 Characterization of T-DNA mutant lines

A The positions of the T-DNA inserts in KO lines in At3g49560 (SALK 031707 and SALK 112126) and in At5g24650 (SALK 053383 and SALK 149871). ATG, start codon; TAG and TGA, stop codon; UTR, untranslated region. Red triangles indicate the location of the TDNA insertion for respective lines. Green boxes correspond to exons. Full length of the gene is indicated (bp).

B Mitochondria isolated from Col-0, *tric1* (SALK 112126), *tric2* (SALK 149871) and *tric1:2* plants were subjected to the SDS-PAGE (40 µg of protein for each line was resolved) and probed with antibodies against TRic1 and TRic2. The apparent molecular mass of the protein detected is indicated by the red arrow (28 kDA). Chloroplasts isolated from Col-0, SALK 112126, SALK 149871 and the *tric1:2* plants were subjected to the SDS-PAGE (20 and 40 µg of protein for each line was resolved) and probed with the antibody against TRic1. The apparent molecular mass of the protein detected is indicated by the red arrow (28 kDA).

C Mitochondria (40 µg), Chloroplasts (40 µg) and cytosolic protein fraction (40 µg) from Col-0 plants were subjected to SDS-PAGE and probed with the antibody againsts TRic1. The apparent molecular mass of the protein detected is indicated by the red arrow (28 kDa). The presence of the TRic1 protein was confirmed in mitochondrial and chloroplastic subcompartments while no protein was detected in the cytosol.

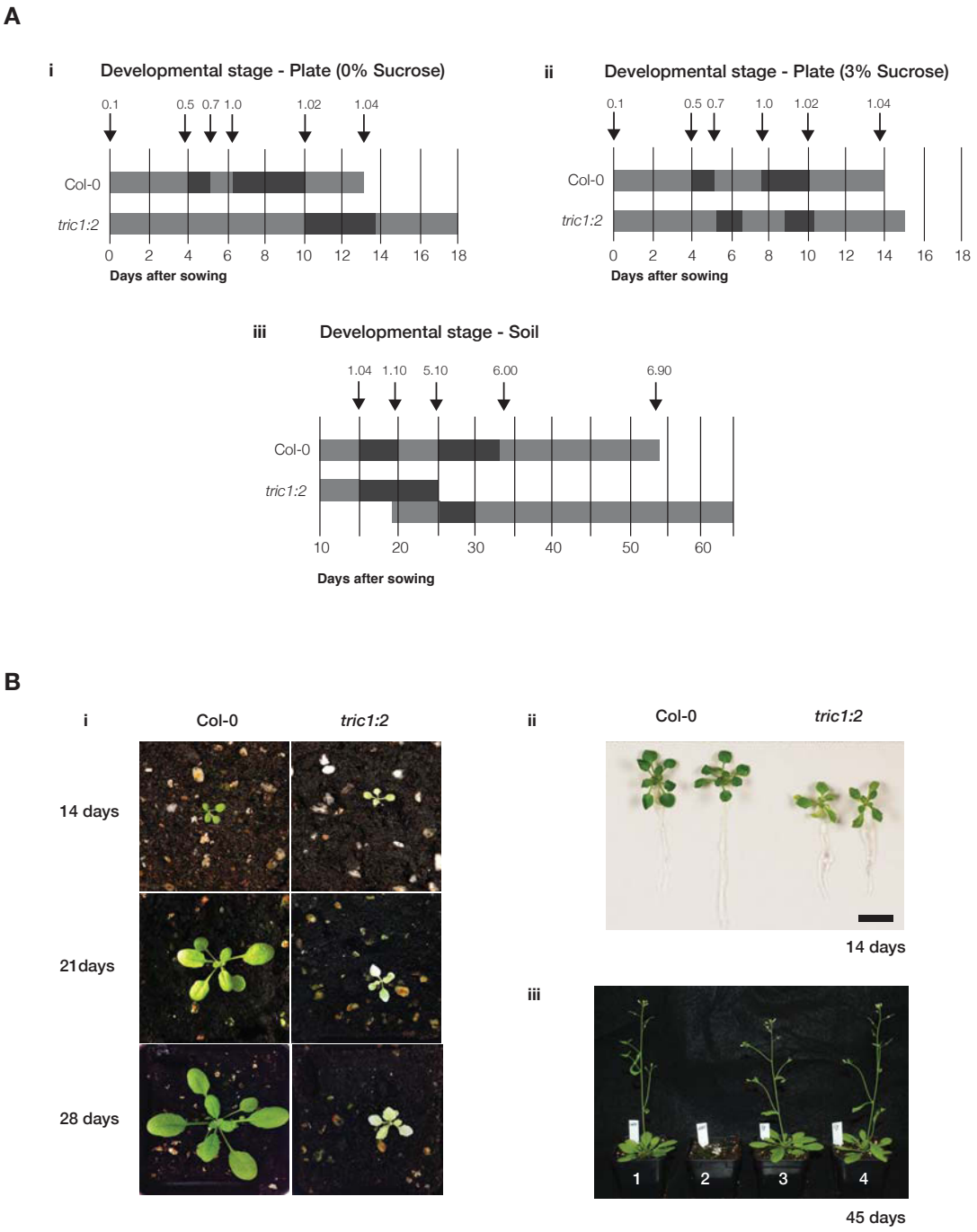

Figure 3.2.2 Quantitative phenotyping of *tric1:2* plants

A Plate-based growth progression analysis of Col-0 and the *tric1:2* on 0 % (w/v) sucrose MS medium. Days after sowing are indicated by arrows, when Col-0 plants have reached the growth stages decribed in Boyes et al. (2001). Boxes define the time between growth stages and shading indicates the occurrence of each growth stage. Stage 0.1, imbibition; stage 0.5 radical emergence; stage 0.7, hypocotyl emergence from seed coat; stage 1.0, cotyledons fully opened; stage 1.02, two rosette leaves > 1 mm in length; stage 1.04. four rosette leaves > 1 mm in length. Data is given as avarages for 10 plants. Days are relative to the days after sowing after a 3 d stratification at 4°C (i). Plate-based growth progression analysis as in (i) on 3 % (w/v) sucrose MS medium (ii). Soil-based growth progression as in (i): stage 1.10, 10 rosette leaves > 1 mm; stage 5.10, first flower bud visible; stage 6.0, first flower opens; stage 6.9, flowering complete (iii).

B Growth phenotypes of Col-0 and the *tric1:2* plants after 14, 18 and 22 days in soil (i). Growth phenotypes of Col-0 and *tric1:2* plants grown on 3 % (w/v) sucrose MS medium before transplanting to soil (ii). Growth phenotypes of Col-0 (1), *tric1:2* (2), *tric1* (3) and *tric2* (4) plants at the flowering stage (around 45 days) (iii).

A

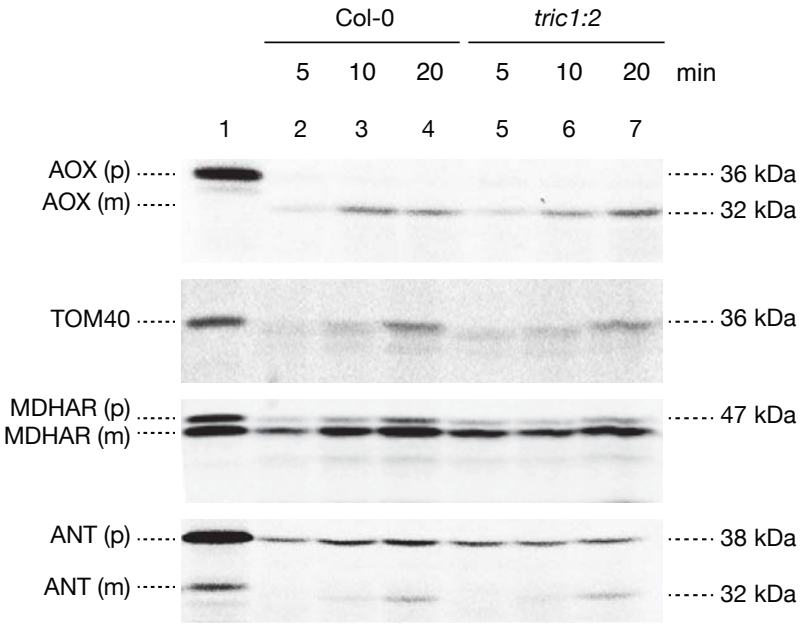

B

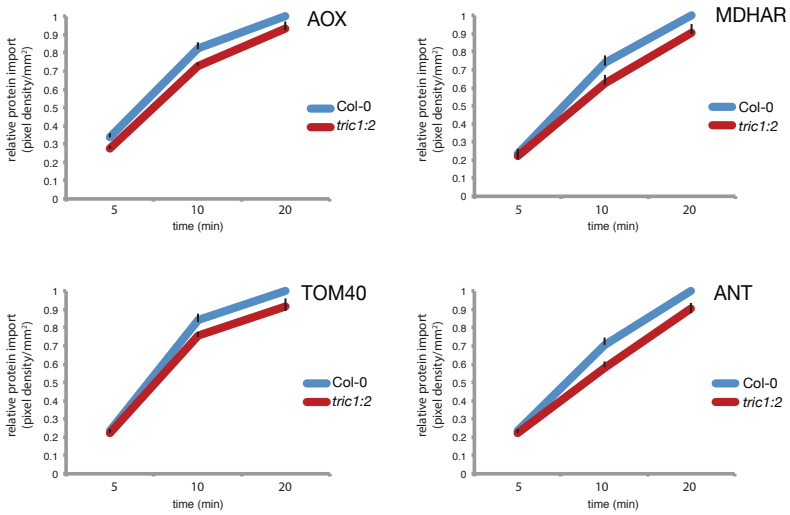

Figure 3.3.1 *In vitro* protein import into *tric1:2* mitochondria

A [^{35}S]-labelled precursor proteins AOX, TOM40, MDHAR and ANT were incubated with mitochondria isolated from Col-0 and *tric1:2* plants under conditions that support the protein import. Aliquots were removed at 5, 10 and 20 min and treated with pK. pK-protected mature radiolabeled protein was quantified at each time point. 100 µg of mitochondrial protein was used in each import reaction.

B Graphs representing the rate of the protein import as intensity of the mature products, protected by proteinase K. The maximal intensity of the replicates was normalised to one and other values expressed relatively. Experiments were conducted three times, giving three independent replicates.

A

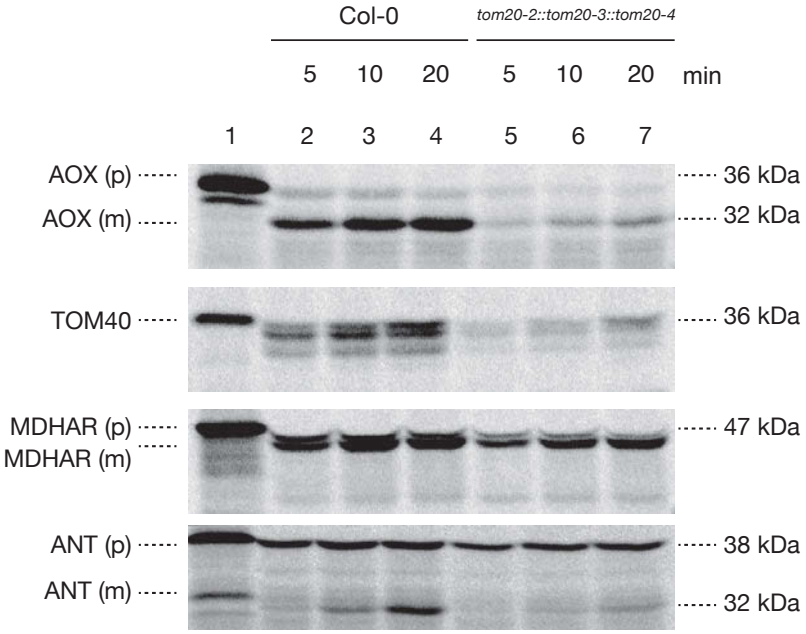

B

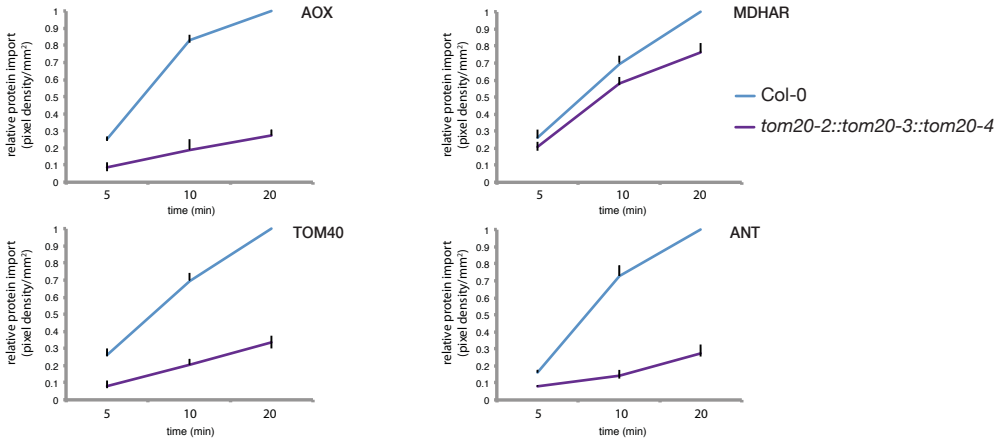

Figure 3.3.2 *In vitro* protein import into *tom20-2::tom20-3::tom20-4* mitochondria

A [^{35}S]-labelled precursor proteins AOX, TOM40, MDHAR and ANT were incubated with mitochondria isolated from Col-0 and *tom20-2::20-3::tom20-4* plants under conditions that support the protein import. Aliquotes were removed at 5, 10 and 20 min and treated with pK. pK-protected mature radiolabeled protein was quantified at each time point.

B Graphs representing the rate of the protein import as intensity of the mature products, protected by proteinase K. Quantification was carried out in three replicates. The maximal intensity of the replicates was normalised to one and other values expressed relatively.

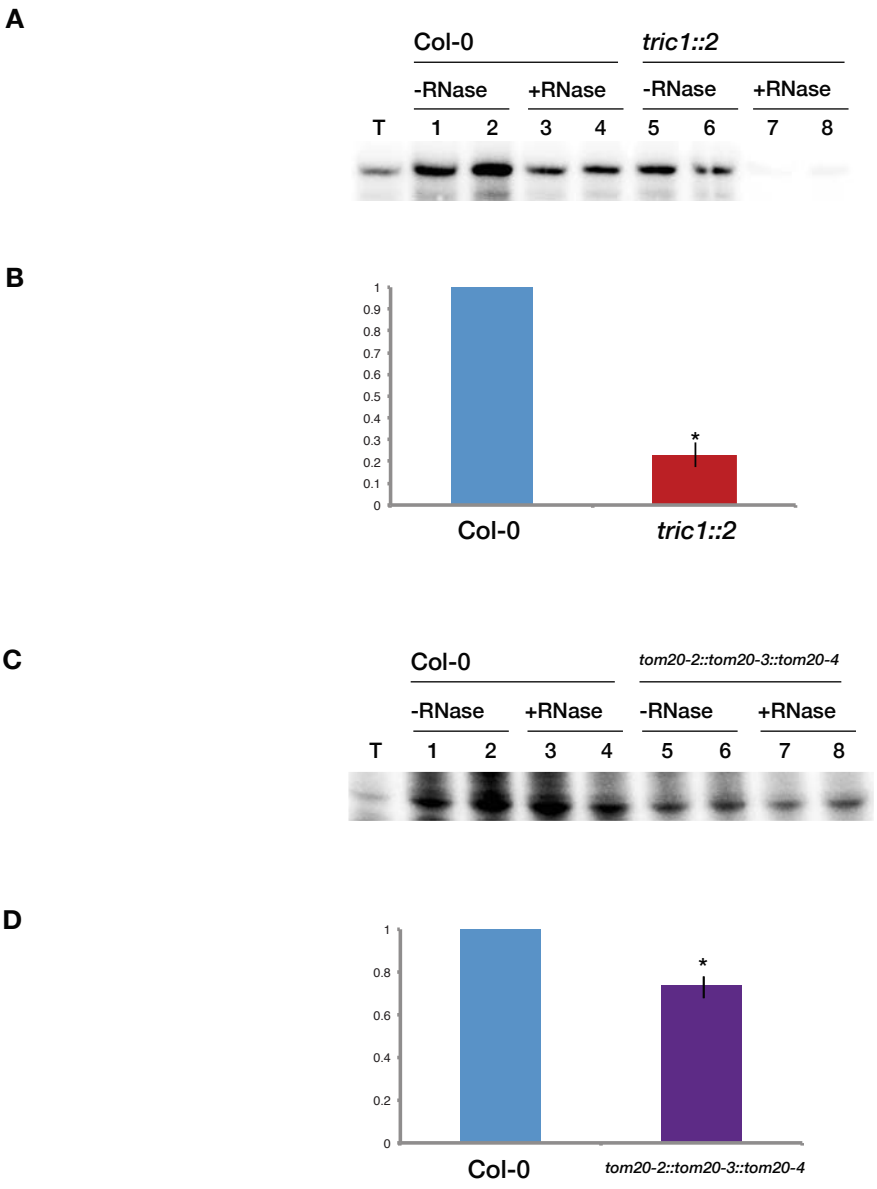

Figure 3.4 In vitro import of radiolabeled tRNA^{Ala}

A [^{32}P]-labeled tRNA^{Ala} was incubated with mitochondria isolated from Col-0 and *tric1::2* under conditions that support the tRNA import (see Chapter 2). Reactions were stopped after 20 min and treated with RNase mix to esure the bad corresponded to the size of the radiolaballed probe (T). Protected radiolabeled tRNA molecules were quantified.

B Graph representation of the tRNA import in *tric1::2* mitochondria in comparison to Col-0. The amount of import was measured as band intensity of the imported, RNase-protected substrate and quantified in three experimental replicates. Measurments were normalised by setting the maximal intensity to one. n=3, P value < 0.05, student's t test, +/- SE.

C [^{32}P]-labeled tRNA^{Ala} was incubated with mitochondria isolated from Col-0 and *tom20-2.3.4* under conditions that support the tRNA import (see Chapter 2). Reactions were stopped after 20 min and treated with RNase mix to esure the band corresponded to the size of the radiolaballed probe (T). Protected radiolabeled tRNA molecules were quantified.

D Graph representation of the tRNA import in *tom20-2.3.4* mitochondria in comparison to Col-0. The amount of import was measured as band intensity of the imported, RNase-protected substrate and quantified in three experimental replicates. Measurments were normalised by setting the maximal intensity to one. n=3, P value < 0.05, student's t test, +/- SE.

A

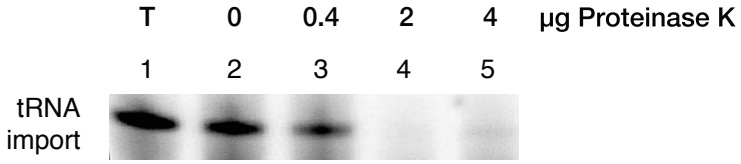

B

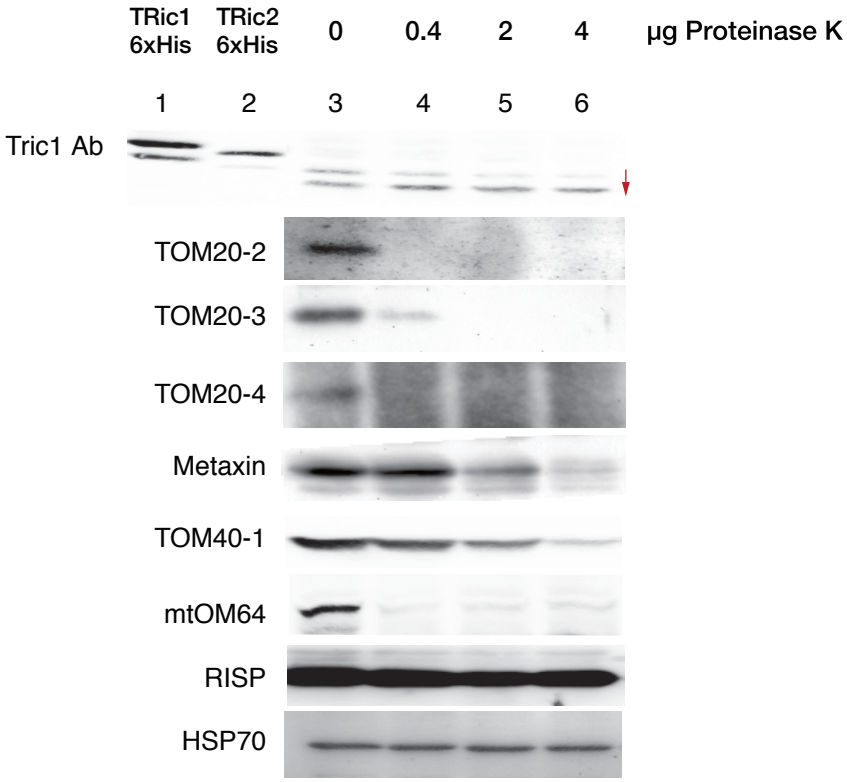

Figure 3.5 Import of tRNA^{Ala} is sensitive to pK

A Proteinase K (pK) titrations (0, 0.4, 2 and 4 µg) were carried out on mitochondria isolated from Col-0, followed by *in vitro* tRNA^{Ala} import assay as described in Chatper 2. The red arrow indicates the shift corresponding to the degradation of the putative receptor portion of TRic protein. TRic1 6xHis and TRic2 6xHis, recombinant proteins used to raise the TRic1 and TRic2 antibodies.

B Mitochondria were immunodetected with antibodies against TRic1, along with markers for peripheral outer membrane components (Tom20-2, 20-3, 20-4, metaxin), integral outer membrane components (Tom40), inner membrane components (RISP) and matrix located mtHSP70.

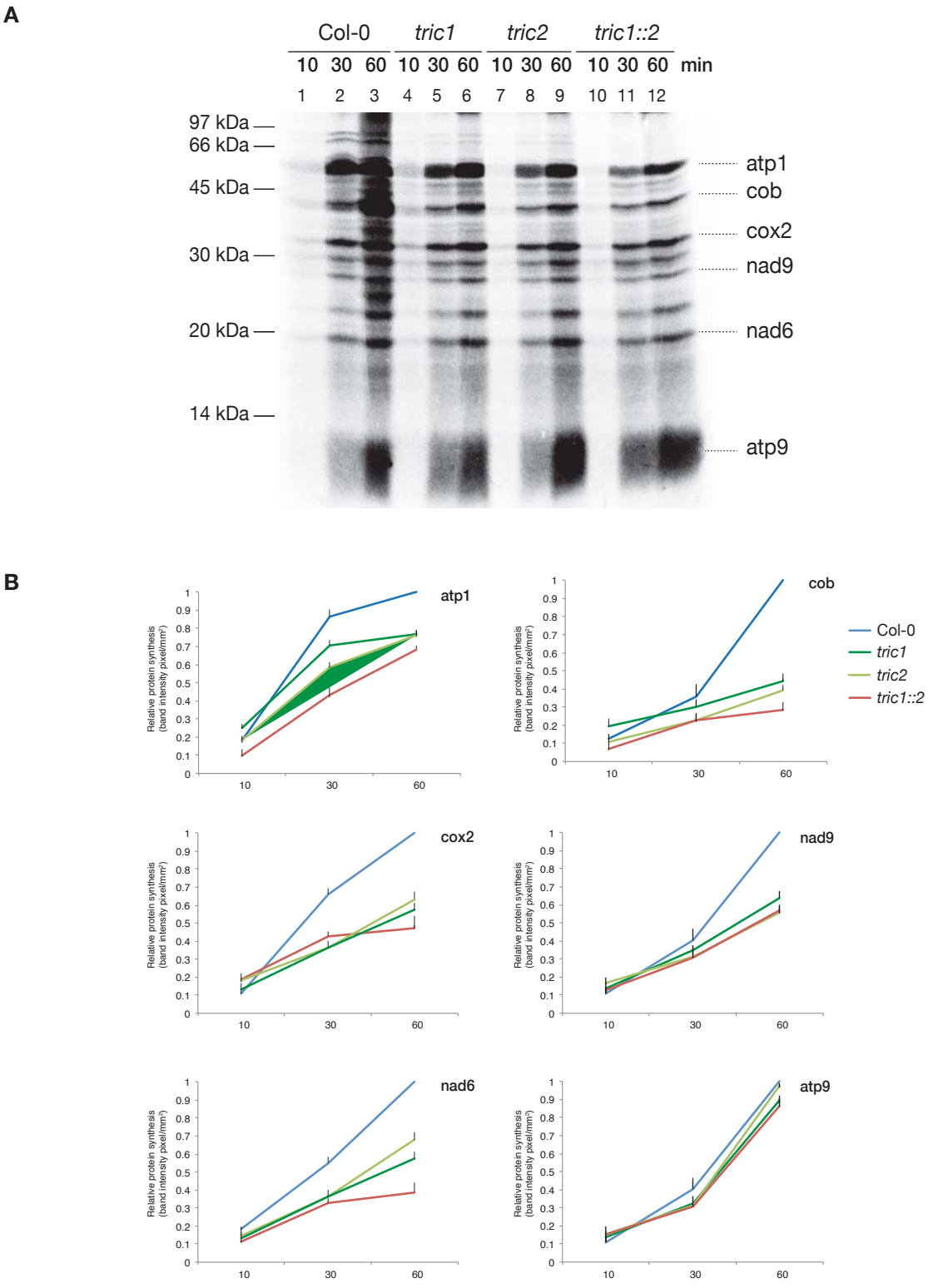

Figure 3.6 Analysis of mitochondrial *in organello* protein synthesis

A Mitochondria isolated from 14 day-old Col-0, *tric1*, *tric2* and *tric1::2* plants were subjected to *in organello* protein synthesis assay, which showed the incorporation of [^{35}S]-methionine into mitochondria-encoded proteins. Apparent molecular weight of mitochondria-encoded proteins as determined by previous studies is shown.
B The relative protein synthesis rate of *in organello* synthesis of mitochindria-encoded proteins was measured in triplicate and graphed. Band intensity was measured as pixel density/mm^2

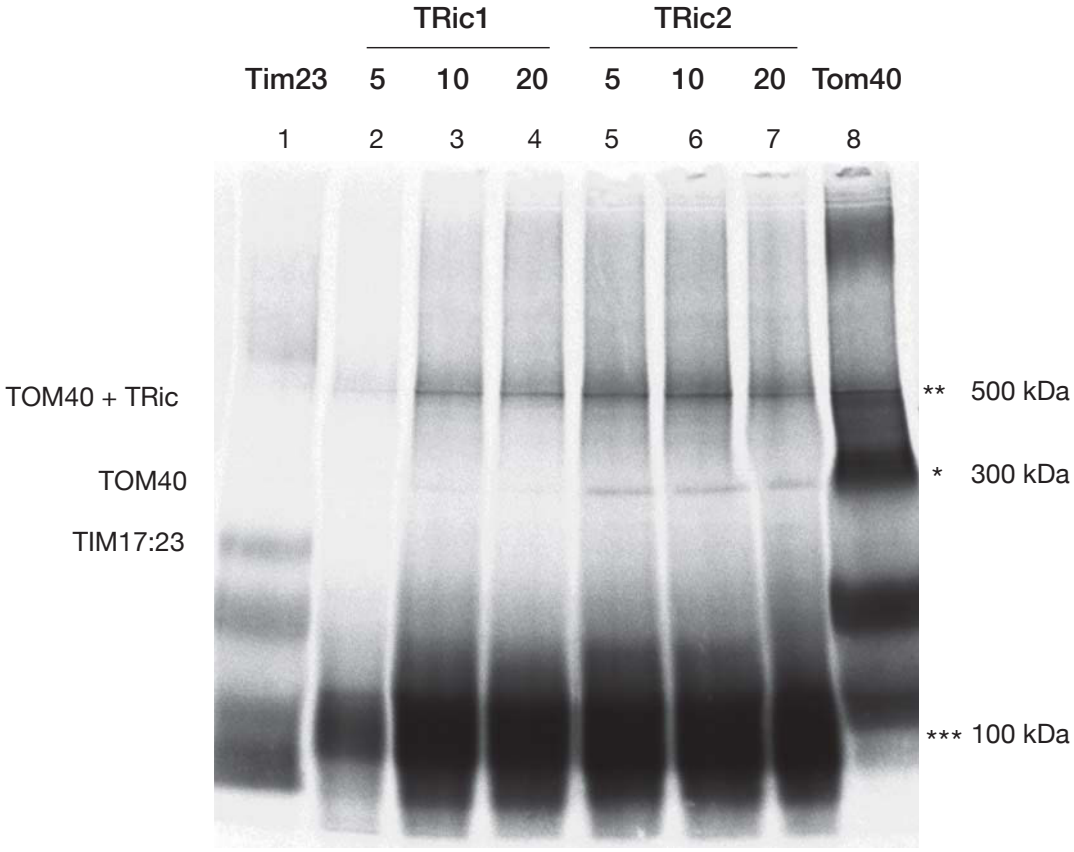

Figure 3.7 Association of TRic1 and TRic2 proteins into mitochondrial protein complexes

[^{35}S]-labeled TRic1 and TRic2 proteins were incubated with Col-0 mitochondria under conditions supporting the protein import. Blue Native PAGE of the time course analysis (min) of TRic1 and TRic2 import into isolated mitochondria was carried out. Incorporation of radiolabled proteins into TOM + TRics complex (**), TOM complex (*) and TIM17:23 complex (***) is indicated with the apparent mass of the complexes.

A

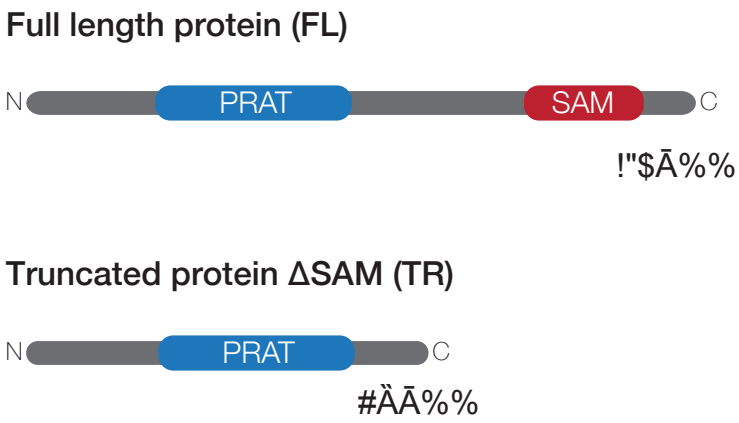

B

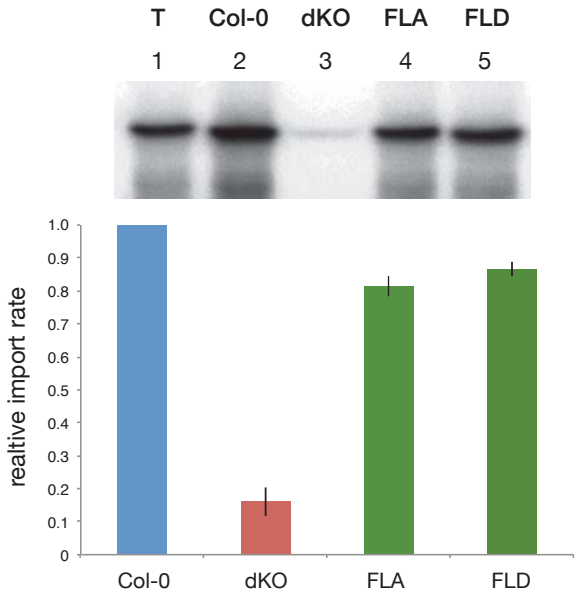

Figure 3.8.1 *In vivo* complementation of the TRic dKO line

A Diagrams representing constructs used in the complementation of TRic dKO line. Full lenght (FL) construct contained the full coding sequence of TRic2 (PRAT and SAM domains). Truncated (TR) construct contained first 150 aa of TRic2 (PRAT domain only). aa amino acid

B Mitochondria isolated from Col-0, dKO, FLA and FLD lines were incubated in the presence of $tRNA^{Ala}$ under conditions supporting the tRNA import as described in Chapter 2.

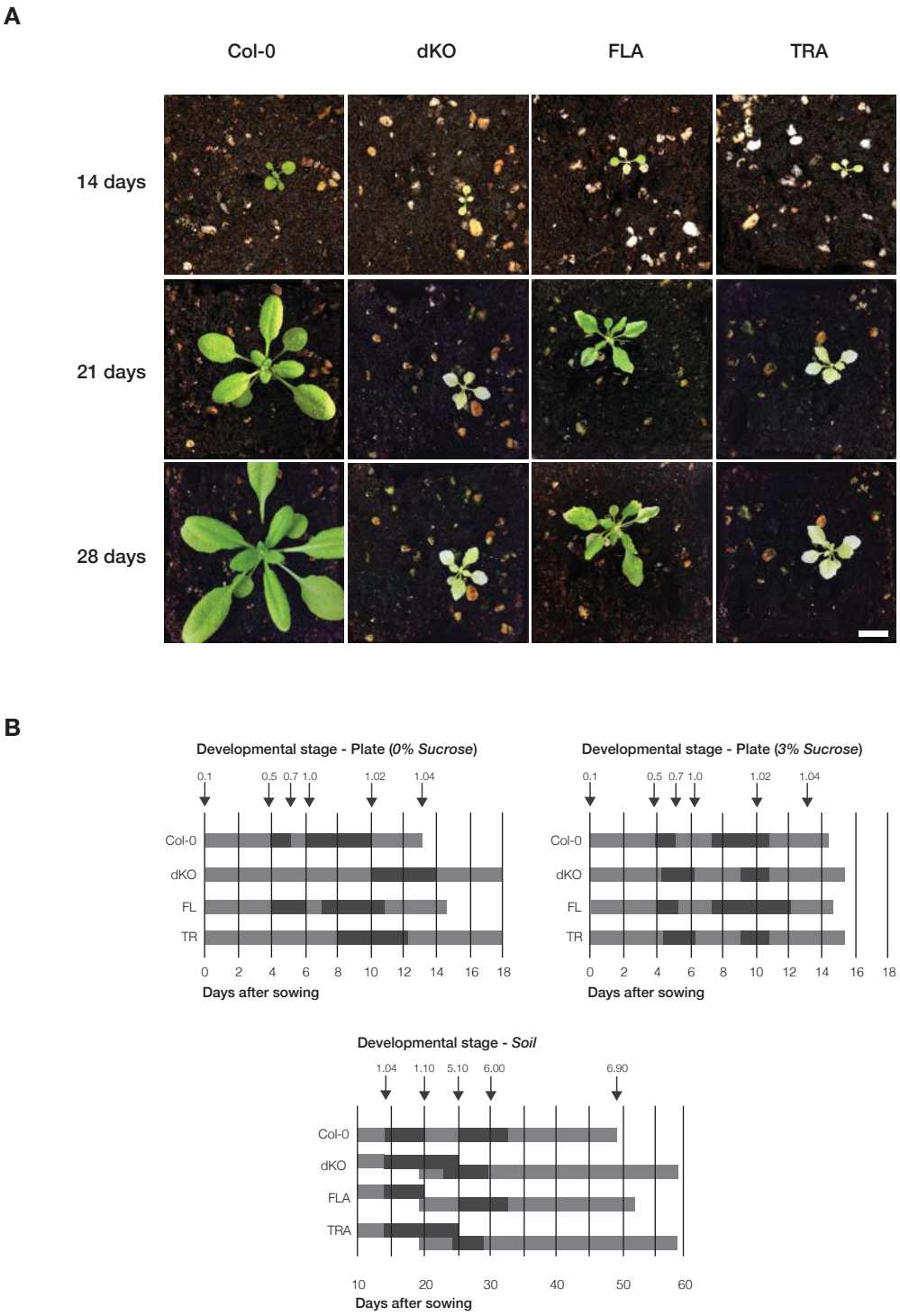

Figure 3.8.2 Quantitavie phenotyping of the TRic dKO complemented lines

A Growth phenotypes of Col-0, dKO, FLA and TRA plants after 14, 21 and 28 days in soil.

B Plate-based growth progression analysis of Col-0, dKO, FLA and TRA plants. Days after sowing are indicated by arrows, when Col-0 plants have reached the growth stages decribed in Boyes et al. (2001). Boxes define the time between growth stages and shading indicates the occurrence of each growth stage. Stage 0.1, imbibition; stage 0.5 radical emergence; stage 0.7, hypocotyl emergence from seed coat; stage 1.0, cotyledons fully opened; stage 1.02, two rosette leaves > 1mm in length; stage 1.04. four rosette leaves > 1 mm in length. Data is given as avarages for 10 plants. Days are relative to the days after sowing after a 3 d stratification at 4C (i). Plate-based growth progression analysis as in (i) on 3 % MS medium (ii). Soil-based growth progression as in (i): stage 1.10, 10 rosette leaves > 1 mm; stage 5.10, first flower bud visible; stage 6.0, first flower opens; stage 6.9, flowering complete (iii).

OM47

Chapter 4 – OM47

4.1 Introduction

The mitochondrial outer membrane formed in the process of endosymbiosis of the ancestral α-proteobacterium with the eukaryotic precursor cell [1]. The lipid composition of both membranes has changed significantly, however crucial protein functions have remained in part unchanged. Proteins of β-barrel topology are present in the outer membrane of Gram-negative bacteria and outer membranes of eukaryotic organelles (mitochondria and chloroplasts) and unlike Gram-negative bacteria, the outer membranes of mitochondria and chloroplast also contain α-helically anchored membrane proteins (reviewed in [211, 212]).

β-barrel topology is characterized by amphipathic and antiparallel β-strands, connected by loops, which creates the barrel-shaped structure across the membrane. Number of β-strands varies between different proteins of that topology and can be between 8-22 and average number of amino acids in one β-strand is between 8-11, which is sufficient to span across the membrane [213]. In bacteria β-barrel proteins predominantly mediate the exchange of metabolites, act as enzymes and virulence factors [214].

In yeast mitochondria, four β-barrel topology proteins have been identified: VDAC (two isoforms), Tom40, Sam50 and recently described Mdm10. VDACs have been characterized as major mediators between the cytoplasm and the mitochondria and their main function is the exchange of small metabolites, which are similar functions to the typical bacterial outer membrane β-barrel proteins [215]. As mentioned before, Tom40 proteins are core components of the TOM translocon and form the channel for the import of preproteins into mitochondria [216]. The third β-barrel-topology protein present in mitochondria is Sam50 (also known as Tob55), which acts as the pore of the SAM complex, responsible for sorting and assembly of other β-barrel proteins [217]. The Mdm10 protein, which has been described as involved in the maturation of mitochondrial outer membrane complexes, is also predicted to have the β-barrel structure and associates with the ERMES complex in yeast [218]. Moreover, it doesn't seem to

be present in other eukaryotes such as plants and mammals and has no homologs in bacteria, making it a fungi-specific β-barrel protein [98].

Recently a novel β-barrel outer membrane mitochondrial protein in *Trypanosoma brucei* mitochondria has been identified and named tripartite attachment complex 40 (TAC40). Unlike other eukaryotes, trypanosomes possess a single mitochondrion with a singe-unit genome connected to the flagellum. TAC40 localizes to the connection site of the genome and the flagellum and it has been described as essential for mitochondrial genome inheritance in *T. brucei*. Interestingly, TAC40 is not specifically related to any of the other β-barrel proteins mentioned above [219].

Most of the β-barrel proteins are highly conserved across all species and fulfil a variety of essential functions. It is however of particular importance to study β-barrel proteins, which evolved specific functions and are specific to particular groups of organisms. A recent in depth study of highly purified mitochondria analysed by shotgun mass spectrometry identified a novel β-barrel protein in the mitochondrial outer membrane of Arabidopsis [181], which was named the outer membrane protein 47 (OM47) and is encoded by At3g27930 gene.

4.2 Aims

The aim of this set of experiments was to investigate the function of OM47. Phylogenetic analysis suggests that OM47 is a plant specific protein and it was of interest to determine, what specific roles OM47 confers in plant mitochondria. Absence of OM47 in plants resulted in no obvious phenotype. Analysis of *OM47* gene expression profiles suggested a putative role of OM47 in the senescence process, which was further characterised by a variety of physiological assays. To functionally characterize the OM47 protein the following approaches were undertaken.

1. Bioinformatic analysis of OM47
2. Functional complementation of yeast YNL055c (*por*$^{-}$) strain
3. Characterization of the T-DNA insertion lines
4. Localization of OM47
5. *In vitro* import of various protein precursors
6. Mitochondrial outer membrane protein composition
7. Dark induced senescence assay
8. Starch and reactive oxygen species (ROS) determination

4.3 Results

4.3.1 Bioinformatic analysis of OM47 protein

The amino acid sequence of OM47 protein was retrieved from The Arabidopsis Information Resource (TAIR, http://www.arabidopsis.org/) TAIR10 genome release. The Conserved Domain Database (CDD) [184] indicated that OM47 belongs to the eukaryotic mitochondrial outer membrane porin family (Porin3 super family) as it contains the Porin3 motif within amino acids 183-361 (Figure 4.1 A) [184]. The β-strands of the OM47 protein were identified using the PRED TMBB (http://bioinformatics.biol.uoa.gr/PRED-TMBB/) based on a Hidden Markov Model [186]. Sequences corresponding to 18 putative β-strands (amino acids: 33-41, 60-68, 74-84, 96-104, 109-117, 122-130, 133-141, 156-162, 165-173, 18-201, 204-214, 233-243, 249-259, 273-289, 301-309, 324-332, 336-346 and 359-371) were indicated in red. Loops predicted outside of the membrane were indicated in blue while loops inside of the membrane were indicated in green (Figure 4.1.1 A). The 2-dimension (2D) prediction of β-strands of OM47 was generated by PRED TMBB (http://bioinformatics.biol.uoa.gr/PRED-TMBB/) based on a Hidden Markov Model (Figure 4.1.1 B).

Primary amino acid sequences of OM47, Tom40 and VDAC from Arabidopsis were compared for similarity and identity scores using the Matrix Global Alignment Tool (MatGAT) version 2.01 as described in Chapter 2. The similarity scores between OM47 and Tom40-1, Tom40-2, VDAC1, VDAC2, VDAC3 and VDAC4 were estimated at 34 %, 36 %, 33 %, 30 %, 33% and 29 % respectively while identity scores were estimated at 18 %, 17 %, 19 % 15 %, 18 % and 17 % respectively (Figure 4.1.2 A).

A search for all putative OM47 orthologs was carried out as described in Chapter 2. The BLASTP search [188] against *Homo sapiens* (human, http://www.hprd.org), *Caenorhabditis elegans* (roundworm http://www.wormbase.org), *Neurospora crassa* (mould, http://www.ncbi.nlm.nih.gov), *Dictyostelium discoideum* (slime mould, http://dictybase.org/) and *Saccharomyces cerevisiae* (budding yeast http://www.yeastgenome.org) in their respective databases revealed no direct orthologs to OM47. The search was continued using genome databases such as:

Phytozome v9.1 (http://www.phytozome.net/), Cyanidioschyzon merolea Genome Project (http://merolae.biol.s.u-tokyo.ac.jp/) and Online resource for community annotation of eukaryotes OrcAE (http://bioinformatics.psb.ugent.be/orcae/overview/Ectsi) for various plant species (including green algae), *Cyanidioschyzon merolea* (red algae) and *Ectocarpus siliculosus* (brown algae) according to the parameters described in Chapter 2. It was concluded that OM47 is specific to photosynthetic eukaryotes and was identified in 16 plant species (including green algae) and is not present in human, roundworm, mould, slime mould and budding yeast. Direct orthologs of OM47 are also absent in red and brown algae suggesting their important role in the early evolution of land plants. The phylogenetic trees were drawn as described in Chapter 2 using MEGA 5.2.2 [189]. The full-length protein alignments were generated using the Clustal option followed by the generation of the phylogenetic tree using the maximum likelihood tree setting according to the Jones-Thornton-Taylor model after 1000 replications (Figure 4.1.2 B).

4.3.2 Functional complementation of yeast mutant YNL055c

To find out whether OM47 has the ability to function as a VDAC protein a complementation experiment was carried out according to the experimental design described in [220]. A yeast mutant strain lacking VDAC1 protein (*por*$^{-}$) (YNL055c) [221] and wild type yeast strain (BY4742) were used in this experiment. YNL055c exhibits delayed growth on non-fermentable media such as the ones with glycerol as the exclusive carbon source however it grows well on media with glucose. In order to test the hypothesis that OM47 can functionally replace a VDAC protein, a full length coding sequence of OM47 was cloned into yeast vector pAG426GPD [222] under the constitutive promoter GPD and URA3 selectable marker and transformed into the YNL055c line. Additionally, the YNL055c line was transformed with yeast VDAC1 protein as the functional control. BY4742, YNL055c and transformed strains (YNL055c + ScVDAC and YNL055c + AtOM47) were plated on media with 2 % (w/v) glucose or 2.5 % glycerol as sole carbon source. As anticipated all four transformed strains were growing well on media with glucose. BY4742 strain grew well on media with glycerol while

YNL055c did not grow in glycerol medium as shown previously [221]. YNL055c yeast strain expressing AtOM47 protein was capable of growth in media containing glycerol as the sole source of carbon similarly to YNL055c strain transformed with ScVDAC (Figure 4.2). These results suggest that AtOM47 can functionally replace the yeast VDAC1.

4.3.3 Characterization of the *om47* lines

The initial screening and genotyping of the knock out lines in At3g27930 was performed by Dr Owen Duncan, who obtained the mutant lines from: The Arabidopsis Biological Resource Centre (http://abrc.osu.edu/) and the Genomanalyse im biologischen System Pflanze (http://www.gabi-kat.de/). The following lines: SALK_016767 (knockout 1, KO1) and GABI_369G03 (knockout 2, KO2) insertion lines were screened and homozygous lines were obtained by PCR-based genotyping using specific primers designed with T-DNA Primer Design (http://signal.salk.edu/tdnaprimers.2.html) (Figure 4.3 A). These plants were grown in long day conditions as described previously. A detailed phenotypic analysis was carried out according to [206] on both soil and MS media with and without sucrose supplement, (long day conditions: 16 hour day/8 hour night at 22°C under 100 µmol m^{-2} s^{-1} light intensity).

Growth on MS media with 0 % (w/v) sucrose indicated that none of the *om47* lines exhibited any significant phenotype under the parameters tested and all three lines (Col-0, KO1 and KO2) reached the radical emergence stage (0.5) on average four days after sowing (Figure 4.2 Ai). On average, both *om47* lines reached the opened cotyledons stage (1.0) one day later than Col-0 plants however all three lines completed the principal growth stage 1 after 14 days from sowing at which point they were transplanted to soil for further phenotypical analysis (Figure 4.3 B iii). Similar growth pattern was observed for all three lines, when grown on MS media with 3 % (w/v) sucrose (Figure 4.3 B ii).

The soil-based phenotyping was initiated at 14 days following sowing and stratification and indicated that all three lines reached the 10 rosette leaves stage (1.10) at day 18 and first flower visible stage (5.10) at day 24 however *om47* lines didn't reach the first flower open stage (6.0) until day 35, which was on average 5

days after Col-0. Both *om47* lines showed delayed flowering time and didn't complete it until day 55, which was on average 6 days after Col-0 (Figure 4.3 B iii).

Total mitochondrial protein was isolated from each of the *om47* lines and from Col-0 plants and analysed by SDS-PAGE and immunodetection. 20 and 40 µg of mitochondrial proteins were loaded to ensure semi-quantitative results. Immunodetection was performed using the polyclonal antibody raised against the full length OM47 protein. The recombinant OM47 protein expressed with the poly-histidine tag (R) was run as a control (Figure 4.3 C, lane 1). The intensity of bands was measured (pixel density/mm^2) for each of the lanes. The maximal intensity (Figure 4.3 C, lane 3) was normalised to one and other values were expressed relatively. A decrease to approximately 1 % was observed for *om47* mitochondria (Figure 4.3 C, lanes 4-7). These western blots show that insertions in both *om47* lines resulted in the absence of the OM47 protein (47 kDa).

4.3.4 Subcellular localization of OM47

In order to confirm the outer membrane localization of OM47, the full-length coding sequence was cloned and fused to C-terminal green fluorescent protein (GFP) and transiently transformed into Arabidopsis Col-0 suspended cell culture using biolistic gene gun (see Chapter 2) along with the mitochondrial matrix-targeted red fluorescent protein control AOX:RFP. As reported previously, mitochondrial outer membrane localisation can be studied by GFP-tagging and visualised by fluorescent microscopy as a characteristic green ring around the red mitochondria [181].

A second line of evidence for mitochondrial outer membrane localization of OM47 was carried out using *in vitro* protein import experiments (Figure 4.4 B). The full-length OM47 protein was cloned under a T7 promoter and translated using the rabbit reticulocyte lysate and radiolabelled with [^{35}S]-methionine. Translation of OM47 indicates the production of a protein band resolving at 47 kDa, which is similar to the endogenous protein size of 47 kDa (Figure 4.2 C). Radiolabelled protein was incubated with freshly isolated Col-0 mitochondria under conditions that support protein uptake [192]. Import was also carried out in the presence of valinomycin, an ionophore, which dissipated the membrane

potential and prevents protein import. The mitochondria were treated with pK in order to digest the external protein in case of rapture of mitochondria and release of MPP, which could cause protein processing unspecific to the protein import.

Incubation of mitochondria (M) with the radiolabelled protein (P) resulted in import (lane 2), which was indicated by a presence of band, which corresponded to the size of the radiolabelled protein (lane 1). Reactions were treated with pK (lanes 3), valinomycin, Val (lane 4) or both (lane 5). Subsequently mitoplasts were generated and treated as described above (Figure 4.4 B lanes 6-9). These results indicated that OM47 is imported into the mitochondrial outer membrane as visible in lane 3 but not in lane 5 and is not present in mitoplast lanes.

Finally, protease titrations where carried out. Radiolabelled OM47 was imported into Col-0 mitochondria, which were subsequently treated with increasing amounts of pK from 0 µg pK, to 6.5 µg pK. Upon import and increased pK degradation, the band corresponding to the radiolabelled protein decreases in signal intensity (lanes 1-5). Additionally, the same pK-treated mitochondria were immunodetected using polyclonal antibodies against OM47 and Tom20-2 (as a marker of a peripheral outer membrane component) (Figure 4.4 C). The gradual disappearance of the OM47 signal suggests that OM47 is an integral mitochondrial outer membrane protein unlike Tom20-2, which is a cytosolically facing, peripheral attached protein.

4.3.5 Depletion of OM47 does not influence the *in vitro* protein import

As OM47 is an integral mitochondrial outer membrane protein of β-barrel topology it was of interest to test whether it could be potentially involved in the process of import of protein precursors into mitochondria similarly to a known β-barrel protein Tom40. Protein precursors selected for the *in vitro* protein import experiments included an N-terminal presequence-containing protein (AOX), a plant carrier protein (ANT), a β-barrel protein (TOM40) and a dual-targeted to mitochondria and chloroplasts monodehydroascorbate reductase (MDHAR). *In vitro* translation of these proteins using the rabbit reticulocyte lysates in presence of [^{35}S]-methionine resulted in products of 36 kDa, 38 kDa, 30 kDa and 47 kDa respectively. Incubating precursor proteins with mitochondria isolated from Col-0,

KO1 and KO2 plants resulted in the accumulation of the processed, mature form of the protein, which was measured as the rate of the protein import as described in Chapter 2 and sampled over a time course of 5 (lanes 1-3), 10 (lanes 4-6) and 20 (lanes 7-9) minutes in order to determine the rate of protein uptake into mitochondria from Col-0 and KO1 and KO2 plants. The reactions were treated with pK following import to digest precursor protein external to the mitochondria outer membrane. Products of the reactions were separated by SDS-PAGE and imaged by storage phosphor autoradiography as described in Chapter 2 (Figure 4.5 A). Intensity of the mature products, protected by pK, was quantified over three biological replicates. The maximal intensity of the replicates was normalised to one from Col-0, and other values expressed relatively. The normalised results were graphed (Figure 4.5 B, $p<0.05$, +/- SE).

No significant changes in the rate of protein import could be observed between Col-0 and KO1 and KO2 at any time points tested suggesting that OM47 is not a component required for mitochondrial protein import and that deletion of OM47 does not alter the protein import pathways.

4.3.6 Mitochondrial outer membrane protein composition of *om47* lines

Mitochondria from Col-0 and *om47* plants were isolated and subjected to SDS-PAGE for immunodetection against a variety of mitochondrial outer membrane proteins such as Tom40, Sam50 and VDAC (all markers of integral, β-barrel proteins). Moreover Tom20-2, Tom20-3 and Tom20-4 proteins were tested (as markers of peripheral outer membrane components). 20 and 40 µg of mitochondrial proteins were loaded to ensure semi-quantitative results. No changes in the amount of Tom40, Tom20-2 and Tom20-3 proteins were observed in the mitochondria isolated from the *om47* lines. A decrease of about 40 % and 50 % in Sam50 protein abundance was observed in KO1 and KO2 lines respectively (Figure 4.6 lanes 3-4 and 5-6) comparing to Col-0 (lanes 1-2). An increase of about 50 % and 40 % of Tom20-4 abundance was observed in KO1 and KO2 lines respectively. Similarly an increase of about 30 % of VDAC abundance was observed in *om47* lines comparing to the Col-0 mitochondria (Figure 4.6).

4.3.7 Blue Native PAGE analysis of OM47

In order to determine the association of OM47 protein within mitochondrial protein complexes Blue Native-PAGE (BN-PAGE) analysis of mitochondria isolated from Col-0, KO1 and KO2 plants was carried out as described in Chapter 2. After separation, proteins were transferred onto a PVDF membrane and used for immunodetection using OM47 and Tom40 polyclonal antibodies. Detection against OM47 resulted in a single band at approximately 150 kDa (Figure 4.7 A, lane 1). No band was detected in mitochondrial isolated from KO1 and KO2 lines (Figure 4.7 A, lanes 2 and 3 versus 1). The Tom40 complex was detected in all three lines and appeared unchanged in *om47* lines compared to Col-0 (Figure 4.7 A, lanes 4-6). A Coomassie stain of the BN-PAGE gel shows equal protein abundances and no significant changes in the abundance of any detectable protein complexes such as the respiratory complexes I, V, III and supercomplex I+III indicated on the left (Figure 4.7 A, 7-9). These results suggest that OM47 does not co-migrate with Tom40 and could be in a complex by itself. Additionally a large-scale *in vitro* protein import assay into isolated Col-0 mitochondria, using radiolabelled OM47 proteins was carried out and analyzed by BN-PAGE as described in Chapter 2 (Figure 4.7 B). This assay was carried out to confirm the incorporation of OM47 into the protein complex of 150 kDa (marked as *) and to characterize the assembly of this protein complex in a time-dependent manner. A time-course experiment was performed, where import was carried out for 10, 20 and 40 minutes followed by BN-PAGE analysis (Figure 4.7 B, lanes 1-9). Radiolabelled Tom40 (lane 10) was used as a control. The resulting products were resolved on BN-PAGE and imaged as described above. The Tom40 can be seen to incorporate into a protein complex at about 300 kDa (Figure 4.7 B, lane 10, marked as **) whereas OM47 is incorporated into a complex of 150 kDa. The intensity of incorporation is seen to increase in a time-dependent manner suggesting that the band visualized is a result of import and not due to non-specific incorporation of radiolabelled methionine. Additional bands can be observed at 500, 600 and 1000 kDa (indicated by #) and are likely to be a result of non-specific incorporation of radiolabelled methionine. It is interesting to note that the intensity of incorporation of OM47 is less into mitochondria isolated from KO1 and KO2 (Figure 4.7 B). The apparent molecular weight markers are indicated

as well as the location of the respiratory chain complexes as determined by Coomassie stain.

4.3.8 Plants depleted of OM47 exhibit a delayed senescence phenotype

The lack of the visible phenotype of the OM47 depleted plants invited for a comprehensive gene expression analysis of OM47 expression patterns using the GENEVESTIGATOR plant biology tool (https://www.genevestigator.com/gv/plant.jsp). This search revealed that while OM47 gene expression is at medium levels throughout most developmental stages, it is significantly high in the last stage of development i.e. the senescence (Figure 4.8 A).

The loss of chlorophyll as well as yellowing of leaves is a distinct trait of the plant senescence process [223]. In order to assess the putative function of OM47 in the senescence process in Arabidopsis, a dark induced senescence experiment was carried out. Leaves from 4-week-old Col-0 and *om47* plants were excised and covered with foil in order to deplete them of light for three days (Figure 4.8 B). The chlorophyll content was measured before (0 d) and after (3 d) treatment using a SPAD 500 chlorophyll meter. Chlorophyll content measured at 0 d from Col-0 was normalised to one and values obtained were expressed relatively (Figure 4.8 C). The measurements were carried out in biological triplicate and standard errors are shown (n=3, $p<0.05$, +/- SE). These results showed that chlorophyll content in leaves from *om47* plants degraded to about 90 % and 92 % in KO1 and KO2 respectively after 3 days of darkness while in Col-0 leaves the degradation was observed at 50 % after 3 days (Figure 4.8 C).

4.3.9 Determination of reactive oxygen species and starch content in leaves of *om47* plants before and after the dark-induced senescence treatment

Senescence can be triggered by a variety of external factors such as drought, extremes of temperature and darkness and one of the earliest responses of plant cells to various biotic and abiotic stresses as well as during senescence is

the burst of large quantities of reactive oxygen species (ROS) such as superoxide, hydrogen peroxide, hydroxyl radicals and singlet oxygen [197]. To determine the production of cellular ROS in leaves of *om47* plants, 4-week-old leaves were stained with 600 µM nitroblue tetrazolium (NBT) to visualize the superoxide anions (O_2^-), followed by incubation in 80 % (v/v) ethanol to remove the chlorophyll. Leaves were collected from plants grown in standard conditions as described in Chapter 2 as well as from plants subjected to the dark-induced senescence. These results showed there are no observable differences in steady state levels of ROS in untreated Col-0 and *om47* plants (Figure 4.9 A). The same assay was carried out on leaves following a 3-day dark-induced senescence treatment (Figure 4.9 B). The production of ROS in *om47* plants was less evident than in Col-0 leaves when senescence was induced.

In addition starch content was determined in 4-week old rosette leaves from Col-0 and *om47* plants collected in the morning (AM) and evening (PM) in order to determine the starch content. It was observed that leaves collected from *om47* plants in the morning showed a higher content of starch then Col-0. Leaves collected in the evening showed no observable differences between Col-0 and *om47* lines (Figure 4.10 A). These results suggest that *om47* plants are able to retain starch. Similarly differences in starch content could be observed with Col-0 leaves, comparing to *om47* plants both in the morning (AM) and in the evening (PM). Starch content in Col-0 leaves seems to be much lower after 3-day dark-induced senescence treatment in the morning (AM) and in the evening (PM). Leaves of *om47* plants seem to retain starch after 3 days of dark induced senescence in the morning and the evening (Figure 4.10 B).

4.4 Discussion

Comparing to the diversity of β-barrel membrane proteins in prokaryotic organisms, number of mitochondrial outer membrane proteins classified as this structural type is much more limited. Some predictions propose that yeast mitochondrial outer membrane could contain up to 100 β-barrel proteins [213] but latest proteomic and bioinformatic studies suggest the number is much smaller. Generally in all eukaryotes there is a number of highly conserved β-barrel proteins

such as VDACs, Tom40 and Sam50, which all confer vital functions in mitochondria. It is becoming increasingly evident that in various groups of organism, specific β-barrel proteins evolved to perform specific roles tailored for specific needs of these organisms such as fungi-specific Mdm10 or trypanosome-specific TAC40 [98, 219]. Prior to these experiments, the number of known β-barrel proteins in Arabidopsis mitochondria was as follows: four VDAC isoforms expressed (from six predicted genomic sequences) [224], two isoforms of Tom40 (of which Tom40-1 is the prevalent isofom and known to be essential [72]), and two isoforms of Sam50 [18]. These experiments have confirmed that an additional β-barrel protein encoded by a single gene, At3g27930, termed outer membrane protein 47 (OM47) is located in the outer mitochondrial membrane.

Bioinformatic analysis of OM47 revealed it belongs to the Porin3 superfamily, a eukaryotic porin family that forms channels in the mitochondrial outer membrane (Figure 4.1 A), and also contains VDAC and Tom40 proteins. However, unlike these highly conserved β-barrel proteins, OM47 is not conserved across all mitochondria-containing organisms but it appears to be a plant specific protein as indicated by the phylogenetic studies. Direct orthologs of OM47 were found in all 16 plant species analysed including the early plant taxa such as *Chlamydomonas reinhardtii* and *Volvox carteri.* This is indicative of this protein putative involvement in the early evolution of photosynthesizing eukaryotes. As indicated by the protein sequence similarity and identity scores obtained using MatGAT (Figure 4.1.2 A) OM47 could be a distant relative of other protein members of this porin superfamily such as Tom40 and VDAC. Interestingly, obtained *om47* lines in At3g27930 didn't produce any drastic phenotype as shown by the quantitative phenotyping, despite the confirmed absence of the protein in *om47* mitochondria, however it was observed that *om47* lines flowering time was extended (Figure 4.2). As mentioned before, OM47 has been identified as a mitochondrial outer membrane protein initially identified by a mass spectrometry study of the Arabidopsis mitochondrial outer membrane proteome and confirmed by GFP-tagging [181]. Subsequent *in vitro* import assays of radiolabelled OM47, pK titrations and immunodetection confirm the location of OM47 in the mitochondrial outer membrane and suggest it is an integral membane protein.

It was of interest to establish whether OM47 can be involved in functions similar to those of other known β-barrel proteins such as Tom40 and VDAC. Protein import assays into *om47* lines did not result in any significant changes in the import rate of any of the tested precursors suggesting that it is not likely to be involved in the process of translocation of tested protein precursors across the outer membrane. Furthermore, it has been previously shown that the depletion of AtTom40-1 protein results in embryo-lethality [72] while results presented here show no obvious deleterious effects in *om47* plants. Therefore most likely OM47 doesn't act as a protein import channel.

Voltage-dependant anion channel (VDAC) is known to be a highly conserved mitochondrial outer membrane protein present in all eukaryotes and is the most abundant protein in the outer membrane and as such it is a crucial component of the traffic of metabolites and anions across the outer membrane [225]. Moreover, despite its conserved function among fungi, animals and plans, its amino acid sequence homology between these groups is relatively low [226]. *In vivo* complementation of yeast VDAC1 knock out strain (YNL055c) was carried out to assess whether OM47 can functionally replace the yeast VDAC1. YNL055c cells are incapable of growth on media with glycerol as the only source of carbon unlike the wild type yeast cells (BY4742). It has been shown previously that four Arabidopsis VDAC isoforms are capable of complementing the yeast VDAC knock out strains and act as VDAC in the yeast mitochondrial outer membrane, despite the relatively low primary amino acid sequence similarity [220]. Results presented here suggest that similarly, despite its low amino acid sequence similarity and identity to AtVDACs, OM47 can also functionally replace the yeast VDAC1. This raises the question whether OM47, a plant specific protein, originally diverged from the VDAC family of proteins to perform an additional plant specific function.

It is becoming more evident that various mitochondrial processes such as core metabolic pathways like the tricarboxylic acid cycle (TCA), oxidative phosphorylation-driven ATP synthesis, electron transport chain, protein import machinery and their regulation, while being conserved in all organisms, differ substantially in plant mitochondria. Because of the immobile lifestyle, plants had to evolve to adapt to changing environments and as a result, plant mitochondria acquired unique metabolic functions comparing to other species such as

biosynthesis of ascorbate [227], folate [228] or thymidylate [229] and most notably the alternative respiratory pathway [230]. Moreover mitochondria are recognised as important mediators in aging and cell death however molecular mechanisms of these processes are still largely unknown [231] in plants. Gene expression study using the GENEVESTIGATOR Plant Biology tool revealed that while expression profile of *OM47* is stable and at consistent levels during Arabidopsis development it increases during senescence hence a dark-induced senescence assay was carried out. Results obtained showed that senescence-related chlorophyll breakdown in *om47* lines is decreased as compared to Col-0. Similarly the breakdown of starch and reactive oxygen species production was decreased in the *om47* lines before and after the dark-induced senescence. In the recent years it has been suggested that mitochondria produce reactive oxygen species and reactive nitrogen species as signalling molecules during stress acclimation [232, 233]. Chlorophyll breakdown is accepted as one of the fundamental and earliest indicators of the leaf senescence process [223] in which either as a result of development (natural aging) or an external factor (biotic and abiotic stresses), the leaf enters the senescence programme. As an adaptation to immobile lifestyle, plants often face nutrient limitations, which they deal with by sacrificing leaves and other organs, recycling the nutrients and relocating them to the rest of the plant. It has been suggested that individually darkened leaves of Arabidopsis enter the senescence programme where mitochondria actively provide energy and carbon molecules for the process of degradation of cell constituents, which leads to the retrieval of nutrients [234]. It is also becoming increasingly evident that mitochondria in plants can act as stress receptors in the cell and signal to the nucleus to activate expression of responsive genes to sustain or restore the cellular functions in response to stresses, which is described as the mitochondrial retrograde regulation [56-58]. These characteristics suggest that mitochondria are crucial components of the recognition of stress stimuli, production of intercellular signals to other parts of the cell and partake in the senescence. Perhaps OM47, as plant specific protein, evolved specifically to mediate the signalling of senescence either as a transporter of signalling molecules or by interacting with other unknown protein components.

Immunodetection of various previously studied outer membrane proteins from Arabidopsis mitochondria was carried out to see if depletion of OM47 causes any changes in the mitochondrial outer membrane makeup. Antibodies against integral (Tom40, Sam50, Porin) as well as peripheral (Tom20 isoforms) outer membrane proteins were used. It was concluded that in the absence of OM47, an increase in the abundance of Porin (VDAC) can be observed, which could be explained by overcompensation due to some shared functions between these two β-barrel proteins. Interestingly, it was also shown that Tom20-4 isoform was more abundant in the *om47* lines while Sam50 isoforms were down. As SAM complex is involved in assembly of β-barrel proteins in mitochondria, which have to be imported via TOM complex, so perhaps the increase in Tom20-4 abundance can be explained by overcompensation in the absence of OM47. It is interesting to note, that immunodetection in *tom20-4* plants showed slight down-regulation of VDAC in isolated mitochondria [86].

BN-PAGE study was performed to determine the association of OM47 within mitochondrial protein complexes. Results presented here suggest that OM47 doesn't co-migrate with Tom40 complex as shown by the western blot and the import of radiolabelled precursors. The time-course import of radiolabelled OM47 into Col-0 and *om47* lines showed that assembly into its putative complex is decreased when OM47 is knocked out, This decrease in the rate of assembly may be explained by the down-regulation of Sam50 which is required for the import of all β-barrel proteins into mitochondria [217].

In conclusion, OM47 is a plant specific, β-barrel mitochondrial outer membrane protein, which is not implicated in the import of tested proteins. It has the ability to functionally complement the VDAC protein in yeast and seems to be involved in the senescence process. As this project is in its infancy there is still a number of question, which have to be addressed such as what exact proteins does OM47 interact with and what are the putative protein complexes it associates with. Moreover, the exciting possibility of OM47 being involved in senescence process needs to be further investigated by looking at broad spectrum of changes, which possibly occur, in the transcriptome and metabolome of plants deprived of OM47 protein. Additionally to find out whether OM47 is

involved in traffic of certain molecules the electrophysiology study should be considered.

A


```
  1 MGNALVKKEPPPPVVLVPPLFDYPPLSARTRMLESSYNLLFGKLALRCLFEDYFEEANRF
 61 TGKFLLKPTDDPHVDLVASVSGAVDGRVEGDFVGNAEFRWQSDVDDPHTFVDLSVSTSNP
121 VLLMRSSAYYPKYGIGAFAVYPLISKITGKSSEEYRIMGLRYGSTNLSVGATVTPFSANN
181 ELPKHAWLVSKMGSLTVGVQYEPLHGSKDLAKYTDPRNWSCAAGYGVGSQSPLTPSFNIG
241 IELARSSQFIASFYQHVVVQRRVQNPFEENQVVGITNYIDFGFELQSRVDDSKTPPNAPD
301 SLLQVAASWQANKNFLLKGKVGAHSSTLSLAFKSWWKPSFAFNISATTNHRTGNVQCGFG
360 LRVDNLREASYQRADPNFVMLTPNKEHLAEGIVWKMGKRPMYQADVDAENFSELPKELRP
421 SQKIL
```

IN
TM
OUT

B

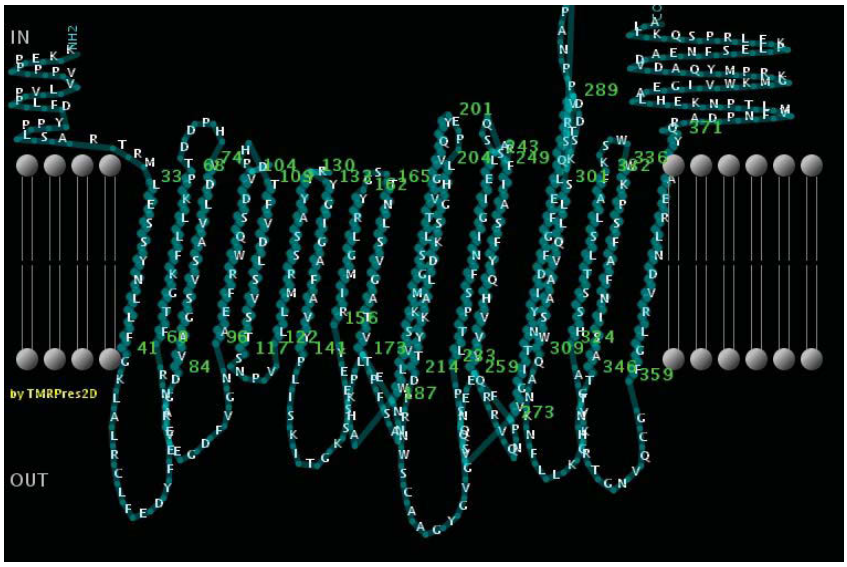

Figure 4.1.1 Bioinformatic analysis of OM47

A Sequence of AtOM47 was retrieved from The Arabidopsis Information Resource (TAIR, http://www.arabidopsis.org/) TAIR10 genome release. OM47 is predicted to belong to the Porin3 superfamily of proteins according to The Conserved Domain Database (**http://www.ncbi.nlm.nih.gov/cdd/**). OM47 β-strands prediction was carried out using the PRED TMBB (**http://bioinformatics.biol.uoa.gr/PRED-TMBB/**) based on a Hidden Markov Model. Sequences corresponding to β-strands were indicated in red. Loops sticking outside of the membrane were indicated in blue while loops inside of the membrane were indicated in green.

B Diagram representing the 2-dimensional prediction of the OM47 β-strands using the PRED TMBB (**http://bioinformatics.biol.uoa.gr/PRED-TMBB/**).

A

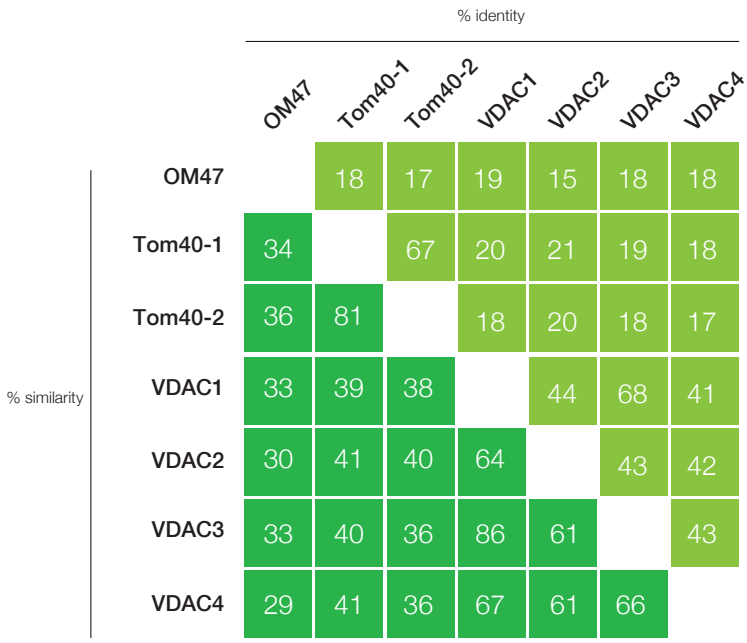

B

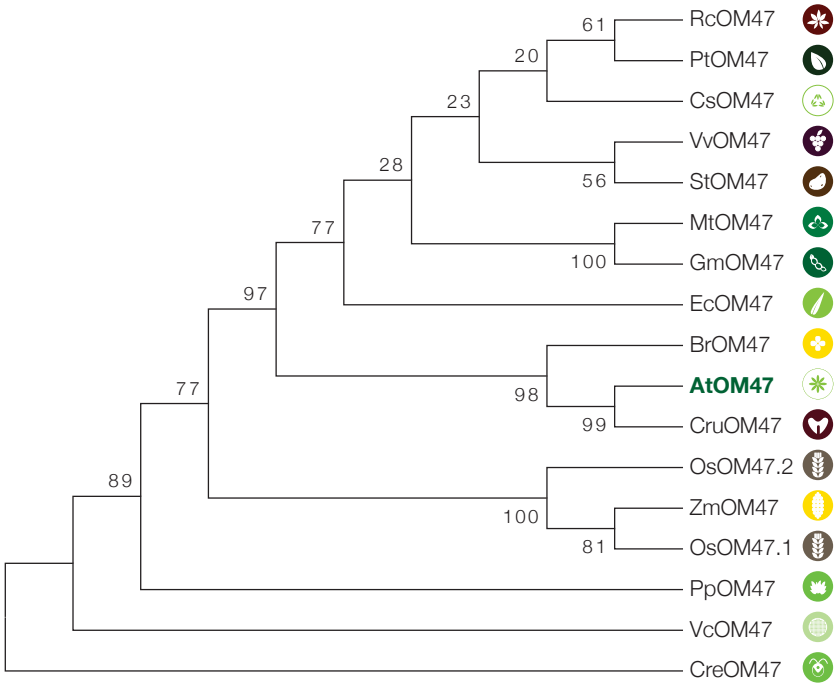

Figure 4.1.2. Protein sequence and phylogenetic analysis

A Matrix showing the percentage similarity and identity scores of amino acid sequences between OM47 and Tom40-1, Tom40-2 and VDAC1, 2, 3 and 4, generated using MatGAT (Campanella *et al*., 2003)

B Sequences of OM47 proteins were retrieved from various databases: Phytozome v9.1 (**http://www.phytozome.net/**), *Cyanidioschyzon merolae* Genome Project (**http://merolae.biol.s.u-tokyo.ac.jp/**) and Online resource for community annotation of eukaryotes OrcAE (**http://bioinformatics.psb.ugent.be/orcae/overview/Ectsi**). The phylogenetic analysis was carried out using MEGA 5.2.2 (Temura *et al*., 2011). Full-length protein alignments were generated using the Clustal option. The phylogenetic tree was generated using the maximum likelihood tree setting according to the Jones-Thornton-Taylor model after 1000 replications.

A

B

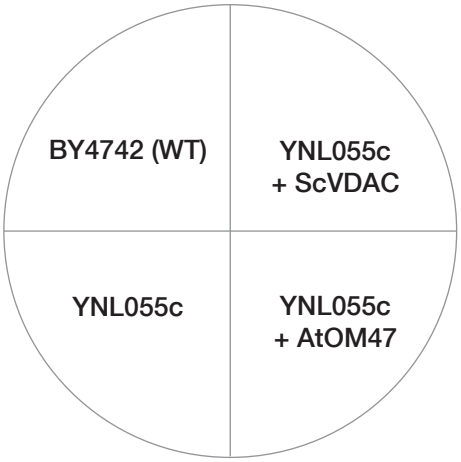

Figure 4.2 Functional complementaion of yeast mutant

A Yeast mutant strain YNL055c was transformed with the AtOM47 and ScVDAC as a control. Cells were streaked on plates containing 2 % (w/v) glucose or 2.5 % (v/v) glycerol as the sole carbon source, and incubated in 30°C for 3 d or 5 d respectively. The wild type yeast strain BY4742 grew well on the medium containing glucose or glycerol. The yeast mutant YNL055c did not grow in the medium containing glycerol as the sole carbon source. The YNL055c + AtOM47 complemented line grew well on the medium with glycerol suggesting that AtOM47 can functionally replace the ScVDAC protein. YNL055c+ ScVDACr was used as a control of transformation.

B The diagram indicates the genotypes of yeast strains and the transformed constructs.

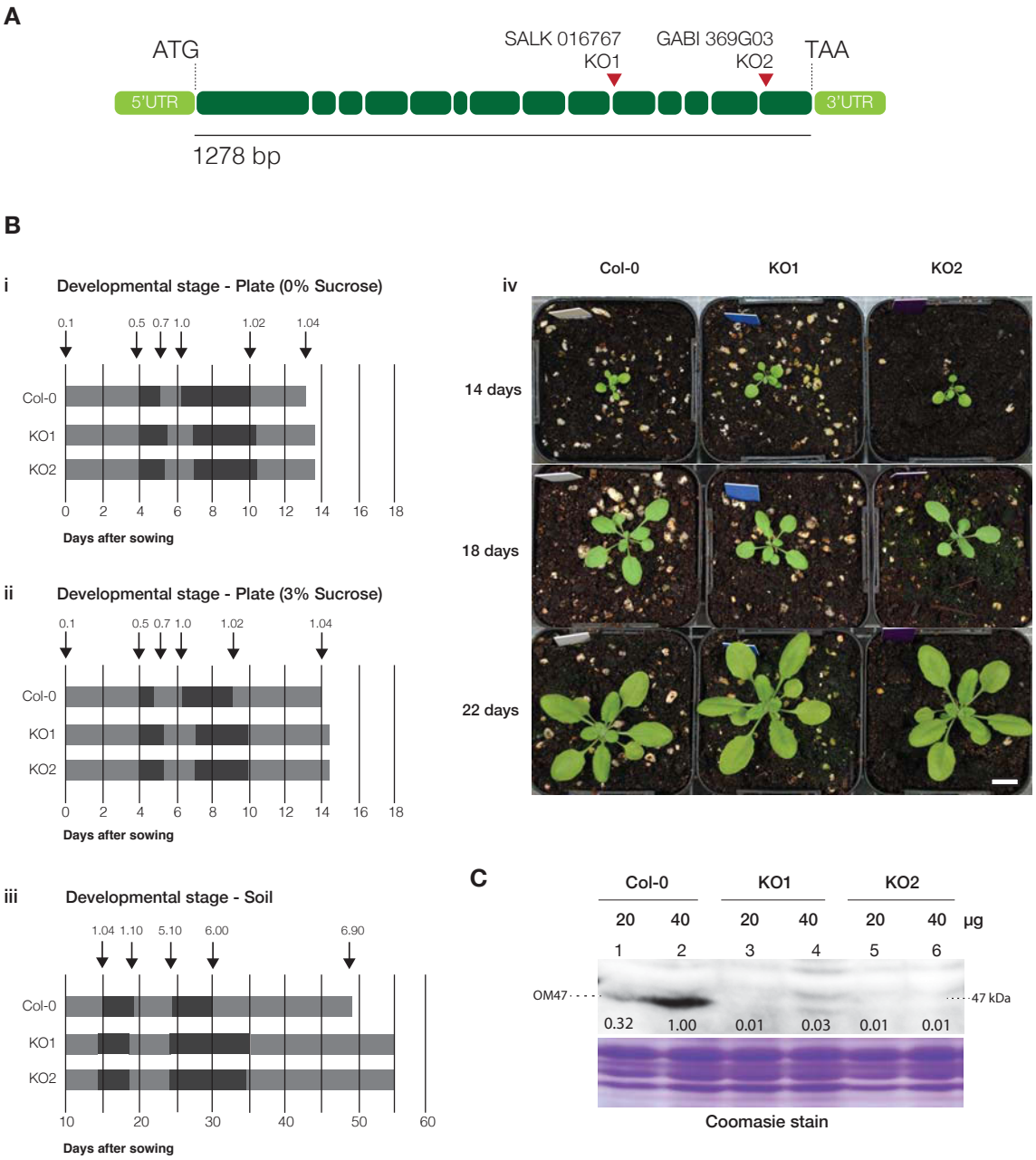

Figure 4.3 Characterisation of T-DNA mutant lines

A The positions of the T-DNA inserts in lines SALK_016767 (KO1) and GABI_369G03 (KO2) lines. UTR, untranslated region, ATG, start codon, TAA, stop codon.

B Plate-based growth progression analysis of Col-0, KO1 and KO2 lines on 0 % sucrose (w/v) MS medium. Days after sowing are indicated by arrows, when Col-0 plants have reached the growth stages described in Boyes *et al*. (2001). Boxes define the time between growth stages and shading indicates the occurrence of each growth stage. Stage 0.1, imbibition; stage 0.5 radical emergence; stage 0.7, hypocotyl emergence from seed coat; stage 1.0, cotyledons fully opened; stage 1.02, two rosette leaves > 1mm in length; stage 1.04. four rosette leaves > 1 mm in length. Data is given as averages for 15 plants. Days are relative to the days after sowing after a 3 d stratification at 4C (i). Plate-based growth progression analysis on 3 % sucrose (w/v) MS medium as in i, (ii). Soil-based growth progression: stage 1.10, 10 rosette leaves > 1 mm; stage 5.10, first flower bud visible; stage 6.0, first flower opens; stage 6.9, flowering complete (iii). Growth phenotypes of Col-0 and the KO plants after 14, 18 and 22 d in soil (iv). Scale: 1 cm

C Mitochondria isolated from Col-0, KO1 and KO2 were subjected to the SDS-PAGE and probed with the antibody against the OM47 protein. The apparent molecular mass of the detected protein (47 kDa) is indicated by the arrow. Coomasie stain is shown as the loading control.

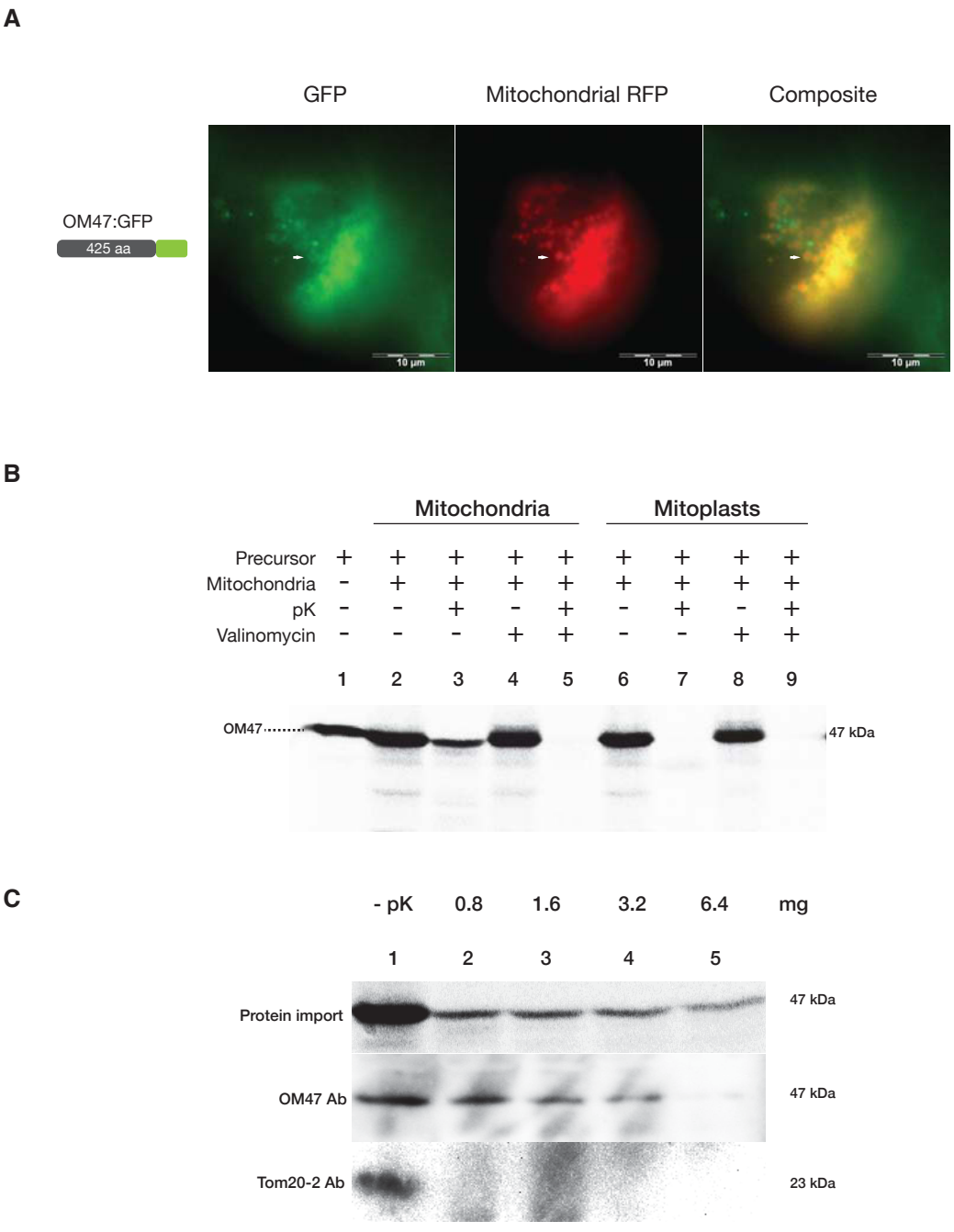

Figure 4.4 Subcellular localization of OM47

A Green fluorescent protein tagging of the OM47 protein confirms the mitochondrial outer membrane localisation as indicated by a characteristic green ring around red mitochondria (white arrows). Full length coding sequence of OM47 protein was cloned and fused to C-terminal GFP and co-transformed with mitochondrial matrix-targeted RFP control into Arabidopsis suspension culture.

B [^{35}S]-labelled full-length OM47 protein precursor was incubated with mitochondria isolated from Col-0 under conditions, which support the protein import. Import reactions were stopped after 20 min and treated with pK and valinomycin, where indicated. Mitoplasts were generated following the import.

C [^{35}S]-labelled full-length OM47 protein precursor was incubated with mitochondria isolated from Col-0 under conditions, which support the protein import. Import reactions were stopped after 20 min and treated with various amounts of pK. The pK digest was inhibited with PMSF. OM47 and Tom20 antibodies (Ab) were used for immunodetection against pK-treated mitochondria.

A

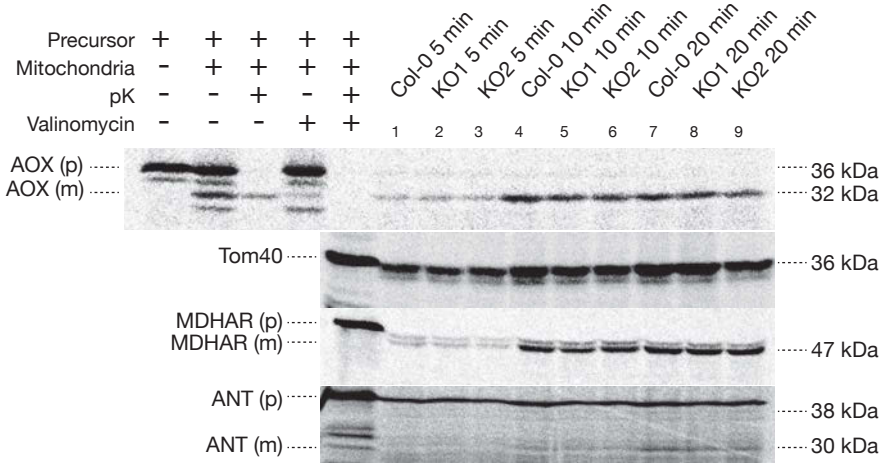

B

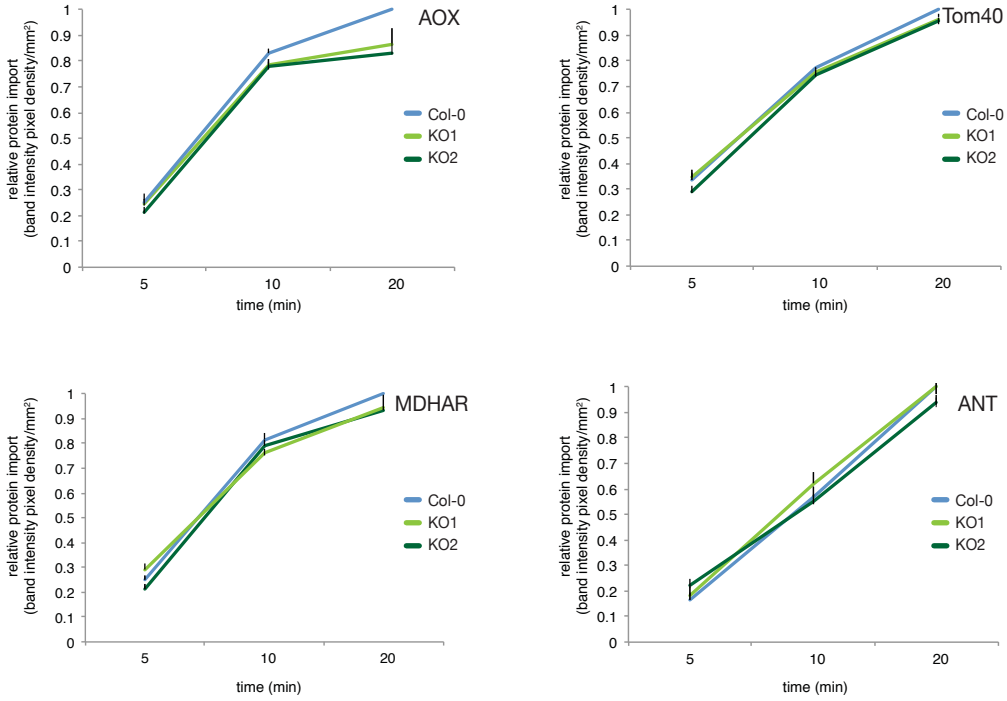

Figure 4.5 In vitro import of radiolabeled protein precursors.

A [^{35}S]-labelled precursor proteins AOX, Tom40, MDHAR and ANT were incubated with mitochondria isolated from Col-0 and *om47* lines (KO1: SALK_016767 and KO2: GABI_369G03) under conditions, which support the protein import. Aliquots were removed at 5, 10 and 20 min and treated with proteinase K.

B Graphs representing the rate of the protein import as intensity of the mature products, protected by proteinase K. Quantification was carried out in three replicates. The maximal intensity of the replicates was normalised to one and other values expressed relatively.

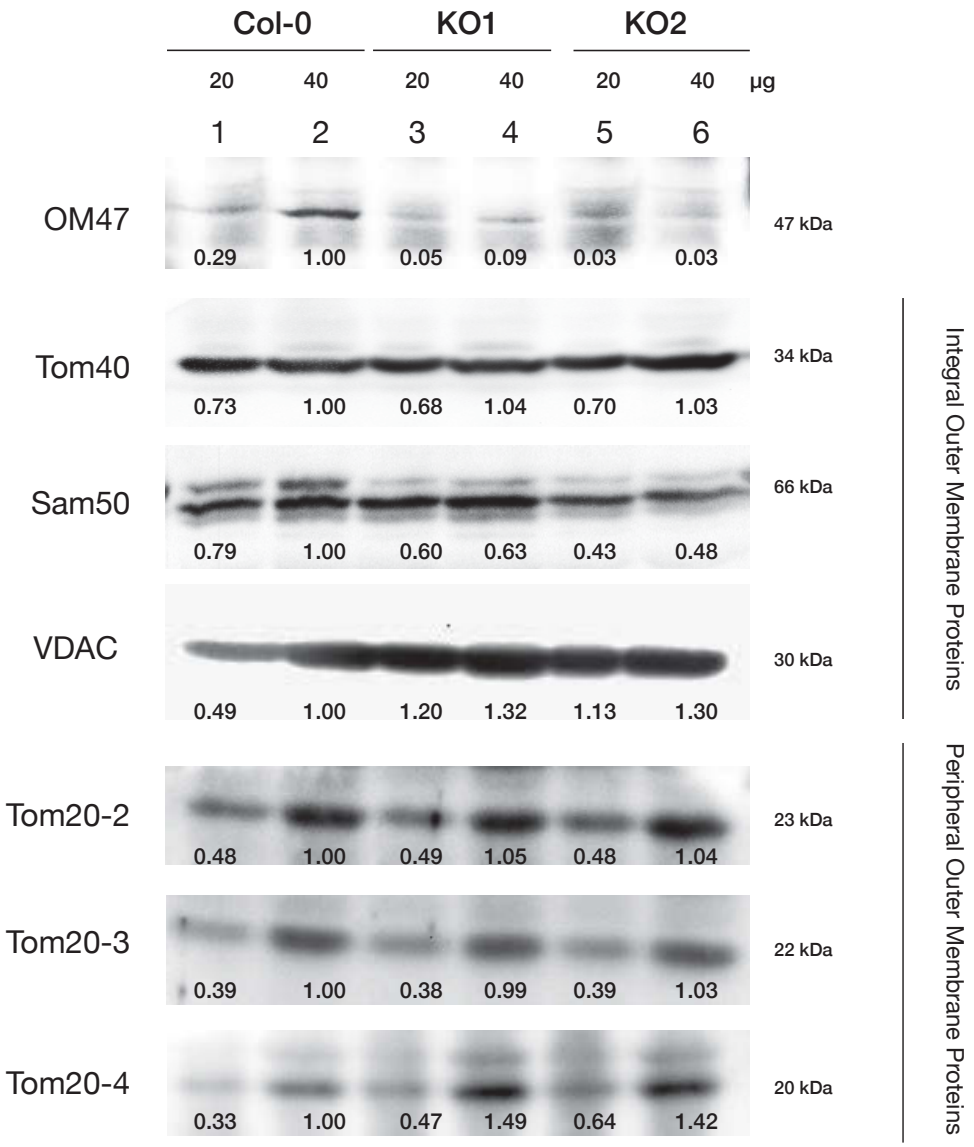

Figure 4.6 Mitochondrial protein composition.

Mitochondria from 14-day-old seedlings of Col-0, KO1 (SALK_016767) and KO2 (GABI_369G03) were isolated and separated via SDS-PAGE. Mitochondrial protein composition was determined by immunodetection using various polyclonal antibodies such as OM47 Ab, Tom40, Sam50 and VDAC (as outer membrane integral protein control) and Tom20-2, -3 and -4 Ab (as outer membrane peripheral protein control). The amount of 20 µg and 40 µg of mitochondrial protein was loaded and resolved on a 12% acrylamide gel. Intensity of bands was measured (pixel density/mm^2). Intensity of Col-0 bands at 40 µg was normalised to one and other values were expressed relatively.

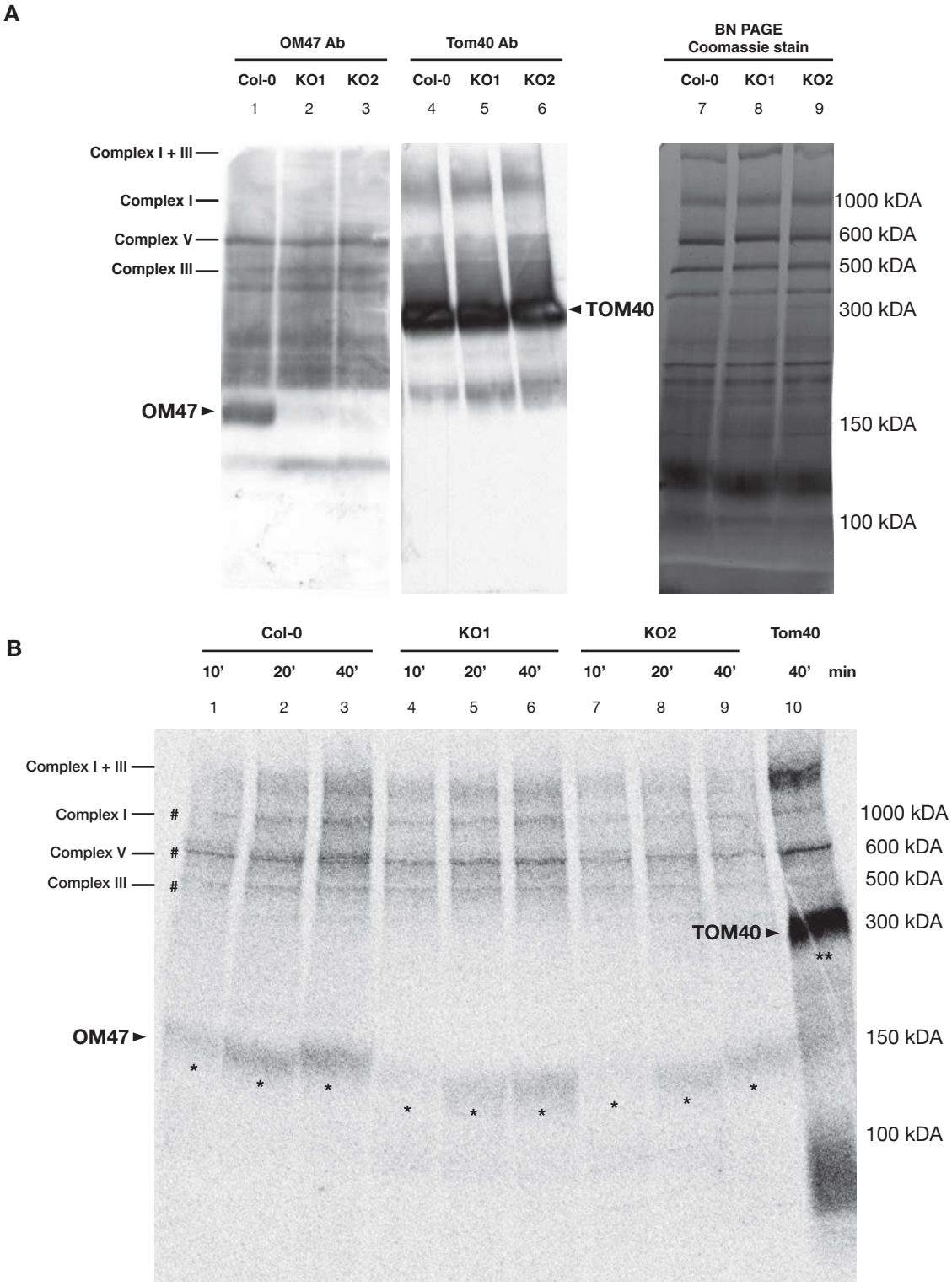

Figure 4.7 Blue Native-PAGE analysis of OM47 protein

A Blue Native-PAGE (BN-PAGE) analysis of the mitochondrial protein complexes in mitochondria isolated from Col-0, KO1 (SALK_016767) and KO2 (GABI_369G03). Immunodetection of OM47 and Tom40 is shown. Arrow indicates the OM47 presence in Col-0 and the depletion in KO lines.

B BN-PAGE time-course (min) of OM47 (*) and Tom40 (**) import into isolated mitochondria. The incorporation of radiolabeled proteins is indicated. #, unspecific incorporation.

A

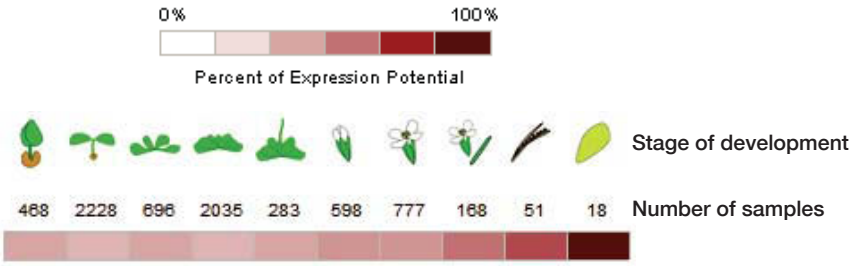

B

Leaves after 3 days of dark-induced senescence treatment

C

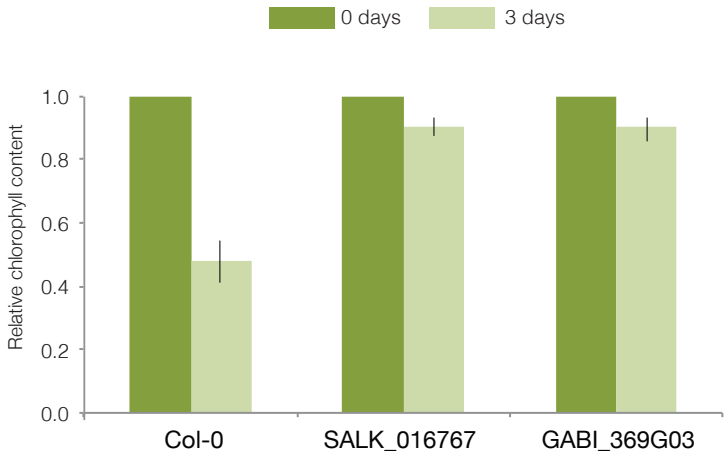

Figure 4.8 Dark induced senesence assay.

A Level of At3g27930 gene expression in Arabidopsis at different stages of the plant development. Data was analysed using GENEVESTIGATOR database and Web-browser data mining interface for Affymetrix GeneChip data (https://genevestigator.com).

B Individual leaves from Col-0, SALK_016767 and GABI_369G03 plants were covered for 3 d to induce the senescence process. Leaves were detached from 4-week-old plants and placed inside of the obscured plates.

C The senescence-related chlorophyll breakdown was measured at 0 d and 3 d using SPAD 502 chlorophyll meter. Chlorophyll content at 0 d was set to one and results obtained at 3 d were normalised. Five leaves per plant and three plants per genotype were sampled (n=3, $p<0.05$, +/- SE).

A

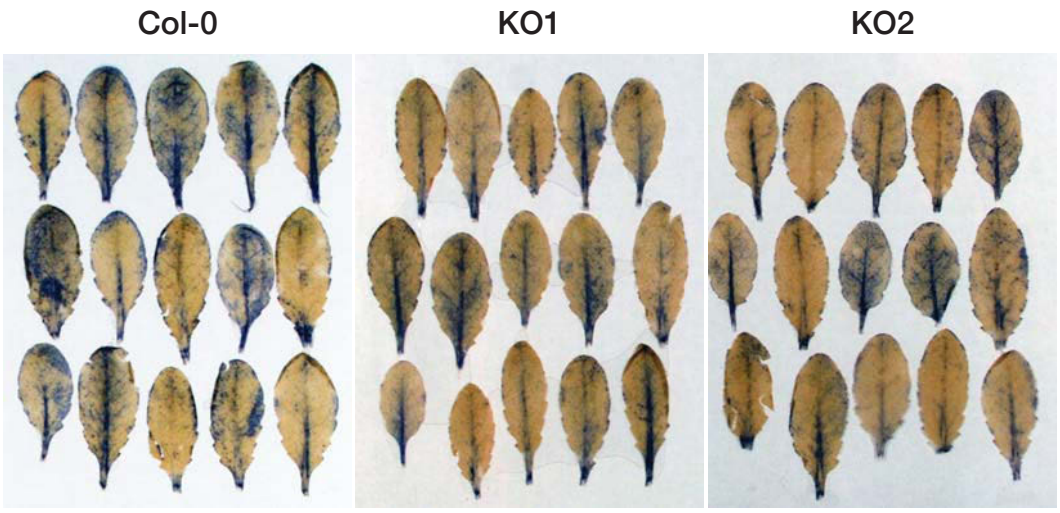

B

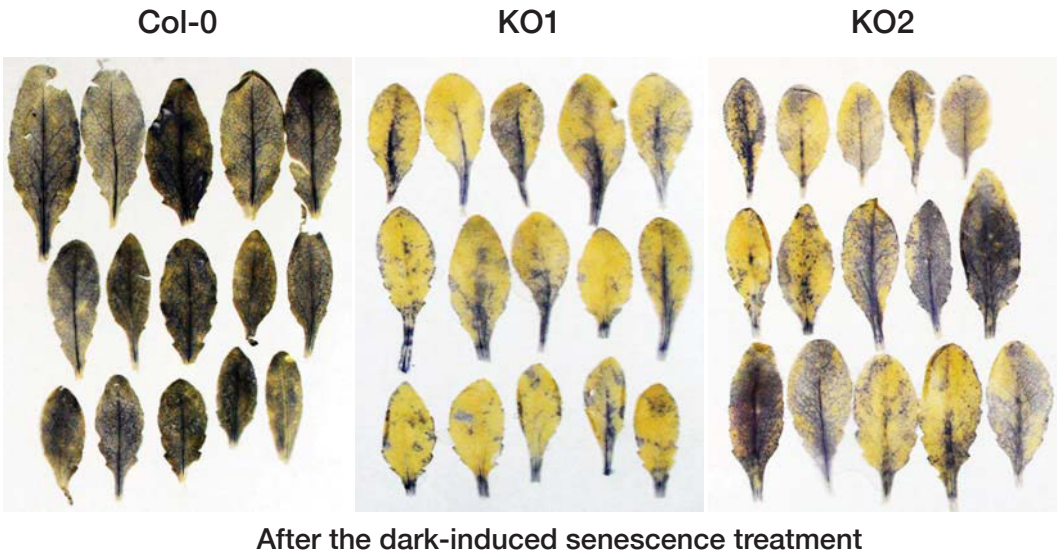

Figure 4.9 Determination of reactive oxygen species (ROS) accumulation

A Leaves from Col-0, KO1 (SALK_016767) and KO2 (GABI_369G03) were collected. Reactive oxygen species in the form of O_2^- were determined by staining the leaves using 600 uM solution of nitroblue tetrazolium (NBT) for 3 h and icubated for 24 h in 80 % ethanol, twice, in order to remove the chlorophyll. Five leaves per plant and three plants per genotype were sampled.

B Leaves from Col-0, KO1 (SALK_016767) and KO2 (GABI_369G03) were collected after 3 days of dark induced senescence treatment. Reactive oxygen species in the form of O_2^- were determined by staining the leaves using 600 µM solution of nitroblue tetrazolium (NBT) for 3 h and incubated for 24 h in 80 % ethanol, twice, in order to remove the chlorophyll. Five leaves per plant and three plants per genotype were sampled.

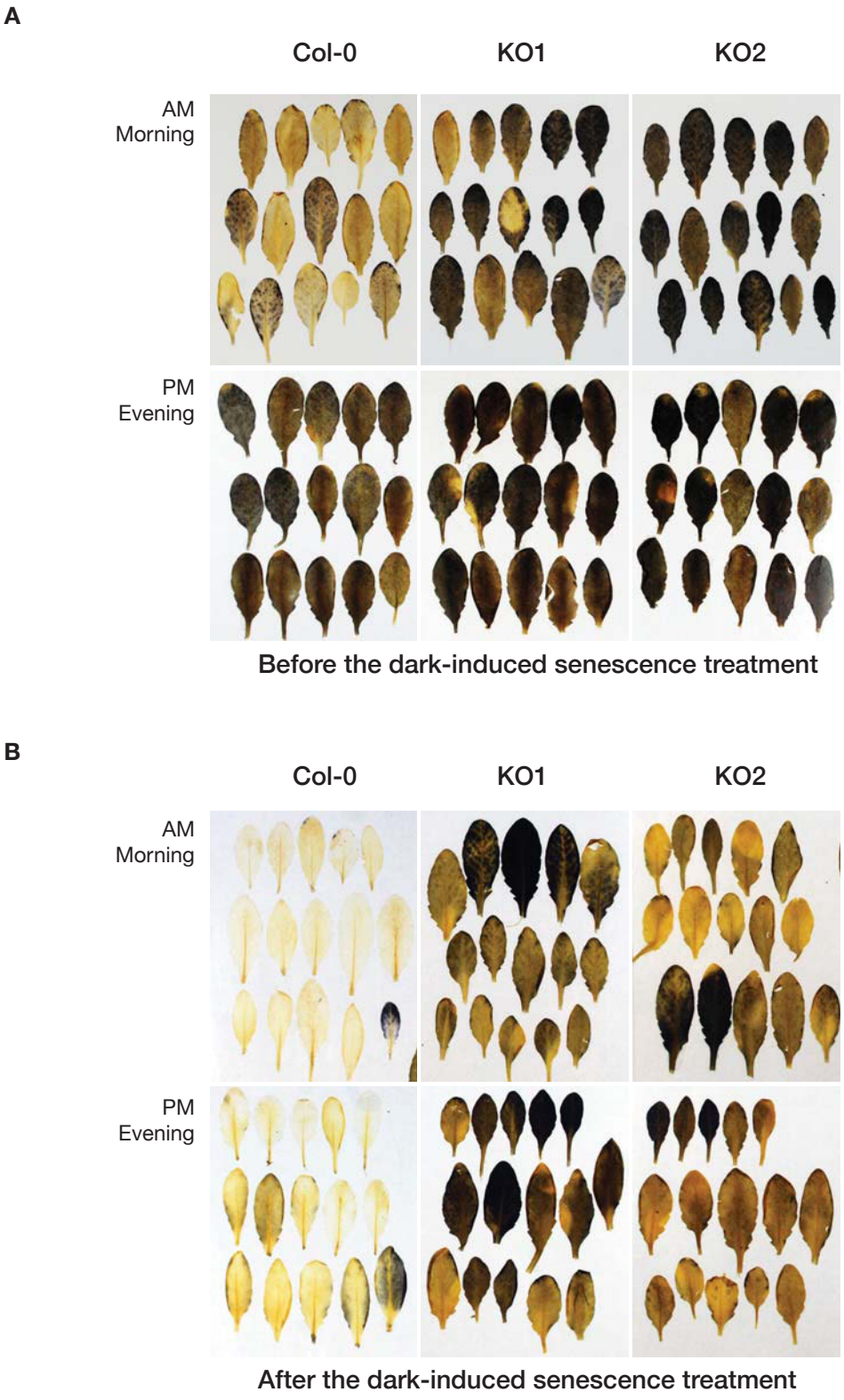

Figure 4.10 Determination of starch content

A Starch content determined by staining the leaves sampled in the morning (**AM**) and in the evening (**PM**) in 50 % (v/v) of Lugol solution for 5 min. After staining leaves were washed with MQ water for 1 h in room temperature. Five leaves per plant and three plants per genotype were sampled.

B Starch content was determined by staining the leaves sampled in the morning (**AM**) and the evening (**PM**), after 3-day dark-induced senescence treatment, in 50 % (v/v) of Lugol solution for 5 min. After staining leaves were washed with MQ water for 1 h in room temperature. Five leaves per plant and three plants per genotype were sampled.

General Discussion

Chapter 5 - General Discussion

5.1 Introduction

The mitochondrial outer membrane acts as an interface between the mitochondrion and other cellular components and is crucial for cellular metabolism by mediating the intricate mechanisms such as passage of small molecules, signalling events between mitochondria and the cytosol and the mechanisms of macromolecule import of nuclear encoded components. It is becoming more obvious, that plant mitochondria evolved plant-specific components and processes. The conservation of fundamental mitochondrial functions among various eukaryotes, such as synthesis of the energy currency - ATP, through the oxidative phosphorylation, the assembly of iron-sulphur clusters as well as the TCA cycle, is undisputable. However, since the primary endosymbiotic event occurred about 1.5 billion years ago, mitochondria underwent a variety of evolutionary changes, which can be observed in various species as well as by the presence of the extremely functionally reduced mitochondria-derived organelles: hydrogenosomes and mitosomes [69]. Those changes involve the changes in the cellular environment as well as the diverse demands that mitochondria had to adjust to during the evolution. The occurrence of the secondary endosymbiotic event, by which the ancestral eukaryote gained the chloroplast and its photosynthetic ability, led to additional subcellular environment alterations, which changed the plant cell energy metabolism. Hence, plant mitochondria had to evolve to cooperate with the new organelle. This can be observed by the interplay between the respiration and photosynthesis, the presence of the alternative respiratory pathway and the implication the alternative oxidase has on the stress signalling in plant cells as well as the import of macromolecules such as proteins and nucleic acids into mitochondria. As shown in the protein import, the presence of chloroplast resulted in the evolution of the dual-targeting process, as both of the endosymbiotic organelles require the translocation of its own set of proteins encoded by the nucleus. The diversification of these various aspects of mitochondrial biology is not surprising and emphasizes the intricacies faced by plant mitochondria during evolution.

Several studies have undertaken a proteomics approach to characterise the composition of the outer membrane of mitochondria in yeast (82 proteins) [179], *Neurospora crassa* (30) [178] and recently in *Trypanosoma brucei* (82) [180]. The composition of the mitochondrial outer membrane proteome is particularly difficult to study as the overall protein content of the outer membrane is relatively low comparing to the inner mitochondrial membrane and the close association with the protein-rich inner membrane and endoplasmic reticulum can lead to contamination during purification of this fraction [181]. This seems to be the problem particularly in plants, which as mentioned above, are characterized by the dynamic nature of mitochondrial inner and outer membranes such as the presence of the C-terminal extensions of Tim17-1 and -2 isoforms, which link both membranes [126] as well as interactions of protein import components with respiratory complexes such as Tim23 and B.14.7 having a dual role in translocation of preproteins to mitochondrial matrix regulation of Complex I [130] and finally with Tim21 and two Tim21-like proteins interacting with respiratory chain machinery [133].

A recent proteomic study to identify novel outer membrane protein candidates in Arabidopsis was carried out [181]. This study identified 42 mitochondrial outer membrane proteins, which accounted for 88% coverage of the known outer membrane components, 27 of which haven't been previously observed to localise in this mitochondrial subcompartment [181]. Many of these proteins had yet to be functionally characterized and several appeared to be plant-specific proteins [181]. Therefore the characterisation of two of these proteins identified in the outer membrane proteome formed the foundation and the concept of this thesis, the first of which was termed the tRNA import component (TRic), a protein found to be involved in the import of tRNA molecules into mitochondria and the second, termed the outer membrane protein 47 (OM47), a β-barrel protein that may have a role in plant senescence and/or programmed cell death.

5.2 TRic1 and TRic2

Unlike the protein import, the import of transfer RNAs is still not very well described [141, 235, 236] Mitochondrial genomes of a majority of eukaryotes, have been predicted to lack number of genes (varying between species) for some tRNAs, therefore the lack of these is compensated by import of a fraction of some cytosolic tRNA species [141, 235, 236]. The process of mitochondrial tRNA import can be divided into two broad mechanisms. In the first one, the tRNA is co-imported with a mitochondrial protein precursor and the translocation happens along the protein import pathway. The best-described example of this tRNA import mechanism is the import of $tRNA^{Lys}$ in yeast mitochondria [145]. The second mechanism, predominantly present in protozoa and plants, is the independent translocation of tRNAs without any additional cytosolic factors [141]. However, results obtained in plant mitochondria suggest that tRNA and protein import pathways might be connected. First protein components proposed to mediate the tRNA import in plants were the protein import receptor - Tom20, the main precursor protein translocation channel - Tom40 and the most abundant porin - VDAC, in potato mitochondria [193], however the assays used were based on the usage of specific antibodies, which obscured tested import components. Additionally specific chemical inhibitors were used to show the involvement of studied proteins in this process. These results showed that protein import machinery could be potentially involved at some stage of the translocation of the tRNA into plant mitochondria.

By using a reverse genetics approach two Arabidopsis genes At3g49560 and At5g24560, encoding for TRic1 and TRic2 respectively, were shown to have a role in the import of tRNA. Depletion of both of the TRic isoforms resulted in a severe phenotypic change in morphology of plants (chlorosis). As these proteins belong to the preprotein and aminoacid transporter (PRAT) family, protein import ability was determined in the double knock-out line and found to have been unaffected. Bioinformatic analysis revealed the presence of an additional domain, the sterile alpha motif (SAM). This domain had previously been shown to have a

role in RNA binding [202-204] therefore the ability of the mutant line to import tRNA was tested and it was found that TRic-deprived mitochondria have significantly decrease ability to import $tRNA^{Ala}$. The combination of the PRAT and SAM domain appears to be specific to plants suggesting that TRics evolved early in the evolution of land plants, with Tric orthologs present in the green algae *Chlamydomonas reinhardtii* and *Volvox carterii* and early land plant *Selaginella moelendorfii*. The expansion and evolution of the PRAT family to mediate the import of tRNA into plant mitochondria may have been a response to the acquisition of the chloroplast and alteration of the cellular, now photosynthetic, metabolism. Whilst this data suggests that TRic may be involved in tRNA import further functional evidence is required. The exact topology of TRic isoforms needs to be elucidated. Proteomic analysis suggests it is an outer membrane protein and both *in vitro* and GFP localisation studies support this finding (Murcha *et al.*, unpublished data). Therefore, the presence of a PRAT domain typical for Tim family of proteins, which spans the inner membrane with its four transembrane regions raised a question of the exact topology of TRics. Perhaps TRic proteins are part of a large tRNA import complex, which involves protein components from both membranes including protein import components. Furthermore the exact location of the SAM domain needs to be determined in order to see whether TRics can act as a receptor on the outer membrane, to recognise cytosolic tRNA. Another possibility could be that TRics do not directly interact with cytosolic tRNAs but mediate their import by recognizing an unknown passenger protein, which binds tRNA, therefore import would occur similarly to the general tRNA import pathway in yeast [145]. A third possibility would be that TRics are necessary for the import of an unknown specific import receptor responsible for recognition of cytosolic tRNAs, which has not been tested here. Moreover, due to the fact that pDHFR assay used in these experiments is not specific to tRNAs, there is a possiblity that TRics are involved in import of other RNA molecules as it has been demonstrated for mammalian mitochondria, which import 5s rRNA *in vivo* [237, 238].

Interestingly, double knock out of TRic, as described, results in a viable plant albeit with obvious deleterious effects such as retarded growth and chlorotic leaves, which could suggest that an additional mechanism of tRNA import is

present in mitochondria. The complementation studies presented here suggest that SAM domain is vital for TRics' function as plants complemented with a construct of just the PRAT domain (amino acids 1-180) showed phenotypic similarities to the knock-out line. Chlorosis of the *tric1::2* leaves also suggests a role in chloroplasts. As described previously [183] TRic dual location to mitochondria and chloroplasts have been demonstrated contrary to the recent study [209], where TRics referred to as HP30-1 and HP30-2 are described as inner plastid envelope membrane proteins involved in transit sequence-less protein import. These reports raise the possibility of diversity of functions and localisations that PRAT protein family could evolve in plants. The Francis Crick codon-anticodon model predicts that 32 tRNA species are needed to read all triplets of the genetic code [239]. However, genomes of plastids, mitochondria and certain parasitic bacteria such as mycoplasmas contain reduced genomes, which lack the complete set of tRNA genes. As mentioned above, mitochondrial tRNA import evolved as a mechanism to compensate for lacking tRNAs, however it is unclear whether this could be the same situation in chloroplasts. It has been suggested that tRNAs might be imported from the cytosol to chloroplasts in some parasitic plants, which don't photosynthesize [240-242], but generally accepted scenario is that chloroplasts of photosynthesizing plants overcome the lack of certain tRNA genes by the extended wobbling principle, which can be defined as the ability of one tRNA molecule to decode all four triplets of the codon family [243]. Thus it is accepted that cytosolic tRNAs are not imported into chloroplasts. This raises the intriguing question, of what is the function of dually targeted TRic isoforms. As PRAT proteins evolved into numerous isoforms in plants it is tempting to speculate that they might have different functions in different organelle membrane systems, as it is the case with B14.7 PRAT protein.

Blue native electrophoresis analysis of TRic1 and TRic2 revealed the location of these proteins in three different complexes. It is possible that isoforms co-migrate with both TOM and TIM complexes as determined by results obtained from the time course import experiment, suggesting the possible dynamic nature of TRics. TRics could potentially form a dynamic complex with the protein import machinery in order to mediate the tRNA recognition and translocation in plant mitochondria. As it has been shown in yeast (co-transport with Eno2p and LysRS)

[145], plants (Tom20, Tom40 and VDAC) [174] and trypanosomes (Tim17 and Hsp60) [161], it seems that protein import machinery is necessary for translocation of tRNAs to mitochondria in these various groups and support the possibility of membrane transporter with a capability to move proteins and tRNAs into mitochondria and suggest that all these groups have similarly functioning tRNA translocons.

5.3 OM47

Four families of mitochondrial β-barrel membrane proteins have been confirmed to date. These four families contain highly conserved VDACs (metabolite transport), Tom40 (preprotein translocation) and Sam50 (β-barrel protein assembly) as well as yeast-specific Mdm10 protein responsible for maintenance of morphology and dynamics. As outer membrane proteome is far less characterized in comparison to other mitochondrial subcompartments the number of known β-barrel topology proteins from mitochondria and chloroplasts is still small comparing to their bacterial ancestors. Nevertheless, in recent years putative novel β-barrel proteins from these organelles have been described. Interestingly, it seems that in the course of the evolution of semi-autonomous organelles, certain eukaryotes evolved specific β-barrel proteins responsible for specific functions such as aforementioned Mdm10 in yeast and trypanosme-specific TAC40 protein, which has been suggested as responsible for mitochondrial genome inheritance in trypanosomes.

Preliminary results from the biochemical characterization of a novel mitochondrial outer membrane protein in Arabidopsis presented in Chapter 4, provide and interesting insight into what could be a plant specific component of the senescence process. Phylogenetic and bioinformatic analyses of the outer membrane protein 47 (OM47) encoded by At3g29370 revealed that it is an integral outer membrane protein of β-barrel topology only present in photosynthesizing organisms, which belongs to a Proin3 superfamily along with VDACs and Tom40 proteins. When the single gene encoding for OM47 is knocked out, no drastic morphological phenotype could be observed suggesting that OM47 is not essential for Arabidopsis. It was concluded that OM47 is not

involved in the import of tested protein precursors. Interestingly, OM47 is stably expressed during the plant development at medium levels but upregulated during senescence as indicated by GENEVESTIGATOR. These results combined with the significantly lower level of chlorophyll degradation, visibly lower levels of reactive oxygen species and visible starch accumulation suggest that OM47 could be involved in plant senescence perhaps as one of the components of the programmed cell death pathway.

Programmed cell death (PCD) or apoptosis is a conserved process, which is crucial for efficient development, homeostasis and removal of dispensable cells in metazoan species [244]. Apoptotic signals from different stimuli are detected by mitochondria, which lead to changes in permeability of mitochondrial membranes and release of mitochondrial intermembrane space proteins such as the canonical apoptotic effector - cytochrome *c*, which leads to the activation of downstream events, which eventually lead to the execution of the cell death process [245]. Some apoptotic stimuli can trigger the formation of permeability transition pore (PTP), which leads to loss of mitochondrial inner membrane potential, osmotic swelling of mitochondria and consequent disruption of the mitochondrial outer membrane, which leads to the release of cytochrome *c* [245, 246]. The major component of this pore is a mitochondrial outer membrane protein - VDAC [245, 246]. Although the transduction of apoptotic signals downstream from mitochondria is somewhat understood, the precise mechanisms of the upstream transmission of apoptotic signals to the organelles have not been yet elucidated. VDAC is a critical component of the release of apoptogenic effectors from mitochondria induced by a variety of stimuli in mammals and in yeast however situation in plants is far less understood [247]. Recent studies in plants link two mitochondrial outer membrane proteins, VDAC and hexokinase, with programmed cell death in plants and there are other reports on similarities between mammalian and plant systems such as appearance of cytochrome *c* in the cytosol [248, 249], mitochondrial permeability transition [250], activation of caspase like proteases [251] as well as cellular and nuclear condensation and fragmentation of DNA [252]. As OM47 is a member of a porin family of proteins and the fact that it is capable to functionally complement the yeast VDAC knock out with the same effect as yeast VDAC it is tempting to speculate that OM47 could be transiting

some sort of signal molecules upstream or downstream the mitochondrial involvement in cell death execution similarly to VDAC during the PTP formation. However, as this project is in its early stage, the research aimed to functionally characterize OM47 continues.

5.4 Conclusion and future work

Results presented in this thesis represent the first evidence of any plant proteins involved in the process of import of the cytosolic tRNA molecules into the plant mitochondria using the reverse genetic approach. It is being hypothesized that these putative tRNA import components, TRic1 and TRic2, are crucial for the efficiency of this process due to their sterile alpha motif (SAM) domain, however they are not essential for the plant and compensating mechanism possibly exists. These plant specific proteins possibly evolved specifically to mediate the tRNA import process in photosynthesizing organisms and are a part of a putative dynamic complex, which involves multiple proteins of both inner and outer membrane complexes.

Future work in this project is required to provide direct evidence for tRNA import and interaction. This may include protein-tRNA interaction assays such as RNA electromobility shift assay (REMSA) and protein-protein interactions should be carried out to identify novel interacting proteins. This could be achieved by he tandem affinity tagged (TAP) lines, which could be generated for biochemical purification of TRic proteins, followed by the masspectrometry and BN PAGE analysis. Additionally a Yeast 2 Hybrid screen of full-length TRics, truncated (without SAM domain) and SAM domain itself against an Arabidopsis cDNA library could be carried out in order to identify novel interacting partner proteins. The SAM domain alone can be tested to identify soluble cytosolic factors that might be involved in the supply of tRNA to the SAM domain on the mitochondrial outer membrane surface. Finally overexpression of TRics in an inducible manner could be carried out in order to follow changes in mitochondrial biogenesis.

This thesis also contains results obtained from the functional analysis of the novel β-barrel protein, which was showed to be an integral, mitochondrial outer membrane protein specific to the plant kingdom. Results presented here suggest

that OM47 is not involved in protein import but rather is a putative component of the senescence process in Arabidopsis. Its ability to restore the phenotype in the VDAC knock out in yeast suggests that it might act as VDACs despite its relatively low similarity and identity scores of the primary amino acid sequence. At this early stage of research the hypothesis is that OM47 could potentially be involved in signaling process during programmed cell death during senescence and it evolved in plants to cater to specific needs of the photosynthesizing organisms. This however needs to be further investigated. Future work could involve several approaches such as detailed study using different senescence assays to confirm that OM47's involvement in this process. This could involve macroscopic experiments such as dark-induced senescence on detached leaves, individually-darkened leaf assays on attached leaves in various light intensity regimes as well as molecular approach such as qRT-PCR study of known senescence markers and global changes in transcriptome and metabolome of the *om47* plants. Additionally the potential involvement in programmed cell death could be studied by looking at characteristic events known to occur during this process such as e.g. cytochrome *c* release, the membrane permeability and caspase-like enzyme activity.

In summary, the in depth study of Arabidopsis mitochondrial outer membrane proteome carried out in our laboratory resulted in the identification of the most extensive list of proteins in this subcompartment and provided the platform for downstream research aiming to functionally characterise these identities. As a direct continuation of that study, this thesis presents the results from characterization of three of these proteins, which might have functions, which arose specifically to mediate intricate processes at the boundary between the cytosol and plant mitochondrial outer membrane.

Bibliography

1. Sagan, L., *On the origin of mitosing cells.* J Theor Biol, 1967. **14**(3): p. 255-74.
2. Keeling, P.J., *Diversity and evolutionary history of plastids and their hosts.* Am J Bot, 2004. **91**(10): p. 1481-93.
3. Martin, W., *Evolutionary origins of metabolic compartmentalization in eukaryotes.* Philos Trans R Soc Lond B Biol Sci, 2010. **365**(1541): p. 847-55.
4. Martin, W. and K. K.V., *Annotated English translation of Mereschkowsky's 1905 paper `Uber Natur und Ursprung der Chromatophoren im Pflanzenreiche'.* Eur. J. Phycol., 1999. **34**: p. 287-295.
5. Gray, M.W., *Mitochondrial evolution.* Cold Spring Harb Perspect Biol, 2012. **4**(9): p. a011403.
6. Gray, M.W., *The endosymbiont hypothesis revisited.* Int Rev Cytol, 1992. **141**: p. 233-357.
7. Gray, M.W., et al., *Genome structure and gene content in protist mitochondrial DNAs.* Nucleic Acids Res, 1998. **26**(4): p. 865-78.
8. Andersson, S.G., et al., *On the origin of mitochondria: a genomics perspective.* Philos Trans R Soc Lond B Biol Sci, 2003. **358**(1429): p. 165-77; discussion 177-9.
9. Gray, M.W., B.F. Lang, and G. Burger, *Mitochondria of protists.* Annu Rev Genet, 2004. **38**: p. 477-524.
10. Lang, B.F., M.W. Gray, and G. Burger, *Mitochondrial genome evolution and the origin of eukaryotes.* Annu Rev Genet, 1999. **33**: p. 351-97.
11. Koonin, E.V., *The origin and early evolution of eukaryotes in the light of phylogenomics.* Genome Biol, 2010. **11**(5): p. 209.
12. Martin, W. and M. Muller, *The hydrogen hypothesis for the first eukaryote.* Nature, 1998. **392**(6671): p. 37-41.
13. Embley, T.M. and W. Martin, *Eukaryotic evolution, changes and challenges.* Nature, 2006. **440**(7084): p. 623-30.
14. Embley, T.M., et al., *Hydrogenosomes, mitochondria and early eukaryotic evolution.* IUBMB Life, 2003. **55**(7): p. 387-95.

15. Hackstein, J.H., et al., *Hydrogenosomes: eukaryotic adaptations to anaerobic environments.* Trends Microbiol, 1999. **7**(11): p. 441-7.
16. Goldberg, A.V., et al., *Localization and functionality of microsporidian iron-sulphur cluster assembly proteins.* Nature, 2008. **452**(7187): p. 624-8.
17. Logan, D.C., *The mitochondrial compartment.* J Exp Bot, 2006. **57**(6): p. 1225-43.
18. Duncan, O., M.W. Murcha, and J. Whelan, *Unique components of the plant mitochondrial protein import apparatus.* Biochim Biophys Acta, 2013. **1833**(2): p. 304-13.
19. Benz, R., *Permeation of hydrophilic solutes through mitochondrial outer membranes: review on mitochondrial porins.* Biochim Biophys Acta, 1994. **1197**(2): p. 167-96.
20. Mesecke, N., et al., *A disulfide relay system in the intermembrane space of mitochondria that mediates protein import.* Cell, 2005. **121**(7): p. 1059-69.
21. Koehler, C.M., *The small Tim proteins and the twin Cx3C motif.* Trends Biochem Sci, 2004. **29**(1): p. 1-4.
22. Chacinska, A., et al., *Essential role of Mia40 in import and assembly of mitochondrial intermembrane space proteins.* EMBO J, 2004. **23**(19): p. 3735-46.
23. Reddehase, S., et al., *The disulfide relay system of mitochondria is required for the biogenesis of mitochondrial Ccs1 and Sod1.* J Mol Biol, 2009. **385**(2): p. 331-8.
24. Reichert, A.S. and W. Neupert, *Contact sites between the outer and inner membrane of mitochondria-role in protein transport.* Biochim Biophys Acta, 2002. **1592**(1): p. 41-9.
25. Fung, S., et al., *The conserved interaction of C7orf30 with MRPL14 promotes biogenesis of the mitochondrial large ribosomal subunit and mitochondrial translation.* Mol Biol Cell, 2013. **24**(3): p. 184-93.
26. Gabaldon, T. and M.A. Huynen, *Shaping the mitochondrial proteome.* Biochim Biophys Acta, 2004. **1659**(2-3): p. 212-20.
27. Unseld, M., et al., *The mitochondrial genome of Arabidopsis thaliana contains 57 genes in 366,924 nucleotides.* Nat Genet, 1997. **15**(1): p. 57-61.

28. Lewis, M.R. and W.H. Lewis, *Mitochondria in Tissue Culture.* Science, 1914. **39**(1000): p. 330-3.
29. Westermann, B., *Mitochondrial fusion and fission in cell life and death.* Nat Rev Mol Cell Biol, 2010. **11**(12): p. 872-84.
30. Westermann, B., *Molecular machinery of mitochondrial fusion and fission.* J Biol Chem, 2008. **283**(20): p. 13501-5.
31. Okamoto, K. and J.M. Shaw, *Mitochondrial morphology and dynamics in yeast and multicellular eukaryotes.* Annu Rev Genet, 2005. **39**: p. 503-36.
32. Hales, K.G. and M.T. Fuller, *Developmentally regulated mitochondrial fusion mediated by a conserved, novel, predicted GTPase.* Cell, 1997. **90**(1): p. 121-9.
33. Westermann, B., *Mitochondrial dynamics in model organisms: what yeasts, worms and flies have taught us about fusion and fission of mitochondria.* Semin Cell Dev Biol, 2010. **21**(6): p. 542-9.
34. Meeusen, S., et al., *Mitochondrial inner-membrane fusion and crista maintenance requires the dynamin-related GTPase Mgm1.* Cell, 2006. **127**(2): p. 383-95.
35. Logan, D.C., *The dynamic plant chondriome.* Semin Cell Dev Biol, 2010. **21**(6): p. 550-7.
36. Arimura, S., et al., *Frequent fusion and fission of plant mitochondria with unequal nucleoid distribution.* Proc Natl Acad Sci U S A, 2004. **101**(20): p. 7805-8.
37. Logan, D.C., *Mitochondrial fusion, division and positioning in plants.* Biochem Soc Trans, 2010. **38**(3): p. 789-95.
38. Fukushima, N.H., et al., *The GTPase effector domain sequence of the Dnm1p GTPase regulates self-assembly and controls a rate-limiting step in mitochondrial fission.* Mol Biol Cell, 2001. **12**(9): p. 2756-66.
39. Ingerman, E., et al., *Dnm1 forms spirals that are structurally tailored to fit mitochondria.* J Cell Biol, 2005. **170**(7): p. 1021-7.
40. Mozdy, A.D., J.M. McCaffery, and J.M. Shaw, *Dnm1p GTPase-mediated mitochondrial fission is a multi-step process requiring the novel integral membrane component Fis1p.* J Cell Biol, 2000. **151**(2): p. 367-80.

41. Arimura, S., et al., *Arabidopsis dynamin-like protein 2a (ADL2a), like ADL2b, is involved in plant mitochondrial division.* Plant Cell Physiol, 2004. **45**(2): p. 236-42.
42. Arimura, S., et al., *Arabidopsis ELONGATED MITOCHONDRIA1 is required for localization of DYNAMIN-RELATED PROTEIN3A to mitochondrial fission sites.* Plant Cell, 2008. **20**(6): p. 1555-66.
43. Pan, R., A.D. Jones, and J. Hu, *Cardiolipin-mediated mitochondrial dynamics and stress response in Arabidopsis.* Plant Cell, 2014. **26**(1): p. 391-409.
44. Chan, D.C., *Fusion and fission: interlinked processes critical for mitochondrial health.* Annu Rev Genet, 2012. **46**: p. 265-87.
45. Fernie, A.R., F. Carrari, and L.J. Sweetlove, *Respiratory metabolism: glycolysis, the TCA cycle and mitochondrial electron transport.* Curr Opin Plant Biol, 2004. **7**(3): p. 254-61.
46. Kayalar, C., J. Rosing, and P.D. Boyer, *An alternating site sequence for oxidative phosphorylation suggested by measurement of substrate binding patterns and exchange reaction inhibitions.* J Biol Chem, 1977. **252**(8): p. 2486-91.
47. Nakamoto, R.K., J.A. Baylis Scanlon, and M.K. Al-Shawi, *The rotary mechanism of the ATP synthase.* Arch Biochem Biophys, 2008. **476**(1): p. 43-50.
48. Futai, M., et al., *Rotational catalysis in proton pumping ATPases: from E. coli F-ATPase to mammalian V-ATPase.* Biochim Biophys Acta, 2012. **1817**(10): p. 1711-21.
49. Rasmusson, A.G., D.A. Geisler, and I.M. Moller, *The multiplicity of dehydrogenases in the electron transport chain of plant mitochondria.* Mitochondrion, 2008. **8**(1): p. 47-60.
50. Michalecka, A.M., et al., *Arabidopsis genes encoding mitochondrial type II NAD(P)H dehydrogenases have different evolutionary origin and show distinct responses to light.* Plant Physiol, 2003. **133**(2): p. 642-52.
51. Bendall, D.S. and W.D. Bonner, *Cyanide-insensitive Respiration in Plant Mitochondria.* Plant Physiol, 1971. **47**(2): p. 236-45.

52. Lambers, H., *Cyanide-resistant respiration: A non-phosphorylating electron transport pathway acting as an energy overflow.* Physiologia Plantarum, 1982. **55**(4): p. 478-485.
53. Ribas-Carbo, M., et al., *Electron Partitioning between the Cytochrome and Alternative Pathways in Plant Mitochondria.* Plant Physiol, 1995. **109**(3): p. 829-837.
54. Rasmusson, A.G., A.R. Fernie, and J.T. van Dongen, *Alternative oxidase: a defence against metabolic fluctuations?* Physiol Plant, 2009. **137**(4): p. 371-82.
55. Van Aken, O., et al., *Alternative oxidase: a target and regulator of stress responses.* Physiol Plant, 2009. **137**(4): p. 354-61.
56. De Clercq, I., et al., *The membrane-bound NAC transcription factor ANAC013 functions in mitochondrial retrograde regulation of the oxidative stress response in Arabidopsis.* Plant Cell, 2013. **25**(9): p. 3472-90.
57. Ivanova, A., et al., *A Functional Antagonistic Relationship between Auxin and Mitochondrial Retrograde Signaling Regulates Alternative Oxidase1a Expression in Arabidopsis.* Plant Physiol, 2014. **165**(3): p. 1233-1254.
58. Ng, S., et al., *A membrane-bound NAC transcription factor, ANAC017, mediates mitochondrial retrograde signaling in Arabidopsis.* Plant Cell, 2013. **25**(9): p. 3450-71.
59. Balk, J. and M. Pilon, *Ancient and essential: the assembly of iron-sulfur clusters in plants.* Trends Plant Sci, 2011. **16**(4): p. 218-26.
60. Bewley, J.D. and M. Black, *Seeds - Physiology and development of germination*. 1994, Plenum: New York.
61. Hodges, M., *Enzyme redundancy and the importance of 2-oxoglutarate in plant ammonium assimilation.* J Exp Bot, 2002. **53**(370): p. 905-16.
62. Alban, C., D. Job, and R. Douce, *Biotin Metabolism in Plants.* Annu Rev Plant Physiol Plant Mol Biol, 2000. **51**: p. 17-47.
63. Vance, J.E., *Phospholipid synthesis in a membrane fraction associated with mitochondria.* J Biol Chem, 1990. **265**(13): p. 7248-56.
64. McBride, H.M., M. Neuspiel, and S. Wasiak, *Mitochondria: more than just a powerhouse.* Curr Biol, 2006. **16**(14): p. R551-60.

65. Millar, A.H., et al., *The plant mitochondrial proteome.* Trends Plant Sci, 2005. **10**(1): p. 36-43.
66. Sickmann, A., et al., *The proteome of Saccharomyces cerevisiae mitochondria.* Proc Natl Acad Sci U S A, 2003. **100**(23): p. 13207-12.
67. Lopez, M.F., et al., *High-throughput profiling of the mitochondrial proteome using affinity fractionation and automation.* Electrophoresis, 2000. **21**(16): p. 3427-40.
68. Carrie, C., et al., *Conserved and novel functions for Arabidopsis thaliana MIA40 in assembly of proteins in mitochondria and peroxisomes.* J Biol Chem, 2010. **285**(46): p. 36138-48.
69. Lithgow, T. and A. Schneider, *Evolution of macromolecular import pathways in mitochondria, hydrogenosomes and mitosomes.* Philos Trans R Soc Lond B Biol Sci, 2010. **365**(1541): p. 799-817.
70. Carrie, C., M.W. Murcha, and J. Whelan, *An in silico analysis of the mitochondrial protein import apparatus of plants.* BMC Plant Biol, 2010. **10**: p. 249.
71. Carrie, C., et al., *How do plants make mitochondria?* Planta, 2013. **237**(2): p. 429-39.
72. Murcha, M.W., et al., *The plant mitochondrial protein import apparatus - the differences make it interesting.* Biochim Biophys Acta, 2013. **1840**(4): p. 1233-45.
73. Model, K., C. Meisinger, and W. Kuhlbrandt, *Cryo-electron microscopy structure of a yeast mitochondrial preprotein translocase.* J Mol Biol, 2008. **383**(5): p. 1049-57.
74. Ryan, M.T., R. Wagner, and N. Pfanner, *The transport machinery for the import of preproteins across the outer mitochondrial membrane.* Int J Biochem Cell Biol, 2000. **32**(1): p. 13-21.
75. Vogtle, F.N., et al., *Global analysis of the mitochondrial N-proteome identifies a processing peptidase critical for protein stability.* Cell, 2009. **139**(2): p. 428-39.
76. Wiedemann, N., N. Pfanner, and M.T. Ryan, *The three modules of ADP/ATP carrier cooperate in receptor recruitment and translocation into mitochondria.* EMBO J, 2001. **20**(5): p. 951-60.

77. Perry, A.J., et al., *Convergent evolution of receptors for protein import into mitochondria.* Curr Biol, 2006. **16**(3): p. 221-9.
78. Rimmer, K.A., et al., *Recognition of mitochondrial targeting sequences by the import receptors Tom20 and Tom22.* J Mol Biol, 2011. **405**(3): p. 804-18.
79. Shiota, T., et al., *In vivo protein-interaction mapping of a mitochondrial translocator protein Tom22 at work.* Proc Natl Acad Sci U S A, 2011. **108**(37): p. 15179-83.
80. Macasev, D., et al., *Tom22', an 8-kDa trans-site receptor in plants and protozoans, is a conserved feature of the TOM complex that appeared early in the evolution of eukaryotes.* Mol Biol Evol, 2004. **21**(8): p. 1557-64.
81. Becker, T., et al., *Assembly of the mitochondrial protein import channel: role of Tom5 in two-stage interaction of Tom40 with the SAM complex.* Mol Biol Cell, 2010. **21**(18): p. 3106-13.
82. Becker, T., et al., *Biogenesis of mitochondria: dual role of Tom7 in modulating assembly of the preprotein translocase of the outer membrane.* J Mol Biol, 2011. **405**(1): p. 113-24.
83. Dukanovic, J., et al., *Genetic and functional interactions between the mitochondrial outer membrane proteins Tom6 and Sam37.* Mol Cell Biol, 2009. **29**(22): p. 5975-88.
84. Jansch, L., et al., *Unique composition of the preprotein translocase of the outer mitochondrial membrane from plants.* J Biol Chem, 1998. **273**(27): p. 17251-7.
85. Werhahn, W., et al., *Purification and characterization of the preprotein translocase of the outer mitochondrial membrane from Arabidopsis. Identification of multiple forms of TOM20.* Plant Physiol, 2001. **125**(2): p. 943-54.
86. Lister, R., et al., *Functional definition of outer membrane proteins involved in preprotein import into mitochondria.* Plant Cell, 2007. **19**(11): p. 3739-59.
87. Esaki, M., et al., *Mitochondrial protein import. Requirement of presequence elements and tom components for precursor binding to the TOM complex.* J Biol Chem, 2004. **279**(44): p. 45701-7.

88. Wiedemann, N., et al., *Machinery for protein sorting and assembly in the mitochondrial outer membrane.* Nature, 2003. **424**(6948): p. 565-71.
89. Curran, S.P., et al., *The role of the Tim8p-Tim13p complex in a conserved import pathway for mitochondrial polytopic inner membrane proteins.* J Cell Biol, 2002. **158**(6): p. 1017-27.
90. Paschen, S.A., et al., *The role of the TIM8-13 complex in the import of Tim23 into mitochondria.* EMBO J, 2000. **19**(23): p. 6392-400.
91. Kutik, S., et al., *Dissecting membrane insertion of mitochondrial beta-barrel proteins.* Cell, 2008. **132**(6): p. 1011-24.
92. Armstrong, L.C., et al., *Metaxin is a component of a preprotein import complex in the outer membrane of the mammalian mitochondrion.* J Biol Chem, 1997. **272**(10): p. 6510-8.
93. Chan, N.C. and T. Lithgow, *The peripheral membrane subunits of the SAM complex function codependently in mitochondrial outer membrane biogenesis.* Mol Biol Cell, 2008. **19**(1): p. 126-36.
94. Yamano, K., S. Tanaka-Yamano, and T. Endo, *Mdm10 as a dynamic constituent of the TOB/SAM complex directs coordinated assembly of Tom40.* EMBO Rep, 2010. **11**(3): p. 187-93.
95. Thornton, N., et al., *Two modular forms of the mitochondrial sorting and assembly machinery are involved in biogenesis of alpha-helical outer membrane proteins.* J Mol Biol, 2010. **396**(3): p. 540-9.
96. Yamano, K., S. Tanaka-Yamano, and T. Endo, *Tom7 regulates Mdm10-mediated assembly of the mitochondrial import channel protein Tom40.* J Biol Chem, 2010. **285**(53): p. 41222-31.
97. Meisinger, C., et al., *The morphology proteins Mdm12/Mmm1 function in the major beta-barrel assembly pathway of mitochondria.* EMBO J, 2007. **26**(9): p. 2229-39.
98. Meisinger, C., et al., *The mitochondrial morphology protein Mdm10 functions in assembly of the preprotein translocase of the outer membrane.* Dev Cell, 2004. **7**(1): p. 61-71.
99. Kornmann, B., et al., *An ER-mitochondria tethering complex revealed by a synthetic biology screen.* Science, 2009. **325**(5939): p. 477-81.

100. Hobbs, A.E., et al., *Mmm1p, a mitochondrial outer membrane protein, is connected to mitochondrial DNA (mtDNA) nucleoids and required for mtDNA stability.* J Cell Biol, 2001. **152**(2): p. 401-10.
101. Osman, C., et al., *The genetic interactome of prohibitins: coordinated control of cardiolipin and phosphatidylethanolamine by conserved regulators in mitochondria.* J Cell Biol, 2009. **184**(4): p. 583-96.
102. Kopec, K.O., V. Alva, and A.N. Lupas, *Bioinformatics of the TULIP domain superfamily.* Biochem Soc Trans, 2011. **39**(4): p. 1033-8.
103. van der Laan, M., et al., *Role of MINOS in mitochondrial membrane architecture and biogenesis.* Trends Cell Biol, 2012. **22**(4): p. 185-92.
104. Harner, M., et al., *The mitochondrial contact site complex, a determinant of mitochondrial architecture.* EMBO J, 2011. **30**(21): p. 4356-70.
105. von der Malsburg, K., et al., *Dual role of mitofilin in mitochondrial membrane organization and protein biogenesis.* Dev Cell, 2011. **21**(4): p. 694-707.
106. Sideris, D.P., et al., *A novel intermembrane space-targeting signal docks cysteines onto Mia40 during mitochondrial oxidative folding.* J Cell Biol, 2009. **187**(7): p. 1007-22.
107. Banci, L., et al., *MIA40 is an oxidoreductase that catalyzes oxidative protein folding in mitochondria.* Nat Struct Mol Biol, 2009. **16**(2): p. 198-206.
108. Muller, J.M., et al., *Precursor oxidation by Mia40 and Erv1 promotes vectorial transport of proteins into the mitochondrial intermembrane space.* Mol Biol Cell, 2008. **19**(1): p. 226-36.
109. Xu, L., et al., *Acquisition, conservation, and loss of dual-targeted proteins in land plants.* Plant Physiol, 2013. **161**(2): p. 644-62.
110. Rehling, P., et al., *Protein insertion into the mitochondrial inner membrane by a twin-pore translocase.* Science, 2003. **299**(5613): p. 1747-51.
111. Young, J.C., N.J. Hoogenraad, and F.U. Hartl, *Molecular chaperones Hsp90 and Hsp70 deliver preproteins to the mitochondrial import receptor Tom70.* Cell, 2003. **112**(1): p. 41-50.
112. Wu, Y. and B. Sha, *Crystal structure of yeast mitochondrial outer membrane translocon member Tom70p.* Nat Struct Mol Biol, 2006. **13**(7): p. 589-93.

113. Rehling, P., K. Brandner, and N. Pfanner, *Mitochondrial import and the twin-pore translocase.* Nat Rev Mol Cell Biol, 2004. **5**(7): p. 519-30.
114. Gebert, N., et al., *Dual function of Sdh3 in the respiratory chain and TIM22 protein translocase of the mitochondrial inner membrane.* Mol Cell, 2011. **44**(5): p. 811-8.
115. Moczko, M., et al., *The intermembrane space domain of mitochondrial Tom22 functions as a trans binding site for preproteins with N-terminal targeting sequences.* Mol Cell Biol, 1997. **17**(11): p. 6574-84.
116. Schleyer, M. and W. Neupert, *Transport of proteins into mitochondria: translocational intermediates spanning contact sites between outer and inner membranes.* Cell, 1985. **43**(1): p. 339-50.
117. Marom, M., et al., *Direct interaction of mitochondrial targeting presequences with purified components of the TIM23 protein complex.* J Biol Chem, 2011. **286**(51): p. 43809-15.
118. Meinecke, M., et al., *Tim50 maintains the permeability barrier of the mitochondrial inner membrane.* Science, 2006. **312**(5779): p. 1523-6.
119. Martinez-Caballero, S., et al., *Tim17p regulates the twin pore structure and voltage gating of the mitochondrial protein import complex TIM23.* J Biol Chem, 2007. **282**(6): p. 3584-93.
120. Meier, S., W. Neupert, and J.M. Herrmann, *Conserved N-terminal negative charges in the Tim17 subunit of the TIM23 translocase play a critical role in the import of preproteins into mitochondria.* J Biol Chem, 2005. **280**(9): p. 7777-85.
121. Albrecht, R., et al., *The Tim21 binding domain connects the preprotein translocases of both mitochondrial membranes.* EMBO Rep, 2006. **7**(12): p. 1233-8.
122. Mokranjac, D., et al., *Role of Tim21 in mitochondrial translocation contact sites.* J Biol Chem, 2005. **280**(25): p. 23437-40.
123. van der Laan, M., et al., *A role for Tim21 in membrane-potential-dependent preprotein sorting in mitochondria.* Curr Biol, 2006. **16**(22): p. 2271-6.
124. van der Laan, M., et al., *Motor-free mitochondrial presequence translocase drives membrane integration of preproteins.* Nat Cell Biol, 2007. **9**(10): p. 1152-9.

125. Wiedemann, N., et al., *Sorting switch of mitochondrial presequence translocase involves coupling of motor module to respiratory chain.* J Cell Biol, 2007. **179**(6): p. 1115-22.
126. Murcha, M.W., et al., *The C-terminal region of TIM17 links the outer and inner mitochondrial membranes in Arabidopsis and is essential for protein import.* J Biol Chem, 2005. **280**(16): p. 16476-83.
127. Van Aken, O., et al., *Defining the mitochondrial stress response in Arabidopsis thaliana.* Mol Plant, 2009. **2**(6): p. 1310-24.
128. Giraud, E., et al., *REDOX regulation of mitochondrial function in plants.* Plant Cell Environ, 2012. **35**(2): p. 271-80.
129. Narsai, R., et al., *In-depth temporal transcriptome profiling reveals a crucial developmental switch with roles for RNA processing and organelle metabolism that are essential for germination in Arabidopsis.* Plant Physiol, 2011. **157**(3): p. 1342-62.
130. Wang, Y., et al., *Dual location of the mitochondrial preprotein transporters B14.7 and Tim23-2 in complex I and the TIM17:23 complex in Arabidopsis links mitochondrial activity and biogenesis.* Plant Cell, 2012. **24**(6): p. 2675-95.
131. Hamasaki, H., et al., *SD3, an Arabidopsis thaliana homolog of TIM21, affects intracellular ATP levels and seedling development.* Mol Plant, 2012. **5**(2): p. 461-71.
132. Chacinska, A., et al., *Mitochondrial presequence translocase: switching between TOM tethering and motor recruitment involves Tim21 and Tim17.* Cell, 2005. **120**(6): p. 817-29.
133. Murcha, M.W., et al., *Evidence for interactions between the mitochondrial import apparatus and respiratory chain complexes via Tim21-like proteins in Arabidopsis.* Front Plant Sci, 2014. **5**: p. 82.
134. Krimmer, T., et al., *Mitochondrial protein import motor: the ATPase domain of matrix Hsp70 is crucial for binding to Tim44, while the peptide binding domain and the carboxy-terminal segment play a stimulatory role.* Mol Cell Biol, 2000. **20**(16): p. 5879-87.

135. van der Laan, M., D.P. Hutu, and P. Rehling, *On the mechanism of preprotein import by the mitochondrial presequence translocase.* Biochim Biophys Acta, 2010. **1803**(6): p. 732-9.
136. Schiller, D., *Pam17 and Tim44 act sequentially in protein import into the mitochondrial matrix.* Int J Biochem Cell Biol, 2009. **41**(11): p. 2343-9.
137. Frazier, A.E., et al., *Pam16 has an essential role in the mitochondrial protein import motor.* Nat Struct Mol Biol, 2004. **11**(3): p. 226-33.
138. Murcha, M.W., et al., *MPIC: a mitochondrial protein import components database for plant and non-plant species.* Plant Cell Physiol, 2015. **56**(1): p. e10.
139. Suyama, Y., *The origins of mitochondrial ribonucleic acids in Tetrahymena pyriformis.* Biochemistry, 1967. **6**(9): p. 2829-39.
140. Small, I., et al., *In vivo import of a normal or mutagenized heterologous transfer RNA into the mitochondria of transgenic plants: towards novel ways of influencing mitochondrial gene expression?* EMBO J, 1992. **11**(4): p. 1291-6.
141. Schneider, A., *Mitochondrial tRNA import and its consequences for mitochondrial translation.* Annu Rev Biochem, 2011. **80**: p. 1033-53.
142. Hopper, A.K., D.A. Pai, and D.R. Engelke, *Cellular dynamics of tRNAs and their genes.* FEBS Lett, 2010. **584**(2): p. 310-7.
143. Grosshans, H., G. Simos, and E. Hurt, *Review: transport of tRNA out of the nucleus-direct channeling to the ribosome?* J Struct Biol, 2000. **129**(2-3): p. 288-94.
144. Tarassov, I.A. and N.S. Entelis, *Mitochondrially-imported cytoplasmic tRNA(Lys)(CUU) of Saccharomyces cerevisiae: in vivo and in vitro targetting systems.* Nucleic Acids Res, 1992. **20**(6): p. 1277-81.
145. Tarassov, I., N. Entelis, and R.P. Martin, *Mitochondrial import of a cytoplasmic lysine-tRNA in yeast is mediated by cooperation of cytoplasmic and mitochondrial lysyl-tRNA synthetases.* EMBO J, 1995. **14**(14): p. 3461-71.
146. Tarassov, I., N. Entelis, and R.P. Martin, *An intact protein translocating machinery is required for mitochondrial import of a yeast cytoplasmic tRNA.* J Mol Biol, 1995. **245**(4): p. 315-23.

147. Kolesnikova, O., et al., *Selection of RNA aptamers imported into yeast and human mitochondria.* RNA, 2010. **16**(5): p. 926-41.
148. Kamenski, P., et al., *Evidence for an adaptation mechanism of mitochondrial translation via tRNA import from the cytosol.* Mol Cell, 2007. **26**(5): p. 625-37.
149. Brandina, I., et al., *tRNA import into yeast mitochondria is regulated by the ubiquitin-proteasome system.* FEBS Lett, 2007. **581**(22): p. 4248-54.
150. Sepuri, N.B., M. Gorla, and M.P. King, *Mitochondrial lysyl-tRNA synthetase independent import of tRNA lysine into yeast mitochondria.* PLoS One, 2012. **7**(4): p. e35321.
151. Rinehart, J., et al., *Saccharomyces cerevisiae imports the cytosolic pathway for Gln-tRNA synthesis into the mitochondrion.* Genes Dev, 2005. **19**(5): p. 583-92.
152. Feng, L., et al., *Aminoacyl-tRNA synthesis by pre-translational amino acid modification.* RNA Biol, 2004. **1**(1): p. 16-20.
153. Rubio, M.A., et al., *Mammalian mitochondria have the innate ability to import tRNAs by a mechanism distinct from protein import.* Proc Natl Acad Sci U S A, 2008. **105**(27): p. 9186-91.
154. Simpson, A.M., et al., *Kinetoplastid mitochondria contain functional tRNAs which are encoded in nuclear DNA and also contain small minicircle and maxicircle transcripts of unknown function.* Nucleic Acids Res, 1989. **17**(14): p. 5427-45.
155. Crausaz Esseiva, A., et al., *The T-stem determines the cytosolic or mitochondrial localization of trypanosomal tRNAsMet.* Mol Biol Cell, 2004. **15**(6): p. 2750-7.
156. Bouzaidi-Tiali, N., et al., *Elongation factor 1a mediates the specificity of mitochondrial tRNA import in T. brucei.* EMBO J, 2007. **26**(20): p. 4302-12.
157. Pusnik, M., et al., *The single mitochondrial porin of Trypanosoma brucei is the main metabolite transporter in the outer mitochondrial membrane.* Mol Biol Evol, 2009. **26**(3): p. 671-80.
158. Rubio, M.A., et al., *Selective importation of RNA into isolated mitochondria from Leishmania tarentolae.* RNA, 2000. **6**(7): p. 988-1003.

159. Yermovsky-Kammerer, A.E. and S.L. Hajduk, *In vitro import of a nuclearly encoded tRNA into the mitochondrion of Trypanosoma brucei.* Mol Cell Biol, 1999. **19**(9): p. 6253-9.
160. Nabholz, C.E., E.K. Horn, and A. Schneider, *tRNAs and proteins are imported into mitochondria of Trypanosoma brucei by two distinct mechanisms.* Mol Biol Cell, 1999. **10**(8): p. 2547-57.
161. Tschopp, F., F. Charriere, and A. Schneider, *In vivo study in Trypanosoma brucei links mitochondrial transfer RNA import to mitochondrial protein import.* EMBO Rep, 2011. **12**(8): p. 825-32.
162. Goswami, S., et al., *A bifunctional tRNA import receptor from Leishmania mitochondria.* Proc Natl Acad Sci U S A, 2006. **103**(22): p. 8354-9.
163. Mukherjee, S., et al., *Necessary and sufficient factors for the import of transfer RNA into the kinetoplast mitochondrion.* EMBO Rep, 2007. **8**(6): p. 589-95.
164. Paris, Z., et al., *Mitochondrial tRNA import in Trypanosoma brucei is independent of thiolation and the Rieske protein.* RNA, 2009. **15**(7): p. 1398-406.
165. Paris, Z., et al., *Futile import of tRNAs and proteins into the mitochondrion of Trypanosoma brucei evansi.* Mol Biochem Parasitol, 2011. **176**(2): p. 116-20.
166. Cristodero, M., T. Seebeck, and A. Schneider, *Mitochondrial translation is essential in bloodstream forms of Trypanosoma brucei.* Mol Microbiol, 2010. **78**(3): p. 757-69.
167. Schekman, R., *Editorial expression of concern: a bifunctional tRNA import receptor from Leishmania mitochondria.* Proc Natl Acad Sci U S A, 2010. **107**.
168. Kumar, R., et al., *Striking differences in mitochondrial tRNA import between different plant species.* Mol Gen Genet, 1996. **252**(4): p. 404-11.
169. Glover, K.E., D.F. Spencer, and M.W. Gray, *Identification and structural characterization of nucleus-encoded transfer RNAs imported into wheat mitochondria.* J Biol Chem, 2001. **276**(1): p. 639-48.
170. Cognat, V., et al., *PlantRNA, a database for tRNAs of photosynthetic eukaryotes.* Nucleic Acids Res, 2013. **41**(Database issue): p. D273-9.

171. Dietrich, A., et al., *A single base change prevents import of cytosolic tRNA(Ala) into mitochondria in transgenic plants.* Plant J, 1996. **10**(5): p. 913-8.
172. Vinogradova, E., et al., *Steady-state levels of imported tRNAs in Chlamydomonas mitochondria are correlated with both cytosolic and mitochondrial codon usages.* Nucleic Acids Res, 2009. **37**(5): p. 1521-8.
173. Delage, L., et al., *In vitro import of a nuclearly encoded tRNA into mitochondria of Solanum tuberosum.* Mol Cell Biol, 2003. **23**(11): p. 4000-12.
174. Salinas, T., et al., *The voltage-dependent anion channel, a major component of the tRNA import machinery in plant mitochondria.* Proc Natl Acad Sci U S A, 2006. **103**(48): p. 18362-7.
175. Zinser, E. and G. Daum, *Isolation and biochemical characterization of organelles from the yeast, Saccharomyces cerevisiae.* Yeast, 1995. **11**(6): p. 493-536.
176. Osman, C., D.R. Voelker, and T. Langer, *Making heads or tails of phospholipids in mitochondria.* J Cell Biol, 2011. **192**(1): p. 7-16.
177. Gaigg, B., et al., *Characterization of a microsomal subfraction associated with mitochondria of the yeast, Saccharomyces cerevisiae. Involvement in synthesis and import of phospholipids into mitochondria.* Biochim Biophys Acta, 1995. **1234**(2): p. 214-20.
178. Schmitt, S., et al., *Proteome analysis of mitochondrial outer membrane from Neurospora crassa.* Proteomics, 2006. **6**(1): p. 72-80.
179. Zahedi, R.P., et al., *Proteomic analysis of the yeast mitochondrial outer membrane reveals accumulation of a subclass of preproteins.* Mol Biol Cell, 2006. **17**(3): p. 1436-50.
180. Niemann, M., et al., *Mitochondrial outer membrane proteome of Trypanosoma brucei reveals novel factors required to maintain mitochondrial morphology.* Mol Cell Proteomics, 2013. **12**(2): p. 515-28.
181. Duncan, O., et al., *Multiple lines of evidence localize signaling, morphology, and lipid biosynthesis machinery to the mitochondrial outer membrane of Arabidopsis.* Plant Physiol, 2011. **157**(3): p. 1093-113.

182. Duncan, O., et al., *The outer mitochondrial membrane in higher plants.* Trends Plant Sci, 2013. **18**(4): p. 207-17.
183. Murcha, M.W., et al., *Characterization of the preprotein and amino acid transporter gene family in Arabidopsis.* Plant Physiol, 2007. **143**(1): p. 199-212.
184. Marchler-Bauer, A., et al., *CDD: conserved domains and protein three-dimensional structure.* Nucleic Acids Res, 2013. **41**(Database issue): p. D348-52.
185. Cserzo, M., et al., *Prediction of transmembrane alpha-helices in prokaryotic membrane proteins: the dense alignment surface method.* Protein Eng, 1997. **10**(6): p. 673-6.
186. Bagos, P.G., et al., *PRED-TMBB: a web server for predicting the topology of beta-barrel outer membrane proteins.* Nucleic Acids Res, 2004. **32**(Web Server issue): p. W400-4.
187. Campanella, J.J., L. Bitincka, and J. Smalley, *MatGAT: an application that generates similarity/identity matrices using protein or DNA sequences.* BMC Bioinformatics, 2003. **4**: p. 29.
188. Altschul, S.F. and E.V. Koonin, *Iterated profile searches with PSI-BLAST--a tool for discovery in protein databases.* Trends Biochem Sci, 1998. **23**(11): p. 444-7.
189. Tamura, K., et al., *MEGA5: molecular evolutionary genetics analysis using maximum likelihood, evolutionary distance, and maximum parsimony methods.* Mol Biol Evol, 2011. **28**(10): p. 2731-9.
190. Looke, M., K. Kristjuhan, and A. Kristjuhan, *Extraction of genomic DNA from yeasts for PCR-based applications.* Biotechniques, 2011. **50**(5): p. 325-8.
191. Day, D.A., M. Neuberger, and R. Douce, *Biochemical characterisation of chlorophyll-free mitochondria from pea leaves.* Australian Journal of Plant Physiology, 1985(12): p. 219-228.
192. Whelan, J., et al., *Evidence for a link between translocation and processing during protein import into soybean mitochondria.* Biochim Biophys Acta, 1996. **1312**(1): p. 48-54.

193. Sieber, F., et al., *A protein shuttle system to target RNA into mitochondria.* Nucleic Acids Res, 2011. **39**(14): p. e96.
194. Aronsson, H. and P. Jarvis, *A simple method for isolating import-competent Arabidopsis chloroplasts.* FEBS Lett, 2002. **529**(2-3): p. 215-20.
195. Jansch, L., et al., *New insights into the composition, molecular mass and stoichiometry of the protein complexes of plant mitochondria.* Plant J, 1996. **9**(3): p. 357-68.
196. Meyer, E.H., et al., *Remodeled respiration in ndufs4 with low phosphorylation efficiency suppresses Arabidopsis germination and growth and alters control of metabolism at night.* Plant Physiol, 2009. **151**(2): p. 603-19.
197. Sedigheh, H.G., et al., *Oxidative stress and leaf senescence.* BMC Res Notes, 2011. **4**: p. 477.
198. Rassow, J., et al., *The preprotein translocase of the mitochondrial inner membrane: function and evolution.* J Mol Biol, 1999. **286**(1): p. 105-20.
199. Meyer, E.H., N.L. Taylor, and A.H. Millar, *Resolving and identifying protein components of plant mitochondrial respiratory complexes using three dimensions of gel electrophoresis.* J Proteome Res, 2008. **7**(2): p. 786-94.
200. Klodmann, J., et al., *Internal architecture of mitochondrial complex I from Arabidopsis thaliana.* Plant Cell, 2010. **22**(3): p. 797-810.
201. Klodmann, J., et al., *Defining the protein complex proteome of plant mitochondria.* Plant Physiol, 2011. **157**(2): p. 587-98.
202. Kim, C.A. and J.U. Bowie, *SAM domains: uniform structure, diversity of function.* Trends Biochem Sci, 2003. **28**(12): p. 625-8.
203. Green, J.B., et al., *RNA recognition via the SAM domain of Smaug.* Mol Cell, 2003. **11**(6): p. 1537-48.
204. Aviv, T., et al., *The RNA-binding SAM domain of Smaug defines a new family of post-transcriptional regulators.* Nat Struct Biol, 2003. **10**(8): p. 614-21.
205. Roston, R.L., et al., *TGD1, -2, and -3 proteins involved in lipid trafficking form ATP-binding cassette (ABC) transporter with multiple substrate-binding proteins.* J Biol Chem, 2012. **287**(25): p. 21406-15.

206. Boyes, D.C., et al., *Growth stage-based phenotypic analysis of Arabidopsis: a model for high throughput functional genomics in plants.* Plant Cell, 2001. **13**(7): p. 1499-510.
207. Kulawiak, B., et al., *The mitochondrial protein import machinery has multiple connections to the respiratory chain.* Biochim Biophys Acta, 2013. **1827**(5): p. 612-26.
208. Murcha, M.W., Y. Wang, and J. Whelan, *A molecular link between mitochondrial preprotein transporters and respiratory chain complexes.* Plant Signal Behav, 2012. **7**(12): p. 1594-7.
209. Rossig, C., et al., *New functions of the chloroplast Preprotein and Amino acid Transporter (PRAT) family members in protein import.* Plant Signal Behav, 2014. **9**(1).
210. Mireau, H., et al., *Expression of Arabidopsis thaliana mitochondrial alanyl-tRNA synthetase is not sufficient to trigger mitochondrial import of tRNAAla in yeast.* J Biol Chem, 2000. **275**(18): p. 13291-6.
211. Yen, M.R., et al., *Protein-translocating outer membrane porins of Gram-negative bacteria.* Biochim Biophys Acta, 2002. **1562**(1-2): p. 6-31.
212. Gabriel, K., S.K. Buchanan, and T. Lithgow, *The alpha and the beta: protein translocation across mitochondrial and plastid outer membranes.* Trends Biochem Sci, 2001. **26**(1): p. 36-40.
213. Wimley, W.C., *The versatile beta-barrel membrane protein.* Curr Opin Struct Biol, 2003. **13**(4): p. 404-11.
214. Schulz, G.E., *The structure of bacterial outer membrane proteins.* Biochim Biophys Acta, 2002. **1565**(2): p. 308-17.
215. Bay, D.C. and D.A. Court, *Origami in the outer membrane: the transmembrane arrangement of mitochondrial porins.* Biochem Cell Biol, 2002. **80**(5): p. 551-62.
216. Hill, K., et al., *Tom40 forms the hydrophilic channel of the mitochondrial import pore for preproteins [see comment].* Nature, 1998. **395**(6701): p. 516-21.
217. Kozjak, V., et al., *An essential role of Sam50 in the protein sorting and assembly machinery of the mitochondrial outer membrane.* J Biol Chem, 2003. **278**(49): p. 48520-3.

218. Flinner, N., et al., *Mdm10 is an ancient eukaryotic porin co-occurring with the ERMES complex.* Biochim Biophys Acta, 2013. **1833**(12): p. 3314-25.
219. Schnarwiler, F., et al., *Trypanosomal TAC40 constitutes a novel subclass of mitochondrial beta-barrel proteins specialized in mitochondrial genome inheritance.* Proc Natl Acad Sci U S A, 2014. **111**(21): p. 7624-9.
220. Lee, S.M., et al., *Pathogen inducible voltage-dependent anion channel (AtVDAC) isoforms are localized to mitochondria membrane in Arabidopsis.* Mol Cells, 2009. **27**(3): p. 321-7.
221. Lee, A.C., et al., *The role of yeast VDAC genes on the permeability of the mitochondrial outer membrane.* J Membr Biol, 1998. **161**(2): p. 173-81.
222. Alberti, S., A.D. Gitler, and S. Lindquist, *A suite of Gateway cloning vectors for high-throughput genetic analysis in Saccharomyces cerevisiae.* Yeast, 2007. **24**(10): p. 913-9.
223. Guiboileau, A., et al., *Senescence and death of plant organs: nutrient recycling and developmental regulation.* C R Biol, 2010. **333**(4): p. 382-91.
224. Robert, N., et al., *Voltage-dependent-anion-channels (VDACs) in Arabidopsis have a dual localization in the cell but show a distinct role in mitochondria.* Plant Mol Biol, 2012. **78**(4-5): p. 431-46.
225. Blachly-Dyson, E. and M. Forte, *VDAC channels.* IUBMB Life, 2001. **52**(3-5): p. 113-8.
226. Young, M.J., et al., *The evolutionary history of mitochondrial porins.* BMC Evol Biol, 2007. **7**: p. 31.
227. Conklin, P.L., E.H. Williams, and R.L. Last, *Environmental stress sensitivity of an ascorbic acid-deficient Arabidopsis mutant.* Proc Natl Acad Sci U S A, 1996. **93**(18): p. 9970-4.
228. Rebeille, F., et al., *Folate biosynthesis in higher plants: purification and molecular cloning of a bifunctional 6-hydroxymethyl-7,8-dihydropterin pyrophosphokinase/7,8-dihydropteroate synthase localized in mitochondria.* EMBO J, 1997. **16**(5): p. 947-57.
229. Webb, M.E., et al., *Elucidating biosynthetic pathways for vitamins and cofactors.* Nat Prod Rep, 2007. **24**(5): p. 988-1008.
230. Millar, A.H., et al., *Organization and regulation of mitochondrial respiration in plants.* Annu Rev Plant Biol, 2011. **62**: p. 79-104.

231. Yao, N., et al., *The mitochondrion--an organelle commonly involved in programmed cell death in Arabidopsis thaliana.* Plant J, 2004. **40**(4): p. 596-610.
232. Gleason, C., et al., *Mitochondrial complex II has a key role in mitochondrial-derived reactive oxygen species influence on plant stress gene regulation and defense.* Proc Natl Acad Sci U S A, 2011. **108**(26): p. 10768-73.
233. He, J., et al., *DEXH box RNA helicase-mediated mitochondrial reactive oxygen species production in Arabidopsis mediates crosstalk between abscisic acid and auxin signaling.* Plant Cell, 2012. **24**(5): p. 1815-33.
234. Keech, O., et al., *The different fates of mitochondria and chloroplasts during dark-induced senescence in Arabidopsis leaves.* Plant Cell Environ, 2007. **30**(12): p. 1523-34.
235. Rubio, M.A. and A.K. Hopper, *Transfer RNA travels from the cytoplasm to organelles.* Wiley Interdiscip Rev RNA, 2011. **2**(6): p. 802-17.
236. Wang, G., et al., *PNPASE and RNA trafficking into mitochondria.* Biochim Biophys Acta, 2012. **1819**(9-10): p. 998-1007.
237. Yoshionari, S., et al., *Existence of nuclear-encoded 5S-rRNA in bovine mitochondria.* FEBS Lett, 1994. **338**(2): p. 137-42.
238. Entelis, N.S., et al., *5 S rRNA and tRNA import into human mitochondria. Comparison of in vitro requirements.* J Biol Chem, 2001. **276**(49): p. 45642-53.
239. Crick, F.H., *Codon--anticodon pairing: the wobble hypothesis.* J Mol Biol, 1966. **19**(2): p. 548-55.
240. Morden, C.W., et al., *Plastid translation and transcription genes in a non-photosynthetic plant: intact, missing and pseudo genes.* EMBO J, 1991. **10**(11): p. 3281-8.
241. Wolfe, K.H., et al., *Rapid evolution of the plastid translational apparatus in a nonphotosynthetic plant: loss or accelerated sequence evolution of tRNA and ribosomal protein genes.* J Mol Evol, 1992. **35**(4): p. 304-17.
242. Bungard, R.A., *Photosynthetic evolution in parasitic plants: insight from the chloroplast genome.* Bioessays, 2004. **26**(3): p. 235-47.

243. Grosjean, H., C. Marck, and V. de Crecy-Lagard, *The various strategies of codon decoding in organisms of the three domains of life: evolutionary implications.* Nucleic Acids Symp Ser (Oxf), 2007(51): p. 15-6.
244. Steller, H., *Mechanisms and genes of cellular suicide.* Science, 1995. **267**(5203): p. 1445-9.
245. Susin, S.A., N. Zamzami, and G. Kroemer, *Mitochondria as regulators of apoptosis: doubt no more.* Biochim Biophys Acta, 1998. **1366**(1-2): p. 151-65.
246. Zoratti, M. and I. Szabo, *The mitochondrial permeability transition.* Biochim Biophys Acta, 1995. **1241**(2): p. 139-76.
247. Godbole, A., et al., *VDAC is a conserved element of death pathways in plant and animal systems.* Biochim Biophys Acta, 2003. **1642**(1-2): p. 87-96.
248. Balk, J., C.J. Leaver, and P.F. McCabe, *Translocation of cytochrome c from the mitochondria to the cytosol occurs during heat-induced programmed cell death in cucumber plants.* FEBS Lett, 1999. **463**(1-2): p. 151-4.
249. Sun, Y.L., et al., *Cytochrome c release and caspase activation during menadione-induced apoptosis in plants.* FEBS Lett, 1999. **462**(3): p. 317-21.
250. Tiwari, B.S., B. Belenghi, and A. Levine, *Oxidative stress increased respiration and generation of reactive oxygen species, resulting in ATP depletion, opening of mitochondrial permeability transition, and programmed cell death.* Plant Physiol, 2002. **128**(4): p. 1271-81.
251. del Pozo, O. and E. Lam, *Caspases and programmed cell death in the hypersensitive response of plants to pathogens.* Curr Biol, 1998. **8**(24): p. R896.
252. Ryerson, D.E. and M.C. Heath, *Cleavage of Nuclear DNA into Oligonucleosomal Fragments during Cell Death Induced by Fungal Infection or by Abiotic Treatments.* Plant Cell, 1996. **8**(3): p. 393-402.

Apendix I

Primers used to clone TRic proteins

Tric1 full-length forward:

5'GGGGACAAGTTTGTACAAAAAAGCAGGCTTCGAAGGAGATAGAACCATGATG GTGGTAGGCGGCGGAGGA3'

Tric1 full-length forward reverse:

3'GGGGACCACTTTGTACAAGAAAGCTGGGTCTCCACCTCCGGATCACTACTTT CGTTTGCCCTTTAT5'

Tric2 full-length forward:

5'GGGGACAAGTTTGTACAAAAAAGCAGGCTTCGAAGGAGATAGAACCATGATG GGGAAAGACGGAGAAGGA3'

Tric2 full-length reverse:

3'GGGGACCACTTTGTACAAGAAAGCTGGGTCTCCACCTCCGGATCATCAACCA CGACTTCCCCGCTT5'

Tric1 1-150 aa forward:

5'GGGGACAAGTTTGTACAAAAAAGCAGGCTTCGAAGGAGATAGAACCATGATG GTGGTAGGCGGCGGAGGA3'

Tric1 1-150 aa reverse:

3'GGGGACCACTTTGTACAAGAAAGCTGGGTCTCCACCTCCGGATCATGCAAAT CCAGATCCTAACGC5'

Tric2 1-150 aa forward:

5'GGGGACAAGTTTGTACAAAAAAGCAGGCTTCGAAGGAGATAGAACCATGATG GGGAAAGACGGAGAAGGA3'

Tric2 1-150 aa reverse:

3'GGGGACCACTTTGTACAAGAAAGCTGGGTCTCCACCTCCGGATCAAGCATTA ACACCAGTTATAGC5'

Tric2 1-180 aa complementation forward

5'GGGGACAAGTTTGTACAAAAAAGCAGGCTTCGAAGGAGATAGAACCATGATG GGGAAAGACGGAGAAGGA3'

Tric2 1-180 aa complementation reverse

3'GGGGACCACTTTGTACAAGAAAGCTGGGTCTCCACCTCCGGATCACCTTTCA
CCCAACTTGAAAAA5'

Primers used to clone OM47 protein

OM47 full-length forward:
5'GGGGACAAGTTTGTACAAAAAAGCAGGCTTCGAAGGAGATAGAACCATGGG
GAATGCTCTTGTCAAAAAAGAACCAC3'
OM47 full-length reverse:
3'GGGGACCACTTTGTACAAGAAAGCTGGGTCTCCACCTCCGGATCATTAGAGA
ATCTTCTGGGACGGTCTAAGTTC5'
OM47 full-length protein import forward:
5'GGGGACAAGTTTGTACAAAAAAGCAGGCTTCGAAGGAGATAGAACCATGATG
ATGGGGAATGCTCTTGTCAAAAAAGAACCAC3'
OM47 full-length protein import reverse:
3'GGGGACCACTTTGTACAAGAAAGCTGGGTCTCCACCTCCGGATCATTACATC
ATGAGAATCTTCTGGGACGGTCTAAGTTC5'

Primers used to clone yeast VDAC1 protein

ScVDAC1 full-length forward:
5'GGGGACAAGTTTGTACAAAAAAGCAGGCTTCGAAGGAGATAGAACCATGATG
TCTCCTCCAGTTTACAGCGATATCTC3'
ScVDAC1 full-length reverse:
3'GGGGACCACTTTGTACAAGAAAGCTGGGTCTCCACCTCCGGATCAAGCGTC
GAAGGACAAAGACCAACC5'